

Portland State University

PDXScholar

Dissertations and Theses

Dissertations and Theses

1998

Xanthoness as Antimalarial Agents : Binding Interactions Between Heme Analogues and Xanthoness

Jane Xu Kelly
Portland State University

Follow this and additional works at: https://pdxscholar.library.pdx.edu/open_access_etds

 Part of the [Chemistry Commons](#)

Let us know how access to this document benefits you.

Recommended Citation

Kelly, Jane Xu, "Xanthoness as Antimalarial Agents : Binding Interactions Between Heme Analogues and Xanthoness" (1998). *Dissertations and Theses*. Paper 6375.
<https://doi.org/10.15760/etd.3521>

This Thesis is brought to you for free and open access. It has been accepted for inclusion in Dissertations and Theses by an authorized administrator of PDXScholar. Please contact us if we can make this document more accessible: pdxscholar@pdx.edu.

THESIS APPROVAL

The abstract and thesis of Jane Xu Kelly for the Master of Science in Chemistry were presented May 6, 1998, and accepted by the thesis committee and the department.

COMMITTEE APPROVALS:



David H. Peyton, Chair



Michael K. Riscoe




Jie Lin



David T. Clark
Representative of the Office of Graduate Studies

DEPARTMENT APPROVAL:



David H. Peyton, Chair
Department of Chemistry

ABSTRACT

An abstract of the thesis of Jane Xu Kelly for the Master of Science in Chemistry presented May 6, 1998.

Title: Xanthenes as Antimalarial Agents: Binding Interactions between Heme Analogues and Xanthenes

Human *falciparum* malaria is caused by *Plasmodium falciparum* parasite, which digests host hemoglobin within its food vacuole, releasing toxic heme. *P. falciparum* detoxifies free heme to hemozoin by polymerization. This process is believed to be the target of most successful antimalarial drugs, chloroquine and quinine, which are now losing their effectiveness due to the spread of multi-drug resistant strains. Xanthenes were recognized in the laboratory of Dr. M. Riscoe (Portland VA Medical Center) to bind to heme, preventing heme polymerization [Ignatushchenko, M., Winter R., and Riscoe, M. (1997) *FEBS Letters* 409, 67].

This thesis reports a study of the interactions of a potential antimalarial agent, 4,5-dihydroxyxanthone (X2), with heme and tin (IV) protoporphyrin IX (SnPP), as well as with other heme analogues, by NMR and optical spectroscopies. It was found that X2 binds to heme with a stoichiometry of two heme molecules to one X2 molecule, exhibiting an apparent dissociation equilibrium constant (K_d) of 5×10^{-6} at pH 5.8. This stoichiometry is identical to that previously found for complexes between heme and chloroquine or quinine. K_d is close to those of chloroquine, 5×10^{-6} and of quinine, 6×10^{-6} . X2 primarily binds to dimeric SnPP, with the stoichiometry of two X2 molecules to one dimer of SnPP and K_d of 1×10^{-5} at pH 5.8. This stoichiometry is identical with that found for complexes of SnPP with chloroquine or quinine, and K_d is

close to those of chloroquine, 1×10^{-5} and of quinine, 1×10^{-5} . The binding was found to be noncooperative in all of the above cases. Axial coordination between the keto of X2 and metal Fe or Sn, π - π interaction between aromatic ring of X2 and porphyrin plane, and hydrogen bonding between 4(5) hydroxy group of X2 with carboxylate side chain of the metalloporphyrin are likely contributions to binding energetics. X2 binds to both sides of monomeric SnPP but to each side of the μ -oxo bridged dimeric SnPP, while X2 binds to β -hematin dimer through coordination between the keto of X2 and the unbound iron with a 1:1 stoichiometry. Structural confirmation and characterization of 29 xanthone derivatives by ^1H NMR is presented.

XANTHONES AS ANTIMALARIAL AGENTS:
BINDING INTERACTIONS BETWEEN HEME ANALOGUES AND
XANTHONES

by

JANE XU KELLY

A thesis submitted in partial fulfillment of the
requirements for the degree of

MASTER OF SCIENCE

in

CHEMISTRY

Portland State University
1998

ACKNOWLEDGMENTS

I would like to extend my warmest thanks to my husband, Bryan, for his love, caring, and commitment. He has never doubted that I could finish whatever I put my mind to. A special thanks goes to my wonderful son, Sean, the light of my life, and constant source of joy and inspiration. I am indebted to my parents, and my sister Shelby for their constant encouragement and support. A big thanks to my research advisor, Dr. David H. Peyton, for his assistance in helping me achieve research excellence, for his willingness to share scholarly expertise, and for his patience and support throughout the process of completing this study. I also extend my great appreciation and gratitude to Dr. Michael Riscoe and Dr. Rolf Winter for their encouragement, advice and support, and for giving me the opportunity to work on this project. Their enthusiasm in science spills over into everything and everyone they touch. Dr. Rolf Winter synthesized all the xanthone compounds, made the project possible. I would like to thank Dr. Jie Lin and Dr. David Clark for serving on my committee, and critically reviewing my dissertation. I am especially grateful to Dr. Jie Lin for having always been there to listen (and to give me advice). My sincere appreciation to Dr. Carl Wamser, who was very gracious in sharing his computer facilities. Last, but not least, I would like to thank our research group: Ayna Alfadhi, Ruth Zhang, Tom Ritter, and Marina Ignatushchenko for all the fun and joy of working with them.

TABLE OF CONTENTS

CONTENT	PAGE
ACKNOWLEDGMENTS.....	i
LIST OF TABLES.....	vi
LIST OF FIGURES.....	vii
CHAPTER	
1. INTRODUCTION.....	1
2. CONFIRMATION AND CHARACTERIZATION OF XANTHONES.....	5
Materials and Methods.....	5
Results and Discussion.....	6
3. OPTICAL SPECTROPHOTOMETRIC STUDIES OF THE INTERACTIONS BETWEEN HEME AND X2, CHLOROQUINE, AND QUININE.....	15
Materials and Methods.....	15
Results and Discussion.....	21
Interaction between Heme and Chloroquine	
Interaction between Heme and Quinine	
Interaction between Heme and X2	
Conclusion.....	26

4. OPTICAL SPECTROPHOTOMETRIC STUDIES OF THE INTERACTIONS BETWEEN TIN PROTOPORPHYRIN (SnPP) AND X ₂ , CHLOROQUINE, AND QUININE.....	36
Materials and Methods.....	36
Results and Discussion.....	37
Interaction between SnPP and Chloroquine	
Interaction between SnPP and Quinine	
Interaction between SnPP and X ₂	
Conclusion.....	39
5. KINETIC STUDIES OF THE INTERACTIONS BETWEEN SnPP AND ANTIMALARIAL AGENTS.....	48
Materials and Methods.....	48
Results and Discussion.....	49
Effect of Chloroquine and X ₂ to the Dimer Formation	
Process of SnPP	
Effect of Chloroquine and X ₂ to the Dimer Dissociation	
Process of SnPP	
Conclusion.....	51
6. NMR STUDY OF THE INTERACTION BETWEEN HEME AND X ₂	56
Materials and Methods.....	57

Results and Discussion.....	57
Interaction between Heme and X2 in Aqueous Solution	
Interaction between Heme and X2 in DMSO	
Conclusion.....	62
7. NMR STUDY OF THE INTERACTION BETWEEN SnPP AND X2.....	68
Materials and Methods.....	69
Results and Discussion.....	69
¹ H NMR Study of Interaction between SnPP and X2 in	
Aqueous solution by X2 Titrating into SnPP	
¹ H NMR Study of Interaction between SnPP and X2	
Aqueous solution by SnPP Titrating into X2	
¹ H NMR Study of Interaction between SnPP and X2 in	
DMSO	
¹¹⁹ Sn NMR Study of the Interaction between SnPP	
and X2 in Aqueous Solution	
Conclusion.....	84
8. NMR STUDY OF THE INTERACTION BETWEEN	
HEMATOPORPHYRIN IX AND X2.....	84
Materials and Methods.....	84
Results and Discussion.....	85

Conclusion.....	86
9. NMR STUDY OF THE INTERACTION BETWEEN ZINC PROTOPORPHYRIN AND X2.....	89
Materials and Methods.....	89
Results and Discussion.....	90
10. MODE OF ACTION FOR X2 AS AN ANTIMALARIAL AGENT.....	92
REFERENCE.....	96
APPENDIX PHOTODEGRADATION OF SnPP.....	99

LIST OF TABLES

TABLE	PAGE
1. Chemical shifts and coupling constants of the protons of hydroxyxanthonenes.....	8
2. Chemical shifts and coupling constants of the protons of methoxyxanthonenes.....	10
3. Chemical shifts and coupling constants of the protons of bromopropoxyxanthonenes.....	12
4. Chemical shifts and coupling constants of the protons of other xanthonenes.....	13
5. Apparent dissociation constants and Hill parameters obtained from optical titrations of heme with antimalarial agents.....	26
6. Apparent dissociation constants and Hill parameters obtained from optical titrations of SnPP with antimalarial agents.....	40
7. Apparent first order rate constant for SnPP dimer formation and dissociation at pH 5.8.....	51

LIST OF FIGURES

FIGURE	PAGE
1. 500 MHz ^1H spectrum of X2, DMSO.....	14
2. Optical titration of heme with chloroquine.....	28
3. Scatchard plots of heme-antimalarial agent associations.....	29
4. Hill plots of heme-antimalarial agent associations.....	30
5. Variation in the absorbance at 362 nm of heme with increasing concentration of chloroquine.....	31
6. Optical titration of heme with quinine.....	32
7. Variation in the absorbance at 362 nm of heme with increasing concentration of quinine.....	33
8. Optical titration of heme with X2.....	34
9. Variation in the absorbance at 362 nm of heme with increasing concentration of X2.....	35
10. Optical titration of SnPP with chloroquine.....	41
11. Scatchard plots of SnPP-antimalarial agent associations.....	42
12. Hill plots of SnPP-antimalarial agent associations.....	43
13. Variation in absorbance at 386 nm of SnPP with increasing concentration of chloroquine.....	44

14. Variation in the absorbance at 386 nm of SnPP with increasing concentration of quinine.....	45
15. Optical titration of SnPP with X2.....	46
16. Variation in the absorbance at 386 nm of SnPP with increasing concentration of X2.....	47
17. Optical spectra of the Soret region of SnPP dimer formation process.....	52
18. A plot of absorbance at 386 nm versus time for the SnPP dimer formation process.....	53
19. Optical spectra of the Soret region of SnPP dimer dissociation process.....	54
20. A plot of the absorbance at 386 nm versus time for SnPP dimer dissociation process.....	55
21. ^1H NMR spectrum of X2 as a function of heme addition in mole percent at pH 9.5.....	64
22. The high-field shifts of aromatic protons of X2 as a function of the molar fraction of heme at pH 9.5.....	65
23. ^1H NMR spectrum of X2 as a function of heme addition in mole percent at pH 11.5.....	66
24. ^1H NMR spectrum of X2 as a function of heme addition in mole percent in nonaqueous solution DMSO.....	67
25. ^1H NMR spectrum of SnPP as a function of X2 addition in mole percent	

at pH 7.2.....	75
26. ^1H NMR spectrum of SnPP as a function of X2 addition in mole percent at pH 9.5.....	76
27. ^1H NMR spectrum of SnPP as a function of X2 addition in mole percent at pH 11.5.....	77
28. ^1H NMR spectrum of X2 as a function of SnPP addition in mole percent at pH 9.5.....	78
29. The high-field shifts of aromatic protons of X2 as a function of the molar fraction of SnPP at pH 9.5.....	79
30. ^1H NMR spectrum of X2 as a function of SnPP addition in mole percent in DMSO nonaqueous solution.....	80
31. ^{119}Sn NMR spectrum of SnPP as a function of X2 addition in mole percent at pH 9.5.....	81
32. The dependence of induced shifts of the Sn resonance of SnPP on the concentration of X2 at pH 9.5.....	82
33. Proposed model for SnPP monomer-X2 complex.....	83
34. Proposed model for SnPP dimer-X2 complex.....	84
35. ^1H NMR spectrum of X2 as a function of hematoporphyrin IX addition in mole percent at pH 9.5.....	88

36. The high-field shifts of aromatic protons of X2 as a function of the molar fraction of hematoporphyrin IX at pH 9.5.....	89
37. ^1H NMR spectrum of X2 as a function of ZnPP addition in mole percent at pH 9.5.....	92
38. Proposed model for heme-X2 complex.....	95

CHAPTER 1

INTRODUCTION

Malaria has had an enormous impact on human history, and remains the most significant parasitic disease in tropical countries today. Forty percent of the world's population is at risk of malaria infection. Each year, 300 million people experience a malarial illness, and over 1 million individuals die, mostly children under 5 years of age.

Human malaria is caused by intracellular protozoa of the genus *Plasmodium*, of which *Plasmodium falciparum* is by far the most lethal, accounting for more than 95% of all malaria morbidity. The clinical symptoms of the disease are caused by *Plasmodium* parasites invading, growing, and replicating within host red blood cells in a 48-hour or 72-hour cycle, depending on the species of *Plasmodium* involved. During this period, up to 80% of the erythrocyte's hemoglobin (roughly 160 grams hemoglobin were consumed per 48 hour cycle in a patient with a 20% parasitemia) is degraded and ingested to provide amino acids as a source of nutrients for the parasite (Golberg, 1992; Olliaro, and Goldberg, 1995). This degradation, which occurs in an acidic organelle called the digestive, or food vacuole (pH range 4.8-5.4), releases large amounts of toxic heme. The parasite lacks a heme oxygenase and therefore cannot enzymatically cleave the porphyrin ring (Sherman, 1979; Slater, 1992). In its free state, heme can be an extremely toxic molecule, it appears to be toxic to cells by both free-radical (Meshnick et al, 1977) and non-free-radical pathways (Chou and Fitch, 1981). By aggregating heme into an insoluble and inert malaria pigment called hemozoin and storing it in acidic food vacuoles, the parasite rids itself a heme problem. Hemozoin, in fact, may become quite toxic to the host after it is released into the circulation. Upon

rupture of the mature schizont, hemozoin is then taken up by macrophages, where it appears to diminish phagocytic capacity (Schwartz et al., 1992) and alter immune cytokine secretion patterns (Prada et al., 1995).

The composition and mechanism of hemozoin synthesis are still controversial. Hemozoin was postulated by some to be a complex of heme and protein (Ashong, et al., 1989; Goldie et al., 1990) but many of the proteins found in hemozoin appear to be contaminants of isolation. Others have suggested that hemozoin is pure heme, but their purification procedures included treatment with proteases (Fitch and Kanjanangguopan, 1987). In another study, it was proposed that the heme of hemozoin may be in the form of β -hematin, a heme polymer with the carboxylate side-group of one heme linked to the central ferric iron of the next heme (Slater et al., 1991), but interpretation of this study is complex due to their use of a high concentration of a carboxylate buffer (acetate) in processing heme for polymer formation.

Malaria has been treated with quinolines such as chloroquine and quinine. The mode of action of these quinoline-based antimalarial drugs remains uncertain. It has been proposed that these drugs either raise the pH of the food vacuole (Homewood and Warhurst, 1972), thereby inhibiting hemoglobin proteolysis, or that they inhibit a putative heme polymerase enzyme, preventing hemozoin formation (Slater and Cerami, 1992). Another explanation is that they coordinate to the heme monomers, blocking the formation of hemozoin (Chou and Fitch, 1980), thus allowing a significant concentration of heme-antimalarial complex to remain in solution from where it exercises a plasmodiotoxic effect by catalyzing the formation of "active" oxygen species (Fitch et al., 1982). In light of the above considerations, it is clear that the nature of the interactions between heme and antimalarial drugs is of considerable relevance to the possible modes of action of such drugs. It appears that a primary

requirement of antimalarial drugs may be to bind to heme so as to inhibit its polymerization. Inhibition of heme polymerization by these drugs would then lead to a build-up of toxic heme.

The traditional antimalarial drugs have been successfully used for more than 45 years but, unfortunately, most *P. falciparum* strains have become resistant to chloroquine, and now multidrug resistance has developed in Southeast Asia and South America (White, 1992). As a result, there is a great need for development of novel antimalarial agents. Chloroquine resistance has been studied extensively and is thought to result from a decreased level of accumulation of this drug rather than an alteration of the drug or in the drug target (Slater, 1993). Therefore, inhibition of heme polymerization can still be the target for the development of novel drugs.

Recently, a new class of antimalarial agents (xanthenes) was discovered by the Riscoe group (Portland VA medical center). It is believed that the xanthenes form soluble complexes with heme. The investigators have demonstrated that the compounds interfere with the process of heme polymerization (Ignatushchenko et al., 1997). A possible model of heme-xanthone complexation was developed which suggests several significant interactions between heme and xanthenes: (1) between the heme iron and the carbonyl oxygen of xanthenes; (2) between the two planar aromatic systems; and (3) between the carboxylate side-groups of the heme and the 4- and 5-position hydroxyls of the xanthone. This model suggests that chemical modifications at the xanthone 4- and 5- positions which improve association with the heme carboxylate groups would result in greater antimalarial activity.

Several studies of the interactions between antimalarial drugs and heme have been reported. Initial studies of the interaction of chloroquine with heme were performed in neutral aqueous solution, and indicated a complex of chloroquine and

heme in a ratio of 1:2 (Chou and Fitch, 1980). It was assumed that binding occurred through the quinoline N-donor atom. Binding has subsequently been confirmed at the relatively high pH employed (Blauer and Ginsburg, 1982; Moreau et al., 1982; Moreau et al., 1985), but the mode of interaction appears to be π - π interaction between the aromatic ring systems of the drug and of the porphyrin. Qualitative experiments in benzene (Warhurst, 1987) indicated that interactions occurs between heme and quinine, cinchonine, mefloquine, and two synthetic antimalarial phenanthrene methanol and quinoline drugs; it was suggested that the quinine epimer, 9-epiquinine, was unable to bind heme. Detailed studies have been performed on the interaction of quinine and chloroquine with uroporphyrin I and Fe(III)-uroporphyrin I using ^{13}C -NMR spectroscopy (Constantinidis and Satterlee, 1988). That work showed that quinine coordinates Fe(III) via the 9-O atom, while a π - π complex is formed with a second uroheme I molecule. Chloroquine, on the other hand, binds to two uroheme I molecules by π - π complexation only.

The aim of this study is to investigate the potential use of an archetypal xanthone, 4,5-X2, as an inhibitor of the heme polymerization process. Thorough binding studies of interactions between heme, tin (IV) protoporphyrin IX (SnPP) and other heme analogs with X2 or the traditional drugs chloroquine and quinine by optical and NMR spectroscopic methods are presented here. SnPP was used because it is a well-behaved porphyrin over a broad pH range: in solution SnPP behaves as a slowly interconverting monomer-dimer system (heme aggregation is much less well-defined), and the equilibrium between monomer and dimer is pH dependent. Most importantly, SnPP, in contrast to heme (paramagnetic), is a diamagnetic porphyrin, so that it is less complex to study the binding of SnPP with drugs using NMR methods.

CHAPTER 2

CONFIRMATION AND CHARACTERIZATION OF XANTHONES

Xanthenes have been widely researched due to their pharmacological properties, mono-amine oxidase inhibition, *in vitro* cytotoxicity and *in vivo* antitumor activity (Hostettmann, 1989). The antimalarial property of xanthenes was recently recognized by Ignatushchenko, Winter and Riscoe group at the Portland VAMC. To date, 29 xanthone derivatives were synthesized by Dr. Winter to construct a structure-activity profile of xanthenes as inhibitors of heme polymerization and as antimalarial agents. ^1H NMR spectroscopy was used to determine the structure of these xanthenes and to assign aromatic protons by comparison with reference data and by analysis of spin-spin coupling. The analysis of the NMR data of these 29 xanthone derivatives is presented in this chapter.

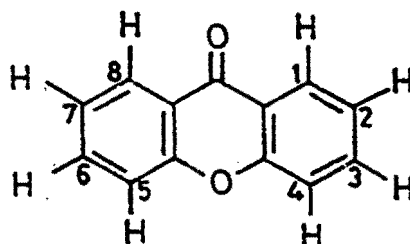
MATERIALS AND METHODS

All xanthenes were synthesized by Dr. Rolf Winter from the Veterans Affairs Medical Center, Portland, OR, and used as supplied. DMSO- d_6 was used as the solvent for all hydroxyxanthenes, and chloroform- d was used as solvent for all methoxyxanthenes and bromopropoxyxanthenes. Spectra of the xanthenes were acquired with the zgpr pulse sequence (relaxation delay- 90°_x -FID) on a Nicolet NT-500 MHz spectrometer equipped with Tecmag Libra interface to a Macintosh computer, and a 5 mm ^1H probe at 25 °C, operating at 500 MHz. Spectra were

referenced against internal Me₄Si (0.00 ppm). All ¹H NMR spectra were processed with MacNMR (Tecmag, TX, v.5.3).

RESULTS AND DISCUSSION

The xanthone skeleton with the notation of Pople, Schneider, and Bernstein (Pople et al., 1959) is shown below.



Chemical shifts and coupling constants of all proton signals of the xanthenes can be analyzed by first-order methods. Figure 1 shows the NMR spectrum of 4,5-hydroxyxanthone (X2) as an example. At 500 MHz, the signals corresponding to the symmetric sets of aromatic protons are well resolved. It has been previously shown (Martin et al., 1965) that the protons at the 1 and 8 position of xanthone skeleton give rise to signals at lowest field because they are deshielded by the ortho ring carbonyl group. So, the signal from H1 and H8 is assigned as an ortho-split doublet ($J=7.8$ Hz) with a small meta coupling ($J=1.9$ Hz) at 8.20 ppm; H2 and H7 give rise to a pseudo triplet at 7.88 ppm due to the coupling of ortho-ortho proton 1(8) and 3(6) ($J=7.8$ Hz), and H3 and H6 give rise to a signal at 7.93 ppm as a doublet of doublets due to the coupling of ortho proton H2 ($J=7.8$ Hz) and meta proton H7 ($J=1.9$ Hz). The chemical shifts and coupling constants for hydroxyxanthone, methoxyxanthone and other xanthenes are listed in Table 1, Table 2, Table 3, and Table 4, respectively.

These assignments were made mainly on the basis of the literature of similar xanthonenes (Barraclough et al., 1970).

Table 1 Chemical shift and coupling constant of the protons of hydroxyxanthenes.

Compound	H1	H2	H3	H4	H5	H6	H7	H8	OH
3-hydroxyxanthone	d,8.06 ppm J=8.8 Hz	dd,6.93 ppm J=8.8 Hz 1.9 Hz		d,6.89 ppm J=1.9 Hz	d,7.61 ppm J=8.8 Hz	t,7.83 ppm J=7.8 Hz 1.9 Hz	t,7.45 ppm J=7.8 Hz	d,8.16 ppm J=7.8 Hz	10.99ppm
2,5-dihydroxyxanthone	d,7.50 ppm J=2.9 Hz		dd,7.35 ppm J=8.8 Hz 2.9 Hz	d,7.59 ppm J=8.8 Hz		dd,7.32 ppm J=7.8 Hz 1.9 Hz	t,7.25 ppm J=7.8 Hz	dd,7.62 ppm J=7.8 Hz 1.9 Hz	10.17ppm
3,4-dihydroxyxanthone	d,7.59 ppm J=8.8 Hz	d,6.96 ppm J=8.8 Hz			dd,7.65 ppm J=8.8 Hz 0.9 Hz	t,7.84 ppm J=7.8 Hz 1.9 Hz	t,7.45 ppm J=7.8 Hz 0.9 Hz	dd,8.17 ppm J=7.8 Hz 1.9 Hz	10.40ppm 9.60ppm
3,5-dihydroxyxanthone	d,8.04 ppm J=8.8 Hz	dd,6.91 ppm J=8.8 Hz 1.9 Hz		d,6.91 ppm J=1.9 Hz		dd,7.28 ppm J=7.8 Hz 1.9 Hz	t,7.23 ppm J=7.8 Hz	dd,7.58 ppm J=7.8 Hz 1.9 Hz	10.94ppm 10.32ppm
1,3,5-trihydroxyxanthone		d,6.22 ppm J=1.9 Hz		d,6.43 ppm J=1.9 Hz		dd,7.32 ppm J=7.8 Hz 1.9 Hz	t,7.26 ppm J=7.8 Hz	d,7.55 ppm J=7.8 Hz	11.06ppm 10.43ppm
3,4,5-trihydroxyxanthone	d,7.55 ppm J=8.8 Hz	d,6.94 ppm J=8.8 Hz				d,7.29 ppm J=7.3 Hz	t,7.25 ppm J=7.3 Hz	dd,7.58 ppm J=7.3 Hz	10.33ppm 9.93ppm 9.43ppm

Continuation of Table 1

Compound	H1	H2	H3	H4	H5	H6	H7	H8	OH
3,4,6-trihydroxyxanthone	d,7.52 ppm J=8.8 Hz	d,6.91 ppm J=8.8 Hz			d,6.90 ppm J=1.9 Hz		dd,6.88 ppm J=8.8 Hz 1.9 Hz	d,7.99 ppm J=8.8 Hz	10.81 ppm 10.32 ppm 9.33 ppm
2,3,4,5-tetrahydroxyxanthone	s,7.05 ppm					dd,7.26 ppm J=7.8 Hz 1.9 Hz	t,7.23 ppm J=7.8 Hz	dd,7.57 ppm J=7.8 Hz 1.9 Hz	9.87 ppm 9.68 ppm 9.42 ppm
2,3,4,6-tetrahydroxyxanthone	s,7.04 ppm				s,6.86 ppm		dd,6.85 ppm J=7.8 Hz 1.9 Hz	d,7.98 ppm J=7.8 Hz	10.73 ppm 9.27 ppm 9.61 ppm 9.34 ppm
1,3,5,6-tetrahydroxyxanthone		s,6.17 ppm		s,6.41 ppm			d,6.93 ppm J=8.8 Hz	d,7.50 ppm J=8.8 Hz	13.12 ppm 10.92 ppm 10.54 ppm 9.44 ppm

Table 2 Chemical shift and coupling constant of the protons of methoxyxanthenes

Compound	H1	H2	H3	H4	H5	H6	H7	H8	OCH3
1-methoxyxanthone	d,7.72 ppm J=1.9 Hz		dd,7.32 ppm J=8.8 Hz 2.9 Hz	d,7.44 ppm J=8.8 Hz	d,7.43 ppm J=8.8 Hz	dd,7.69 ppm J=8.8 Hz 2.9 Hz	t,7.37 ppm J=7.8 Hz	dd,8.34 ppm J=8.8 Hz 1.9 Hz	3.92 ppm
3-methoxyxanthone	d,8.22 ppm J=8.8 Hz	dd,6.90 ppm J=8.8 Hz 2.9 Hz		d,6.83 ppm J=1.9 Hz	d,7.41 ppm J=7.8 Hz	t,7.66 ppm J=7.8 Hz 1.9 Hz	t,7.34 ppm J=7.8 Hz	dd,8.30 ppm J=7.8 Hz 1.9 Hz	3.90 ppm
2,5-dimethoxyxanthone	d,7.70 ppm J=2.9 Hz		dd,7.34 ppm J=8.8 Hz 2.9 Hz	d,7.56 ppm J=8.8 Hz		d,7.13 ppm J=7.8 Hz	t,7.44 ppm J=7.8 Hz	d,8.24 ppm J=7.8 Hz	4.04 ppm
3,4-dimethoxyxanthone	d,8.10 ppm J=8.8 Hz	d,7.03 ppm J=8.8 Hz			d,7.59 ppm J=7.8 Hz	t,7.72 ppm J=7.8 Hz 1.9 Hz	t,7.38 ppm J=7.8 Hz	dd,8.33 ppm J=7.8 Hz 1.9 Hz	4.04 ppm 4.02 ppm
3,5-dimethoxyxanthone	d,8.24 ppm J=8.8 Hz	dd,6.95 ppm J=8.8 Hz 1.9 Hz		d,7.01 ppm J=1.9 Hz		d,7.22 ppm J=7.8 Hz	t,7.29 ppm J=7.8 Hz	dd,7.90 ppm J=7.8 Hz 1.9 Hz	4.03 ppm 3.92 ppm
1,3,5-trimethoxyxanthone		d,6.35 ppm J=1.9 Hz		d,6.63 ppm J=1.9 Hz		d,7.16 ppm J=7.8 Hz	t,7.24 ppm J=7.8 Hz	dd,7.87 ppm J=7.8 Hz 1.9 Hz	4.02 ppm 3.97 ppm 3.90 ppm

Continuation of Table 2

Compound	H1	H2	H3	H4	H5	H6	H7	H8	OCH ₃
3,4,5-trimethoxyxanthone	d,8.07 ppm J=8.8 Hz	d,7.02 ppm J=8.8 Hz				dd,7.2 ppm J=7.8 Hz 1.9 Hz	t,7.28 ppm J=7.8 Hz	dd,7.88ppm J=7.8 Hz 1.9 Hz	4.12 ppm 4.03 ppm 4.01 ppm
3,4,6-trimethoxyxanthone	d,8.07 ppm J=8.8 Hz	d,7.00 ppm J=8.8 Hz			d,6.99 ppm J=1.9 Hz		dd,6.94ppm J=8.8 Hz 1.9 Hz	d,8.23 ppm J=8.8 Hz	4.04 ppm 4.01 ppm 3.94 ppm
1,3,5,6-tetramethoxyxanthone		d,6.35 ppm J=1.9 Hz		d,6.60 ppm J=1.9 Hz			d,6.95 ppm J=8.8 Hz	dd,8.03ppm J=8.8 Hz	4.02 ppm 3.99 ppm 3.97 ppm 3.92 ppm
2,3,4,5-tetramethoxyxanthone	s,7.49 ppm					dd,7.23ppm J=7.8 Hz 1.9 Hz	d,7.30 ppm J=7.8 Hz	dd,7.89ppm J=7.8 Hz 1.9 Hz	4.15 ppm 4.07 ppm 4.04 ppm 3.97 ppm
2,3,4,6-tetramethoxyxanthone	s,7.51 ppm				d,6.96 ppm J=1.9 Hz		dd,6.95 J=8.8 Hz 1.9 Hz	d,8.23 ppm J=8.8 Hz	4.08 ppm 4.06 ppm 3.97 ppm 3.94 ppm

Table 3 Chemical shift and coupling constant of the protons of bromopropoxy xanthenes

Compound	H1	H2	H3	H4	H5	H6	H7	H8	other protons
4,5-bis(δ -bromopropoxy)xanthone $R=CH_2CH_2Br$	dd,7.98ppm $J=7.8$ Hz 2.9 Hz	t,7.31 ppm $J=7.8$ Hz		dd,7.32 ppm $J=7.8$ Hz 2.9 Hz		dd,7.32ppm $J=7.8$ Hz 2.9 Hz	t,7.31 ppm $J=7.8$ Hz	dd,7.98ppm $J=6.84$ Hz 2.9 Hz	O- $\underline{CH_2}$ -CH ₂ t,4.56 ppm $J=6.8$ Hz - $\underline{CH_2}$ -Br t,3.83 ppm $J=5.9$ Hz
3,6-bis(δ -bromopropoxy)xanthone $R=CH_2CH_2CH_2Br$	dd,7.93ppm $J=7.8$ Hz 1.9 Hz	t,7.31 ppm $J=7.8$ Hz	dd,7.28ppm $J=7.8$ Hz 1.9 Hz			dd,7.28ppm $J=7.8$ Hz 1.9 Hz	t,7.31 ppm $J=7.8$ Hz	dd,7.93ppm $J=7.8$ Hz 1.9 Hz	O- $\underline{CH_2}$ -CH ₂ t,4.32 ppm $J=5.8$ Hz - $\underline{CH_2}$ -Br t,3.76 ppm $J=6.8$ Hz CH ₂ - $\underline{CH_2}$ - CH ₂ q,2.47 ppm $J=6.8$ Hz 5.8 Hz
4,5-bis(δ -bromopropoxy)xanthone $R=CH_2CH_2CH_2Br$	d,8.23 ppm $J=8.8$ Hz	dd,6.93 ppm $J=8.8$ Hz 1.9 Hz		d,6.87 ppm $J=1.9$ Hz	d,6.87 ppm $J=1.9$ Hz		dd,6.93 ppm $J=8.8$ Hz 1.9 Hz	d,8.23 ppm $J=8.8$ Hz	O- $\underline{CH_2}$ -CH ₂ t,4.23 ppm $J=5.8$ Hz - $\underline{CH_2}$ -Br t,3.63 ppm $J=5.8$ Hz CH ₂ - $\underline{CH_2}$ - CH ₂ q,2.39 ppm $J=6.8$ Hz 5.8 Hz

Table 4 Chemical shift and coupling constant of the protons of other xanthone

Compound	H1	H2	H3	H6	H7	H8	other protons
4,5-diacetoxy-xanthone 4,5 side chain=OCOCH ₃	d,8.22 ppm J=6.8 Hz	t,7.39 ppm J=7.8 Hz	dd,7.52 ppm J=7.8 Hz 1.9 Hz	dd,7.52 ppm J=7.8 Hz 1.9 Hz	t,7.39 ppm J=7.8 Hz	d,8.22 ppm J=6.8 Hz	OCOCH ₃ s,2.44 ppm
xanthone-4,5-bis-(oxyacetic acid) 4,5 side chain=OCH ₂ COOH	d,7.76 ppm J=7.8 Hz	t,7.37 ppm J=7.8 Hz	d,7.42 ppm J=7.8 Hz	d,7.42 ppm J=7.8 Hz	t,7.37 ppm J=7.8 Hz	d,7.76 ppm J=7.8 Hz	-OCH ₂ COOH s,4.98 ppm -OCH ₂ COOH s,13.19 ppm
xanthone-4,5-bis-ethoxyacete 4,5 side chain of xanthone =OCH ₂ COOCH ₂ CH ₃	dd,7.98 ppm J=7.8 Hz 1.9 Hz	t,7.29 ppm J=7.8 Hz	dd,7.25 ppm J=7.8 Hz 1.9 Hz	dd,7.25 ppm J=7.8 Hz 1.9 Hz	t,7.29 ppm J=7.8 Hz	dd,7.979 J=7.82 1.96	O-CH ₂ -CO s,4.90 ppm O-CH ₂ -CH ₃ q,4.31 ppm J=6.8 Hz 7.8 Hz O-CH ₂ -CH ₃ t,1.31 ppm J=6.8 Hz
4,5-bis-(N,N-diethylaminomethyl)-xanthone 4,5 side chain of xanthone =CH ₂ N(CH ₂ CH ₃) ₂	dd,8.25 ppm J=7.3 Hz 1.4 Hz	t,7.38 ppm J=7.3 Hz	dd,7.96 ppm J=7.3 Hz 1.4 Hz	dd,7.96 ppm J=7.3 Hz 1.4 Hz	t,7.38 ppm J=7.3 Hz	dd,8.25 ppm J=7.3 Hz 1.4 Hz	O-CH ₂ -N s,4.016 N-CH ₂ -CH ₃ q,2.701 J=7.3 Hz 5.8 Hz N-CH ₂ -CH ₃ t,1.128 J=7.33

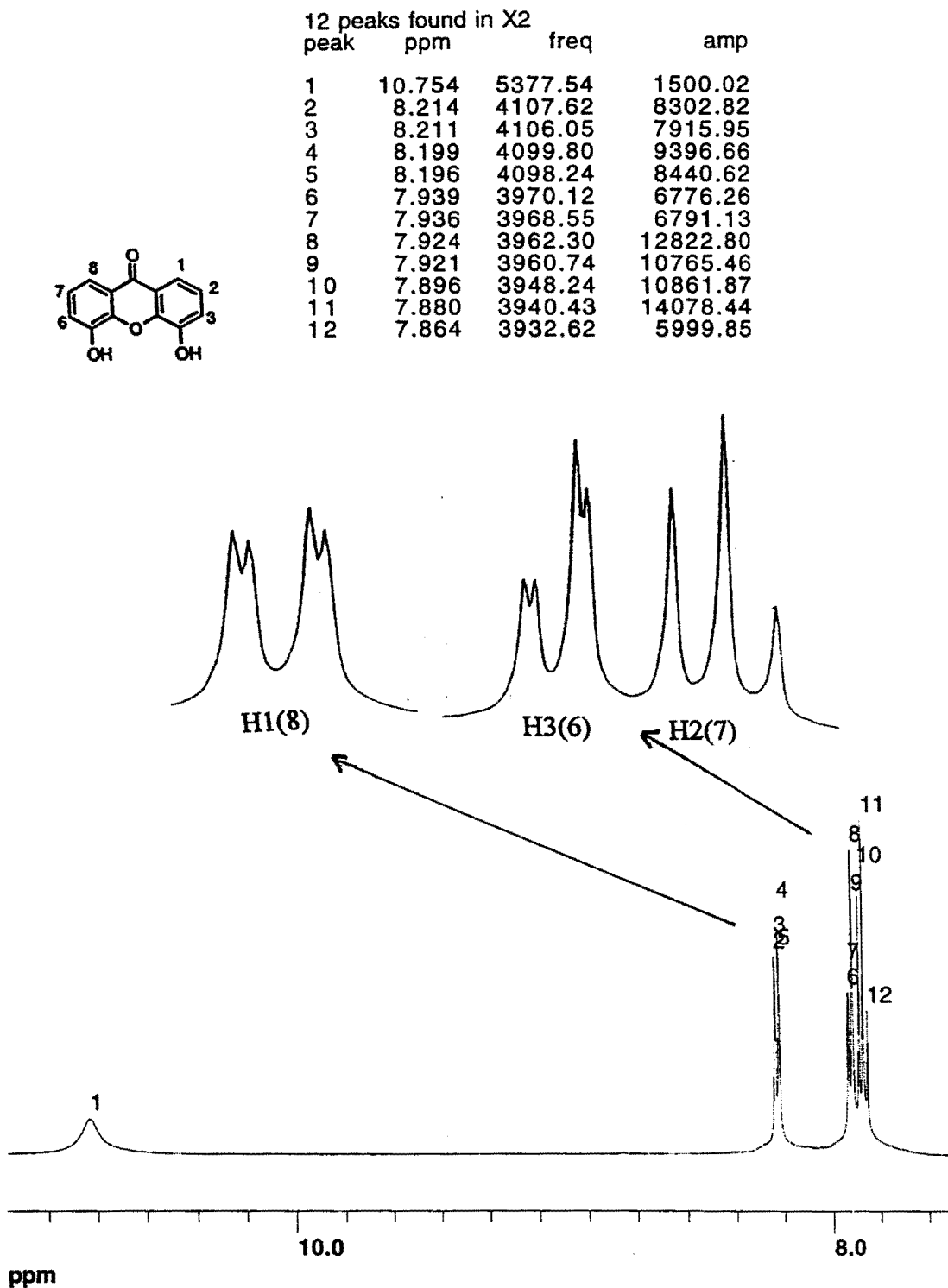


Figure 1. 500 MHz ^1H spectrum of X2 in DMSO solution.

CHAPTER 3

OPTICAL SPECTROPHOTOMETRIC STUDIES OF THE INTERACTIONS BETWEEN HEME AND X2, CHLOROQUINE, AND QUININE

The interactions of certain antimalarial drugs such as chloroquine, quinine, and X2 with heme were investigated by optical methods presented in this chapter. The motivation for this study is twofold. First, previous studies of this type in aqueous solution have been done at pH values at or above 7.5; conditions which do not reflect malaria physiological conditions. Second, although an aqueous environment is more relevant to the physiological chemistry of malaria drug chemotherapy, an extremely interesting study was performed in nonaqueous solution (Behere and Goff, 1984). In an attempt to clarify further the aqueous chemistry of antimalarial drugs in the presence of heme, we chose to study the interactions of these drugs with heme at pH 5.8. Previous work partly characterized the aggregation dynamics of heme (White, 1978), making it possible to derive equilibrium constants, stoichiometry, and Hill parameters by UV-visible methods. The choice of pH 5.8 as an appropriate value was made for its physiological relevance to the acidic food vacuole.

MATERIALS AND METHODS

X2 was synthesized by Dr. Rolf Winter, chloroquine diphosphate (Aldrich) was a gift from Dr. Riscoe, and quinine sulfate dehydrate was purchased from Aldrich. The stock solution of heme was made by dissolving 1.4 mg hemin chloride into distilled water with a minimum amount of 5% NaOH and incubated at room

temperature for at least 30 min to ensure maximal dissolution toward the monomer. Stock solutions of 1 mM X2, chloroquine, and quinine were freshly made in distilled water with a minimum amount of 5% NaOH. The heme stock solution was diluted to 10 μ M with 0.02 M phosphate buffer (pH 5.8) just prior to use. Titrations with X2, chloroquine, and quinine were performed by successive addition of aliquots of their stock solution to the 10 μ M heme solution. Repeated monitoring of the pH throughout all procedures was accomplished with a Radiometer Copenhagen pH meter 26, using an Ingold electrode. In general, once the solution pH was stabilized by appropriate adjustment of the pH by addition of minimum amount of NaOH or HCL solutions before the titration, it remained stable throughout the data collection operation. UV-visible spectroscopy was carried out on a Varian-Cary 3E spectrophotometer using 1 cm quartz cuvettes. All UV-visible spectra data were converted from SPC (Varian-Cary) data to Excel (Microsoft) data with Gram 386 software (Galactic Industries), and then processed with Excel 5.0 software (Microsoft). Absorbance readings and concentrations were corrected for dilution effects, as with all plotted spectra. Equilibrium binding studies were carried out according to Scatchard plot (Cantor and Schimmel, 1980), Hill plot (Van Holde, 1971), direct plot, and nonlinear least-squares analyses (Connors, 1980).

In order to understand the graphical analyses of binding studies between heme and each drug, it is necessary to explain these methods as follows. The basic binding process can be elucidated by the following equation:



in which P represents porphyrin, D represents the antimalarial drug, and n represents the number of D molecules bound to the porphyrin. The dissociation constant is defined as

$$K_d = \frac{[P][D]}{[PD]} \quad (2)$$

For the simplest case where $n=1$, K_d is the dissociation constant of the porphyrin-drug complex, $[P]$ is the concentration of free porphyrin, $[D]$ is the concentration of free drug, and $[PD]$ is the concentration of bound porphyrin.

It is convenient to consider the fraction of porphyrin sites occupied by drug, ν , which can be given by $\nu = \Delta A / \Delta A_{\max}$, where ΔA is the optical change measured.

Then we have

$$\nu = \frac{[PD]}{[PD] + [P]} \quad (3)$$

If equation (2) is solved for $[PD]$ and substitute for $[PD]$ in equation (3), one obtains

$$\nu = \frac{[D]}{K_d + [D]} \quad (4)$$

A plot of ν versus $[D]$ yields a hyperbola, yet it is not easy to decide by this plot binding details such as n or K_d , so it is better to rearrange equation (4) to produce a function that yield a linear graph, such as a Scatchard plot or Hill plot.

Scatchard Plot (Cantor and Schimmel, 1980)

Equation (4) can be readily rewritten as follows:

$$\frac{v}{[D]} = \frac{1}{K_d} - \frac{v}{K_d} \quad (5)$$

A graph of $v/[D]$ versus v is called the Scatchard plot, and it should be linear in this simple 1:1 binding system. A Scatchard plot is found to be particularly useful in the extension of this treatment to multi-site binding, as I outline next.

In a multi-site binding system, if all the binding sites are equivalent and independent of each other, there is no way in which a drug molecule, binding to such a site, can “know” that it is binding to a system that is somehow attached to other sites. The fraction of all the sites in the system that are occupied is v/n (since there are v sites occupied per molecule, out of a total of n sites per molecule). Therefore equation (4) can be extended to

$$v = \frac{n[D]}{K_d + [D]} \quad (6)$$

Then equation (5) can be easily rewritten for this simple case of multiple binding,

$$\frac{v}{[D]} = \frac{n}{K_d} - \frac{v}{K_d} \quad (7)$$

A Scatchard plot of $v/[D]$ versus v will produce a straight line with slope $-(1/K_d)$, and a y-intercept of n/K_d . If the Scatchard plot proves to be curved rather than linear, this may mean that more than one class of sites are present, or there is cooperativity.

Clearly, this plot provides a simple and convenient way to obtain a dissociation constant that characterizes the binding equilibrium.

Hill Plot (Van Holde, 1971):

If binding of a drug molecule to one site on a porphyrin influences the affinity of other sites, the binding is said to be *cooperative*. Such cooperativity can be *positive* (binding at one site increases the affinity of others) or *negative* (if the affinity of the other sites is decreased by binding at one site). In this type of multi-site binding system with interacting binding sites, K_d is defined as

$$K_d = \frac{[P][D]^n}{[PD_n]} \quad (8)$$

If ν again defined as the number of molecules of drug bound per molecule of porphyrin,

$$\nu = \frac{n[PD_n]}{[PD_n] + [P]} \quad (9)$$

we can solve equation (8) for $[PD_n]$, substitute this result for $[PD_n]$ in equation (9), and rearrange the result:

$$\nu = \frac{n[D]^n}{[D]^n + K_d} \quad (10)$$

to give

$$\frac{v}{v-n} = \frac{[D]^n}{K_d} \quad (11)$$

Equation (11) is usually simplified by noting that if θ is defined as the *fraction* of porphyrin sites occupied, then the *number* of occupied sites per porphyrin, v , becomes

$$v=n\theta \quad (12)$$

so that

$$\frac{v}{n-v} = \frac{\theta}{1-\theta} = \frac{[D]^n}{K_d} \quad (13)$$

Finally, by taking the log of both sides of equation (13), one finds

$$\log\left(\frac{\theta}{1-\theta}\right) = n\log[D] - \log K_d \quad (14)$$

so that a so called Hill plot of $\log(\theta/[1-\theta])$ versus $\log[D]$ should give a straight line of slope = n (In optical methods, θ can be simply derived from $\Delta A/\Delta A_{\max}$, in which ΔA is the optical change upon an addition of drug, and ΔA_{\max} is the optical change upon saturation with the drug.). In conclusion, Hill plots can be useful as diagnostic tests for the binding types:

1. If a straight line with slope of unity is found over the whole range, binding is noncooperative and the sites are identical.
2. If the slope of the Hill plot is not unity, the binding is highly cooperative, and the

slope of the Hill plot gives the number of interacting binding sites.

Direct plot methods and nonlinear least-squares calculation methods are discussed in the following section with example of heme-chloroquine binding, because of the convenient elucidation with graphic figures.

RESULTS AND DISCUSSION

Interaction between Heme and Chloroquine

The interaction between heme and chloroquine was characterized by an isosbestic point in the Soret region (near 400 nm) of the spectrum (Figure 2), the UV-visible spectra of heme-only solutions show a broad peak at 362 nm, indicating that principally μ -oxo dimer (White, 1978) or β -hematin is present at pH 5.8 (Slater et al., 1991), this pH was chosen because it is close to the physiological condition in the malaria food vacuole, yet does not lead to precipitation of heme from solution at required concentrations for UV-visible measurements. Chloroquine clearly perturbs the spectrum of heme, indicating that an interaction takes place between the drug and heme. Titrating increasing amounts of chloroquine into a solution of heme reduces the Soret molar absorptivity, and shifts the Soret band maximum to longer wavelength. There is also a small increase in intensity of the Q bands. Both absolute and difference methods were employed in this study (Figure 2A and B). The spectral changes of heme-chloroquine interaction are similar to those observed for molecular complex formation between various metalloporphyrins and other aromatic molecules with a cofacial π - π interaction between them (White, 1978). The loss of Soret band intensity is the consequence of coupling between the transition moments of the two aromatic systems.

A Scatchard plot of heme-chloroquine binding system is shown in Figure 3A. The result is a straight line with slope $1/K_d = 2.5 \times 10^5 \text{ M}^{-1}$ ($K_d = 3.9 \times 10^{-6} \text{ M}$); the linearity of the graph indicates that all of the binding sites on heme are equivalent and independent of each other.

The possibility of cooperativity of the heme-chloroquine complex was tested by the Hill plot method. This is shown in Figure 4A for heme-chloroquine association. The slope of this linear graph is 1.13 ($n \approx 1$), which is the Hill parameter, indicating the binding between chloroquine and heme is non-cooperative. In the cases under consideration here, the overall equilibrium interaction between drug and macrocycle dimer is studied by observing changes in the characteristic heme Soret band at 362 nm.

The direct binding curve as graphed as absorbance difference of heme at 362 nm versus the mole ratio of heme:chloroquine in the system is shown in Figure 5. In order to determine the stoichiometry of the heme-chloroquine complex, n was measured from the extrapolated intersection point of the initial rise and the plateau of the response. n was found to be one heme dimer binding with one chloroquine molecule, which is consistent with those reported in the very first heme-chloroquine binding study performed at pH 7.0 which employed by equilibrium dialysis (Chou and Fitch, 1980).

Since each mole of dimeric heme molecule was found to bind 1 mole of the chloroquine molecule, a nonlinear least-squares calculation from the equation (15) (shown below) that defines the equilibrium process for the 1:1 complex involving heme dimer was employed as the most accurate determination of K_d . Since n was found to be one for heme dimer-chloroquine interaction, dissociation equilibrium may be schematically represented as follows:

$$(\text{Hm})_2 + \text{Cq} = (\text{Hm})_2 \text{Cq} \quad (15)$$

where $(\text{Hm})_2$ represents heme dimer and Cq represents as chloroquine. Hence, the corresponding dissociation constant is

$$K_d = \frac{[(\text{Hm})_2][\text{Cq}]}{[(\text{Hm})_2 \text{Cq}]} \quad (16)$$

The absorbance (A) of dimeric heme solution at 386 nm with chloroquine being present can be considered as the sum of the free and bound dimeric heme contributions, according to the Beer-Lamber law

$$A = \varepsilon_{\text{Hm}_2} [(\text{Hm})_2] + \varepsilon_{(\text{Hm})_2 \text{Cq}} [(\text{Hm})_2 \text{Cq}] \quad (17)$$

The spectrum of dimeric heme was recorded before and after addition of constant volumes of chloroquine solution; the free dimeric heme spectrum was then subtracted from the adduct spectra, after correction for volume dilution.

Therefore,

$$\Delta A = A_n - A_0 \quad (18)$$

where A_n express the absorbance values at 362 nm after the n th addition. Since $C_{\text{Hm}2} = [\text{Hm}_2] + [(\text{Hm})_2 \text{Cq}]$ (and $C_{\text{Hm}2} = [\text{Hm}_2]$ in the absence of drug), one can write

$$\Delta A = (\varepsilon_{(\text{Hm})_2 \text{Cq}} - \varepsilon_{\text{Hm}_2}) [(\text{Hm})_2 \text{Cq}] = \Delta \varepsilon [(\text{Hm})_2 \text{Cq}] \quad (19)$$

Since $[Hm_2] = C_{Hm_2} - [(Hm)_2Cq]$, it follows that

$$[(Hm)_2Cq] = \frac{C_{Hm_2} [Cq]}{K_d + [Cq]} \quad (20)$$

Substituting Equation (20) into Equation (19) one has

$$\Delta A = \Delta \varepsilon \frac{C_{Hm_2} [Cq]}{K_d + [Cq]} = \frac{\Delta A_{\infty} [Cq]}{K_d + [Cq]} \quad (21)$$

where ΔA is the change in absorbance caused by a specific substrate concentration; ΔA_{∞} is the absorbance change at infinite substrate concentration; $[Cq]$ is the free substrate concentration.

ΔA values were correlated with the corresponding $[Cq]$ values using a direct fitting procedure (Figure 5, solid lines) in order to obtain K_d and ΔA_{∞} (from which it is possible to extract $\Delta \varepsilon$ once the analytical heme concentration is known).

K_d was found to be 4.7×10^{-6} M for the heme-chloroquine interaction, which is close to the result derived from the Scatchard plot (3.9×10^{-6} M), and consistent with a previous report performed with isothermal titration microcalorimetry at pH 7.0 (Dorn, 1998).

Interaction between Heme and Quinine

The spectrum of the complex between heme and quinine shows that the Soret band decreases in intensity, but does not shift position, yet a well defined isosbestic point was not observed. There is also a small increase in intensity of the Q band noted. Both absolute and difference methods (Figure 6) were employed in this study.

Scatchard plot of heme-quinine binding system is shown in Figure 3B, the slope of this linear graph, $1/K_d$ is $2.2 \times 10^5 \text{ M}^{-1}$ ($K_d = 4.5 \times 10^{-6} \text{ M}$), the linearity of the graph indicates that all the binding sites on heme are equivalent and independent to each other. The noncooperativity is further proved by Hill plot (Figure 4B), which shows the slope of the linear Hill plot as 1.2 ($n \approx 1$). The stoichiometry was found to be one dimeric heme to one quinine molecule according to the direct plot method described in previous section (Figure 7, broken lines).

Again, a nonlinear least-squares calculation from the equation that defines the equilibrium process for the 1:1 complex involving heme dimer was employed as the most accurate determination of K_d . The K_d was found to be $5.6 \times 10^{-6} \text{ M}$ (close to the result from the Scatchard plot) for the heme-quinine interaction (Figure 7, solid lines). The K_d found here is also similar to the result reported by Dorn et al. (1998) by isothermal titration microcalorimetry at pH 7.0.

Interaction between Heme and X2

In aqueous solution, the interaction of X2 with heme perturbs the UV-visible spectra of heme in the same way chloroquine does. Titration of heme with X2 produces spectra with similarly well defined isosbestic points in the Soret range (shown in Figure 8). The spectroscopic changes is largely a decrease in intensity of the heme Soret band. (The position of this loss in the Soret band maximum may indicate the loss of aggregated heme dimer). The apparent red shift of the Soret, which is induced by X2 binding, is characteristic of molecular complex between aromatic molecules and various metalloporphyrins (White, 1978).

The raw binding data were analyzed by the Scatchard, Hill, and direct, non-linear fitting graphic methods. The straight line in the Scatchard plot (Figure 3C, slope

$1/K_d = 2.0 \times 10^5 \text{ M}^{-1}$, $K_d = 5.0 \times 10^{-6} \text{ M}$), and the Hill parameter (Figure 4C, $n = 1.09 \approx 1$) indicate that X2 binding to heme is noncooperative. The 'breaking point' of direct plot indicate the one heme dimer to one X2 stoichiometry (Figure 9, broken lines), and the non-linear fitting graph leads to a $K_d = 5.1 \times 10^{-6} \text{ M}$ (Figure 9, solid lines).

CONCLUSION

Molecular complexes of heme with each antimalarial agent are formed in aqueous solution at pH 5.8, possibly due to the π - π interaction between the aromatic rings of drug and porphyrin ring of heme. The binding between each type appears to be noncooperative according to both Scatchard and Hill graphical methods. The stoichiometry of all above binding systems seems to involve one dimeric heme molecule with one antimalarial molecule. The values of K_d derived from non-linear fitting methods for all above binding equilibria are listed in Table 5. It should be noted that these K_d values reported here are strictly valid only under our conditions at pH 5.8.

Table 5. Apparent dissociation equilibrium constants and Hill parameter obtained from optical titrations of heme with antimalarial agents.

Binding System	K_d , M (app)	Hill parameter
Heme-Chloroquine	5.1×10^{-6}	1.1
Heme-Quinine	4.7×10^{-6}	1.2
Heme-X2	5.6×10^{-6}	1.1

I call attention to the similarity of the equilibrium constants and stoichiometry for heme-X2 with that determined for the binding of chloroquine and quinine to heme. It seems that heme binding with X2 behaves similarly to those with chloroquine and quinine, but the all the above analyses are somewhat ambiguous because of the aggregation behavior of heme under these experimental conditions. Thus a better-behaved heme analog needed to be investigated with these antimalarial agents under similar conditions. This is reported in the next chapters.

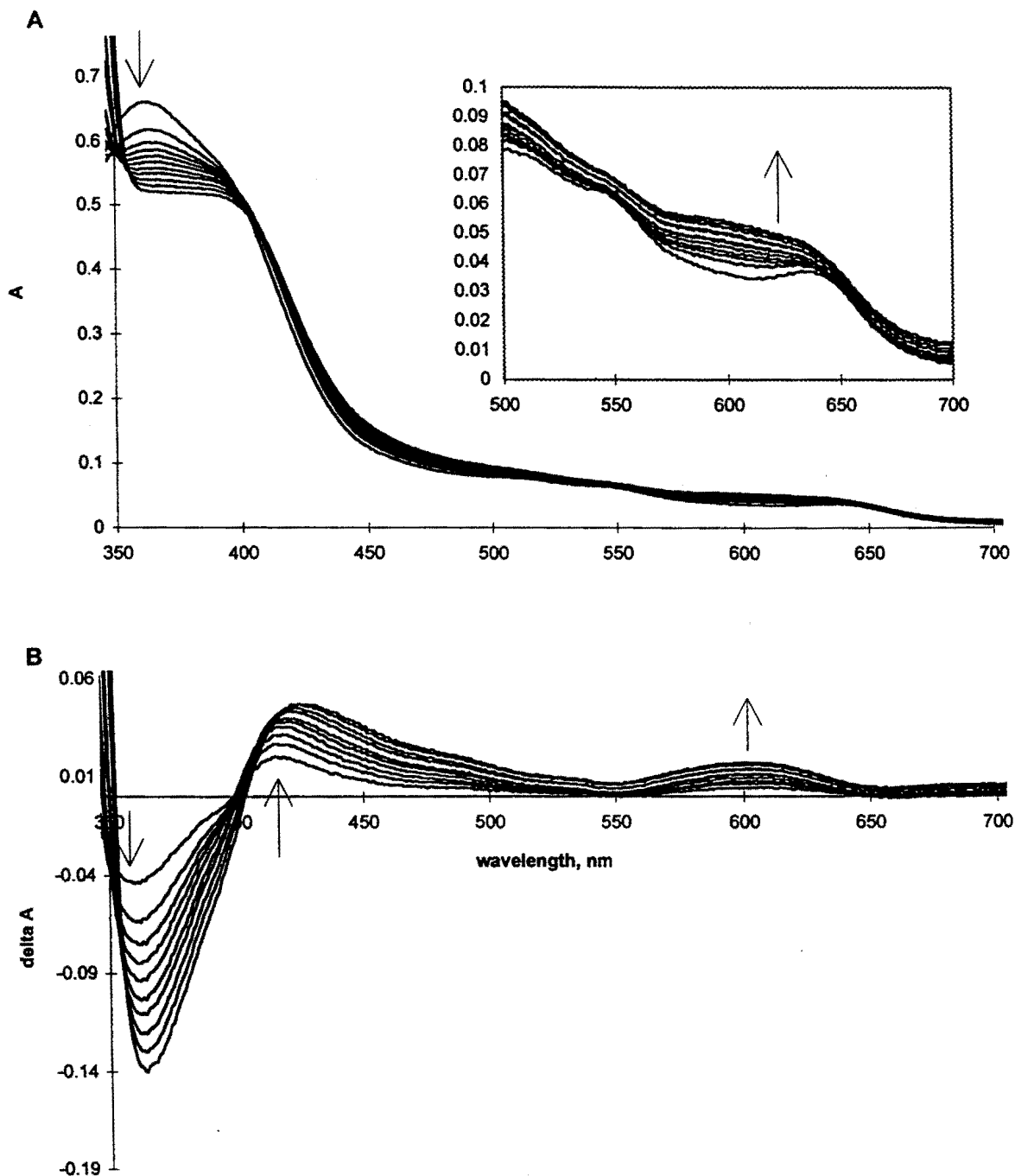


Figure 2. Optical titrations: heme-chloroquine spectroscopic changes, corrected for dilution, accompanying 2-300 μ l additions of 1 mM chloroquine to 10.0 μ M solution of heme. A: absolute spectra. B: difference spectra.

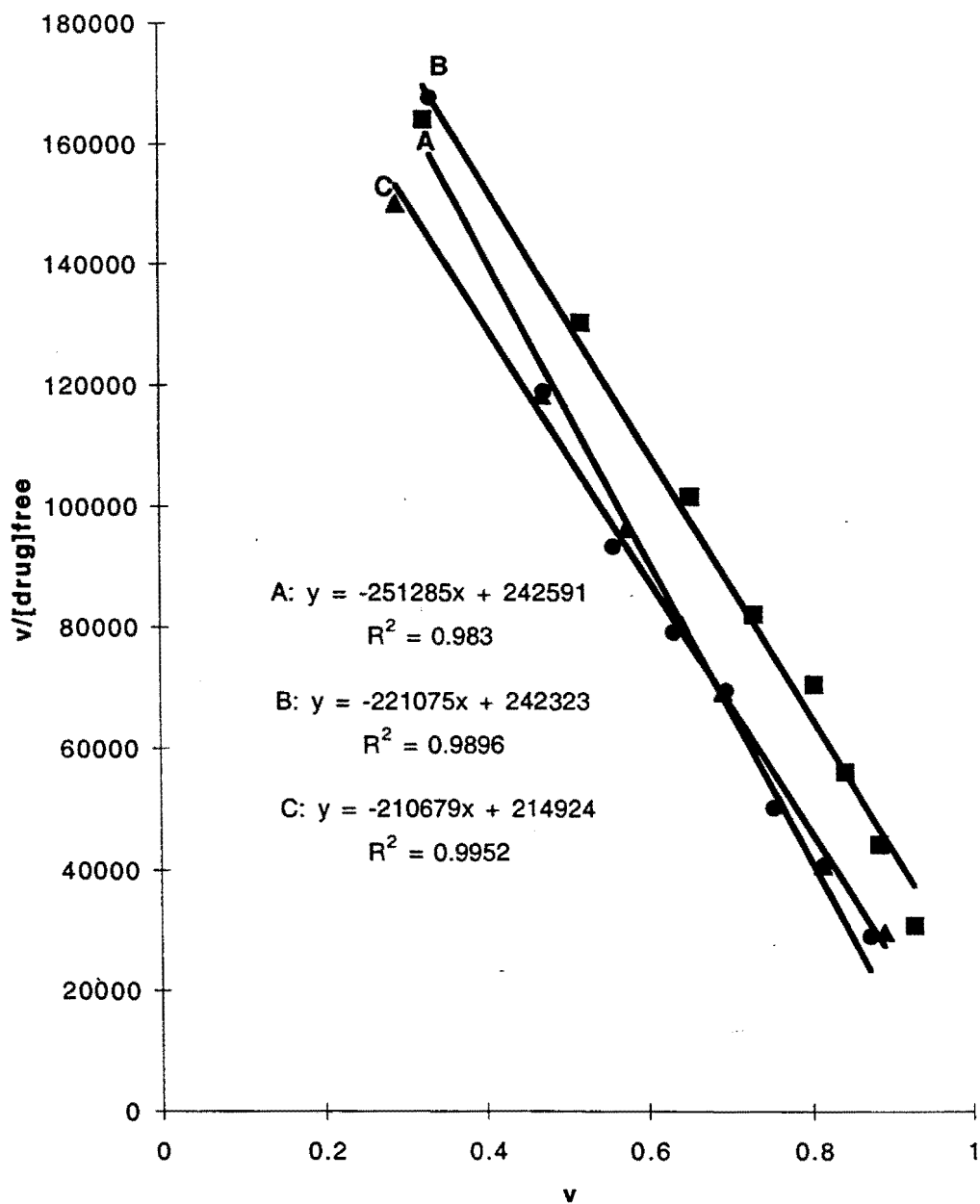


Figure 3. Scatchard plots of A: heme-chloroquine association, B: heme-quinine association, C: heme-X2 association at 362 nm, 10 μ M heme concentration, pH 5.8, 25 $^{\circ}$ C.

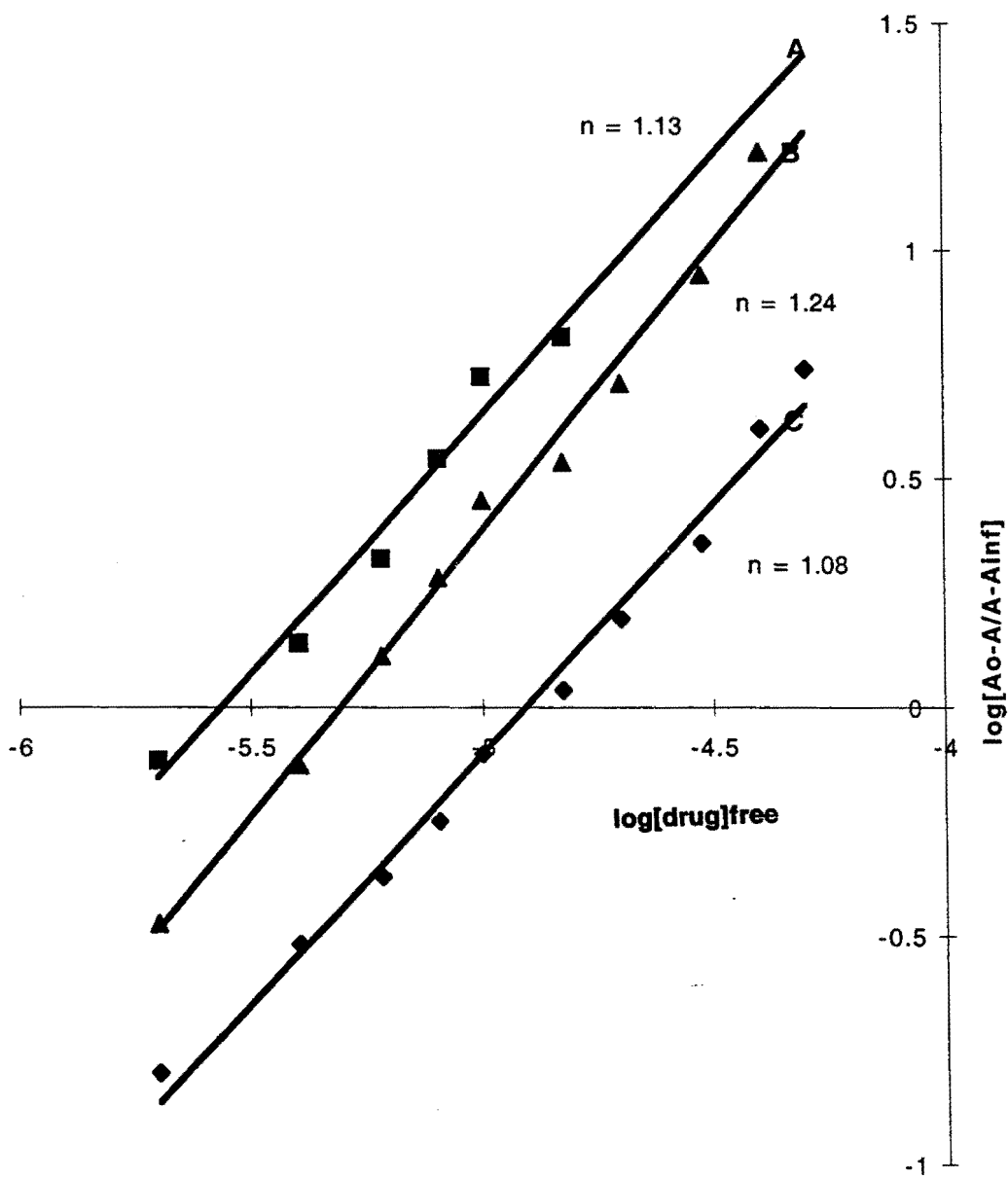


Figure 4. Hill plots of A: heme-chloroquine association, B: heme-quinine association, C: heme-X2 association at 362 nm, 10 μM heme concentration, pH 5.8, 25 $^{\circ}\text{C}$.

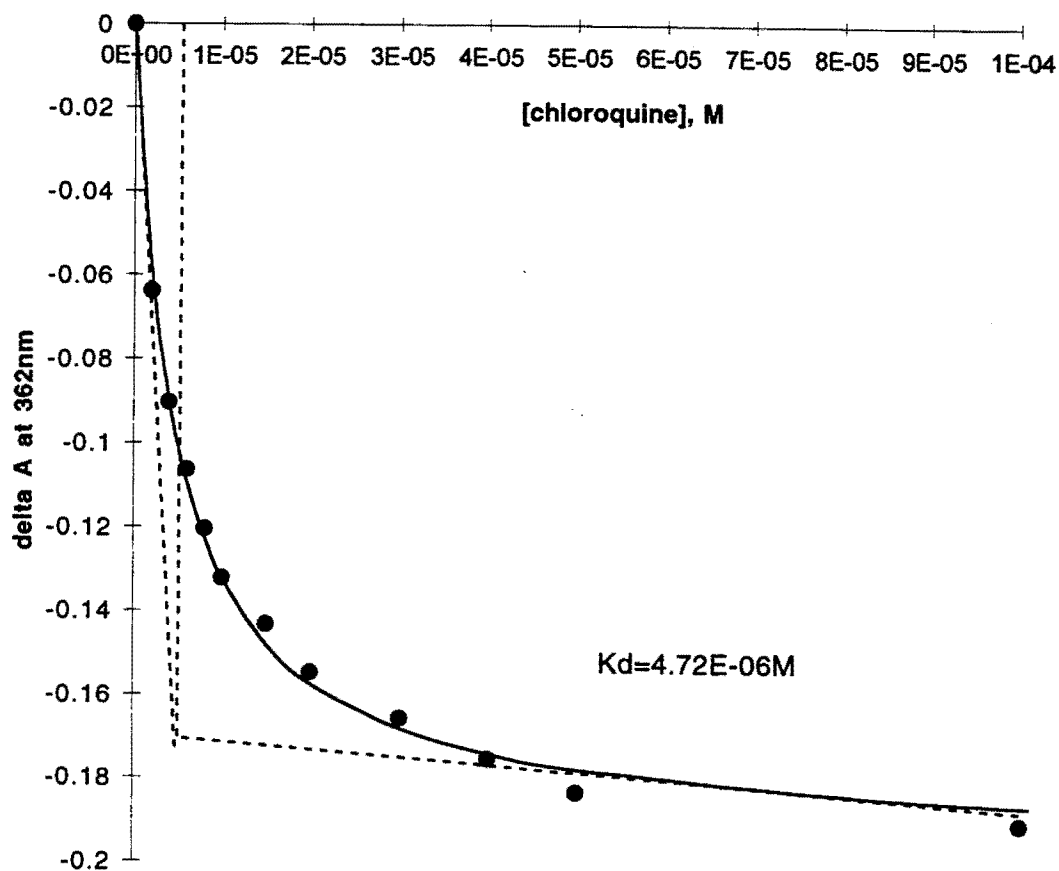


Figure 5. Variation in the absorbance at 362 nm of 10 μ M heme with increasing concentration of chloroquine, pH 5.8, 25 $^{\circ}$ C. The broken lines indicate the 'breaking point' of the plot, the solid lines is the least square fit to equation (21) of the text.

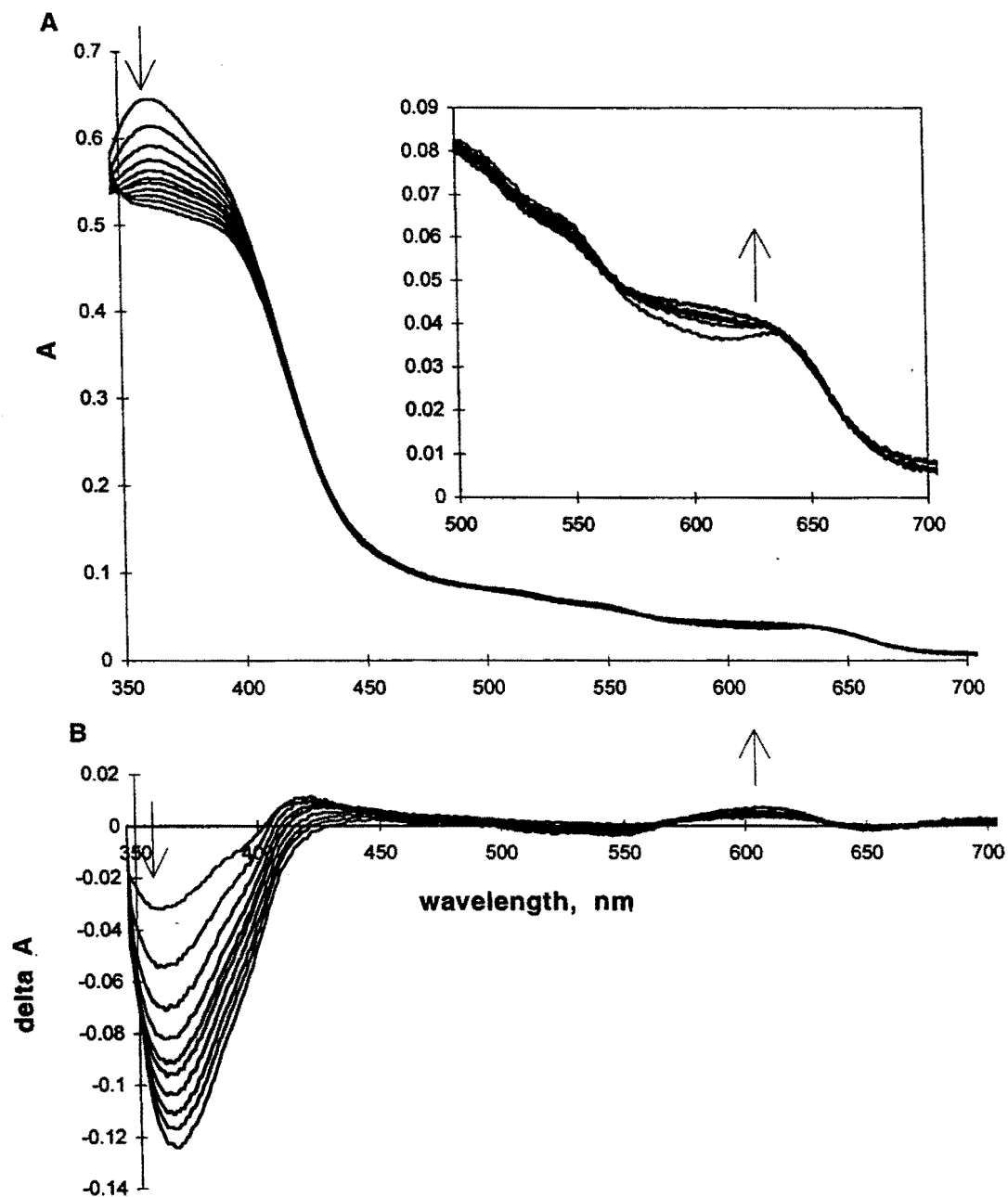


Figure 6. Optical titrations: heme-quinine spectroscopic changes, corrected for dilution, accompanying 2-300 μl additions of 1 mM quinine to 10.0 μM solution of heme. A: absolute spectra. B: difference spectra.

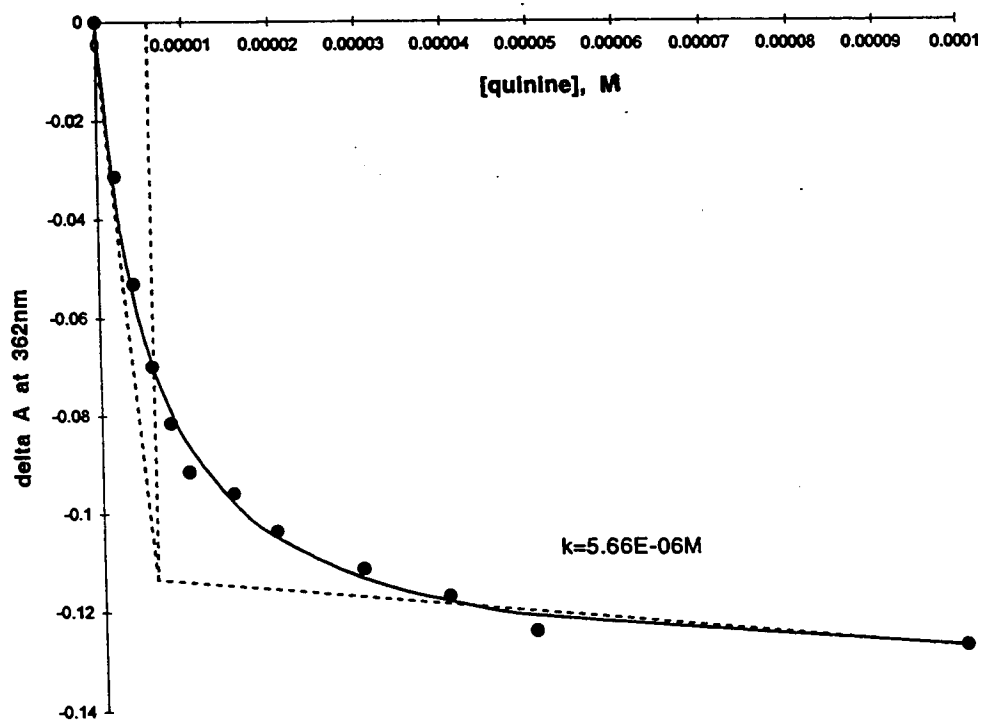


Figure 7. Variation in the absorbance at 362 nm of 10 μM heme with increasing concentration of quinine, pH 5.8, 25 $^{\circ}C$. The broken lines indicate the 'breaking point' of the plot, the solid lines is the least square fit to equation (21) of the text.

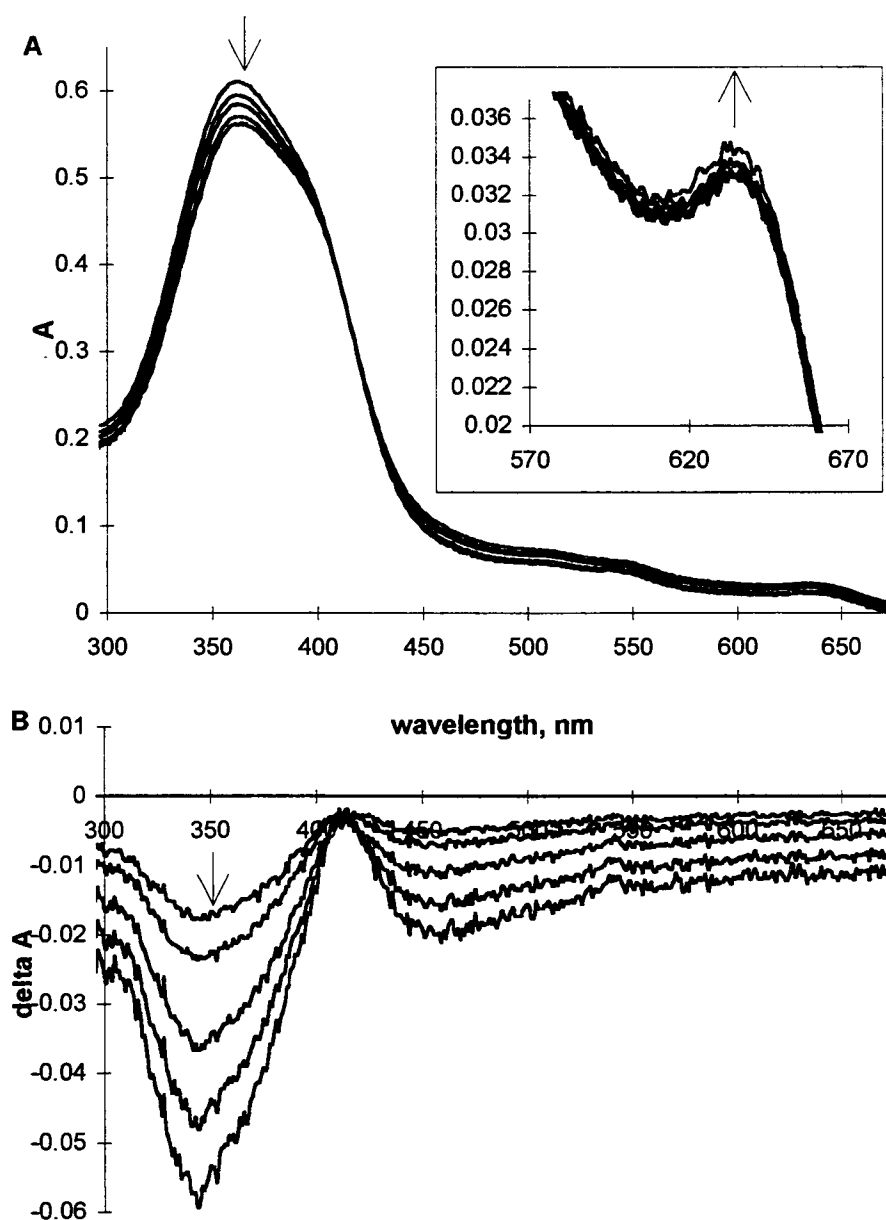


Figure 8. Optical titrations: heme-X2 spectroscopic changes, corrected for dilution, accompanying 2-300 μ l additions of 1 mM X2 to 10.0 μ M solution of heme. A: absolute spectra. B: difference spectra.

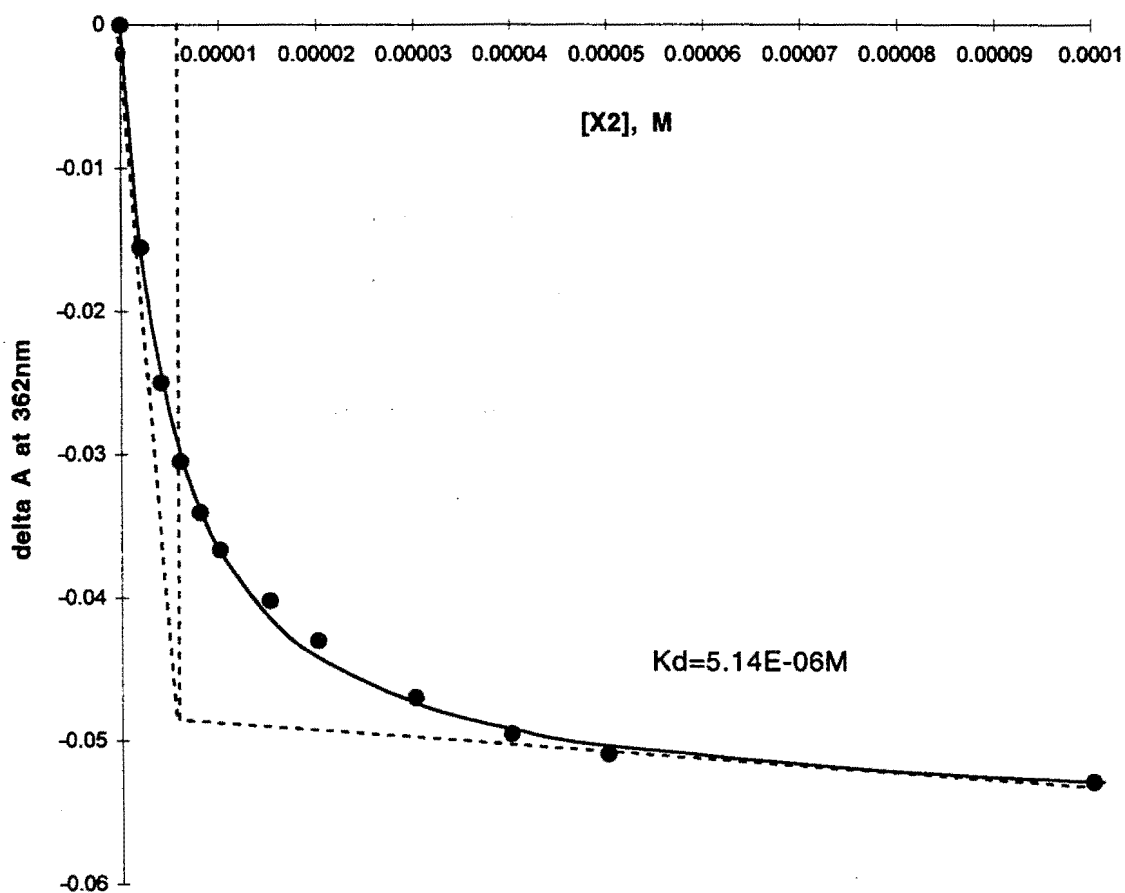


Figure 9. Variation in the absorbance at 362 nm of 10 μM heme with increasing concentration of X2, pH 5.8, 25 $^{\circ}\text{C}$. The broken lines indicate the 'breaking point' of the plot, the solid lines is the least square fit to equation (21) of the text.

CHAPTER 4

OPTICAL SPECTROPHOTOMETRIC STUDIES OF THE INTERACTIONS BETWEEN TIN PROTOPORPHYRIN (SnPP) AND X₂, CHLOROQUINE, AND QUININE

SnPP is a well-behaved porphyrin under varying conditions of pH. In solution SnPP behaves as a slowly interconverting monomer-dimer system, and the equilibrium between monomer and dimer is pH and concentration dependent (Breslow, 1986). Thus, SnPP makes a convenient model for binding studies with optical methods. Optical titrations of SnPP with chloroquine, quinine, and X₂ were performed, and equilibrium constants, stoichiometry, and Hill parameters were derived from the analyses of the experimental data by various graphical methods, including direct plots, Scatchard plots and Hill plots. Details are presented in this chapter.

MATERIALS AND METHODS

Optical titrations of SnPP with chloroquine, quinine, and X₂ were carried out as described in Chapter 3. The stock solution of SnPP was made by dissolving 1.4 mg SnPP chloride into distilled water with minimum amount of 5% NaOH and incubated at room temperature for at least 24 hours to allow the attainment of the monomer-dimer equilibrium of SnPP. All UV-visible spectra data were converted from SPC (Varian-Cary) data to Excel (Microsoft) data with Gram 386 software (Galactic Industries), and then processed with Excel 5.0 software (Microsoft). Absorbance readings and concentrations were corrected for dilution effects. Equilibrium binding

studies were carried out using Scatchard plots, Hill plots, direct plots, and nonlinear least-squares calculations.

RESULTS AND DISCUSSION

Interaction between SnPP and Chloroquine

At pH 5.8, SnPP primarily exists as dimer at 10 μ M (Breslow, 1986).

Although a slight amount of SnPP monomer remains in the solution, only two species (dimer and monomer) appear to be involved in the aggregation process as suggested by the presence of an isosbestic point. That is, in contrast to heme, higher aggregations are not present under these conditions.

The spectrum of the complex between SnPP and chloroquine shows that the Soret band decreases in intensity, but does not shift wavelength, so that a well defined isosbestic point was not observed (Figure 10). There is also a decrease in the intensities of both Q bands. These spectral changes of SnPP-chloroquine interaction are similar to those observed for molecular complex formation between several metalloporphyrins and aromatic molecules with a cofacial π - π interaction, as well as with heme (previous chapter). The loss of intensity of the Soret band and Q bands is a consequence of coupling between the transition moments of the two aromatic systems.

Scatchard, Hill, and direct plots were applied to the interaction between SnPP and chloroquine by monitoring the optical differences at 386 nm (the Soret band maximum of dimeric SnPP). A Scatchard plot of SnPP-chloroquine interaction is shown in Figure 11A. The result is a straight line with the slope $-1/K_d$ as $-9.9 \times 10^4 \text{ M}^{-1}$ ($K_d = 1.00 \times 10^{-5} \text{ M}$); the linearity indicates noncooperativity of binding. A Hill plot (Figure 12A) further demonstrates the noncooperativity of binding, as the Hill

parameter is found to be 1.09 ($n \approx 1$). The stoichiometry of this binding system appears to be one SnPP molecule binding with one chloroquine molecule (Figure 13, broken lines). This can be viewed as one SnPP dimer molecule binding with two chloroquine molecules, in which all the binding sites of SnPP for chloroquine are identical, and the non-linear fitting calculation using Equation (21) still could be applied for each of two independent sites, with each of the sites having the same binding constant. The result of the non-linear fitting is shown in Figure 13, solid line. The apparent K_d for SnPP-chloroquine association was found to be 1.1×10^{-5} M, which is close to the result derived from Scatchard plot (1.0×10^{-5} M).

Interaction between SnPP and Quinine

Like the optical spectral changes observed in the SnPP-chloroquine interaction, titrating increasing amounts of quinine into SnPP solution lowers Soret molar absorptivity and also gives a small decrease in intensity of the Q bands (data not shown). This indicates a π - π interaction between two molecules.

The slope of a linear Scatchard plot (Figure 11B) was found to be $-8.3 \times 10^4 \text{ M}^{-1}$, yielding $-1/K_d$ ($K_d = 1.2 \times 10^{-5}$ M), indicating noncooperativity of binding; the Hill parameter ($n = 1.03 \approx 1$) derived from a Hill plot (Figure 12B) also indicates that quinine binding to SnPP is a noncooperative process. A stoichiometry of one dimeric SnPP to one quinine was found by the 'breaking point' of a direct plot corresponding to the optical differences at 386 nm (Figure 14, broken lines); the most accurate K_d was derived from nonlinear least-square fitting process (Figure 14, solid line). The result is 1.3×10^{-5} M, which is close to that derived from Scatchard plot (1.2×10^{-5} M).

Interaction between SnPP and X2

Unlike the optical spectral changes seen on addition of chloroquine or quinine, titration of SnPP with increasing amounts of X2 induced the Soret band maximum shifting to longer wavelength. This was accompanied by a loss of intensity of the Soret band and a small decrease in intensity of the Q bands (Figure 15). The overall changes are similar to those with chloroquine and quinine, indicating the same type of π - π interaction occurred between two molecules.

The linearity of the Scatchard plot (Figure 11C) indicates that X2 binding to SnPP is a noncooperative process. The slope of the plot is $-8.5 \times 10^4 \text{ M}^{-1}$ which gives $K_d = 1.17 \times 10^{-5} \text{ M}$. A Hill plot (Figure 12C) shows a slope of 1.17 (≈ 1) as the Hill parameter, further demonstrating noncooperativity of the binding process. It also appears that one SnPP dimer molecule binds to two X2 molecules (Figure 16, broken lines), which is the same as the stoichiometry of the interactions of SnPP with chloroquine and quinine. The result from the nonlinear square fitting of SnPP-X2 binding system was found to be $1.1 \times 10^{-5} \text{ M}$ (Figure 16, solid lines), close to the result derived from Scatchard plot ($1.2 \times 10^{-5} \text{ M}$).

CONCLUSION

Molecular complexes of SnPP and each antimalarial agent are formed in aqueous solution at pH 5.8, possibly due to the π - π interaction between the aromatic ring of the drug and the porphyrin ring of SnPP. The binding between each type appears to be noncooperative according to Scatchard and Hill graphic methods. The stoichiometry of all the above binding systems seems to be one dimeric SnPP molecule binding to two antimalarial drug molecules. The values of K_d derived from non-linear

fitting method for all above binding equilibria are listed in Table 6. It should be noted that the K_d values reported here are strictly valid only under our conditions at pH 5.8.

Table 6. Apparent dissociation equilibrium constants and Hill parameter obtained from optical titrations of SnPP with antimalarial agents.

Binding System	K_d , M (app)	Hill parameter
SnPP-Chloroquine	1.1×10^{-5}	1.1
SnPP-Quinine	1.3×10^{-5}	1.0
SnPP-X2	1.1×10^{-5}	1.2

I call attention to the similarity of the equilibrium constants and stoichiometry for SnPP-X2 with that determined for the binding of chloroquine and quinine to heme. It seems that SnPP binding with X2 behaves similarly to those with chloroquine and quinine. It also should be noted that the binding of SnPP with these antimalarial agents appears to be weaker than those of heme with these compounds (Table 5). Therefore, the a more detailed mechanism of the binding process needed to be elucidated with a more powerful (structurally speaking) spectroscopic technique, such as NMR spectroscopy. The efforts of investigating the binding process of heme analogs with antimalarial agents by NMR are stated starting from Chapter 6.

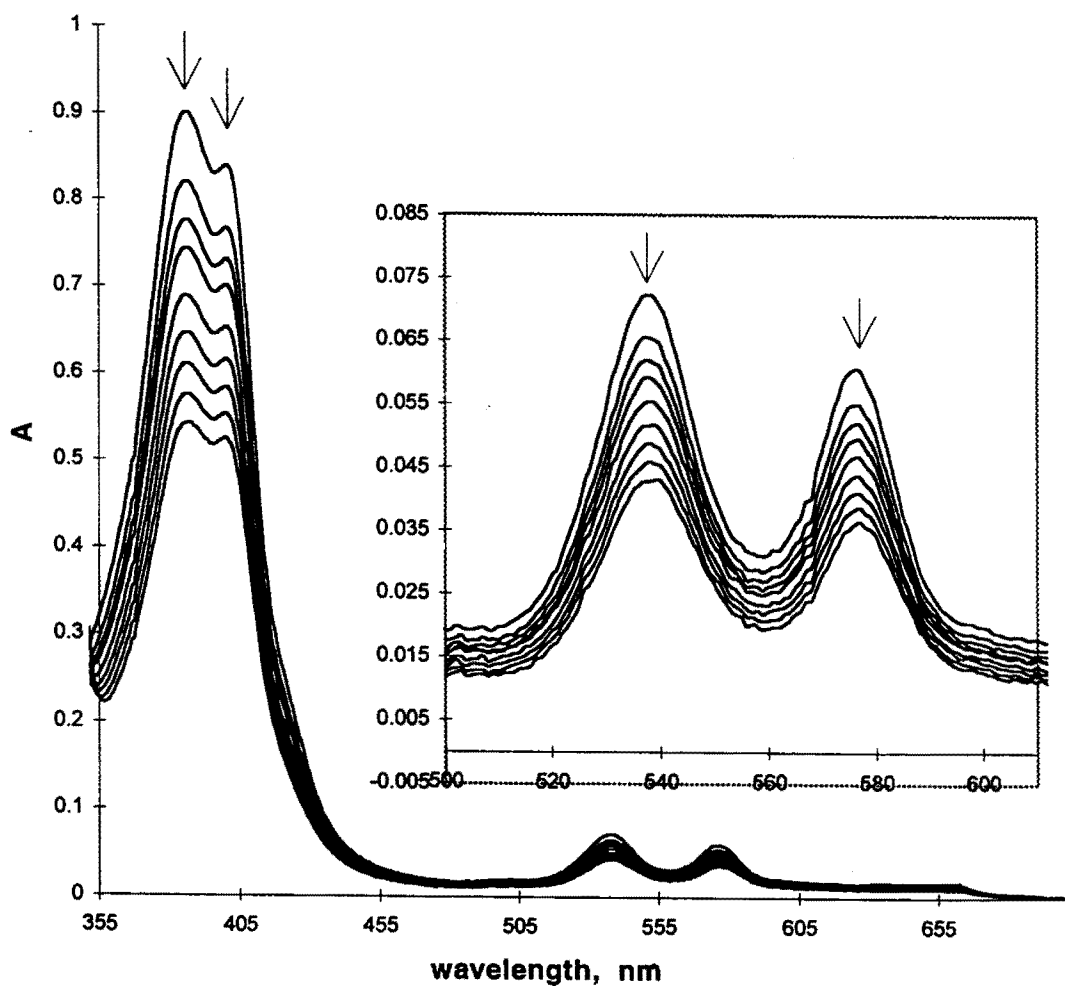


Figure 10. Optical titrations: SnPP-chloroquine spectroscopic changes, corrected for dilution, accompanying 2-300 μ l additions of 1 mM chloroquine to 10.0 μ M solution of SnPP. A: absolute spectra. B: difference spectra.

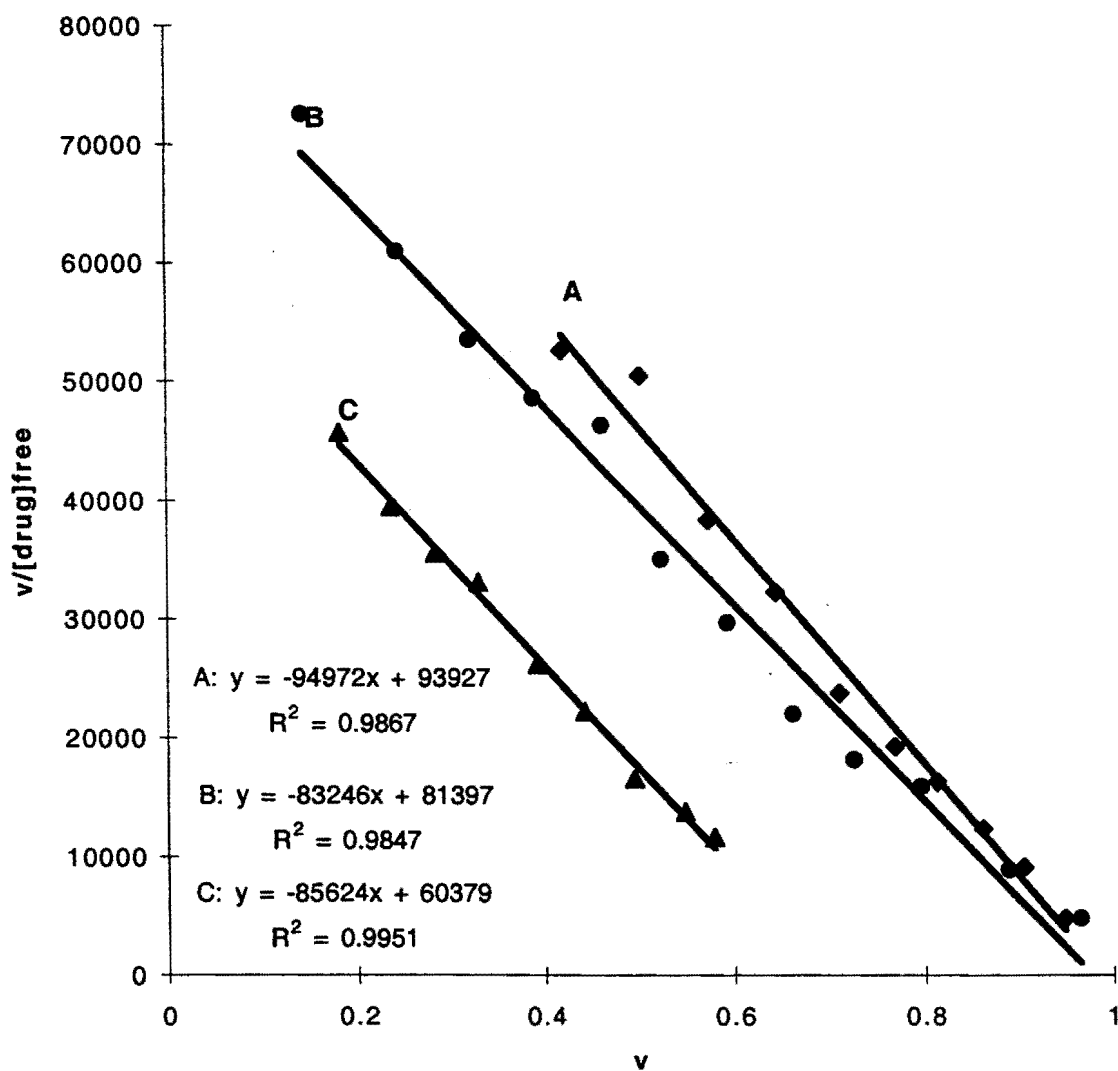


Figure 11. Scatchard plots of A: SnPP-chloroquine association, B: SnPP-quinine association, C: SnPP-X2 association at 386 nm, 10 μ M SnPP concentration, pH 5.8, 25 $^{\circ}$ C.

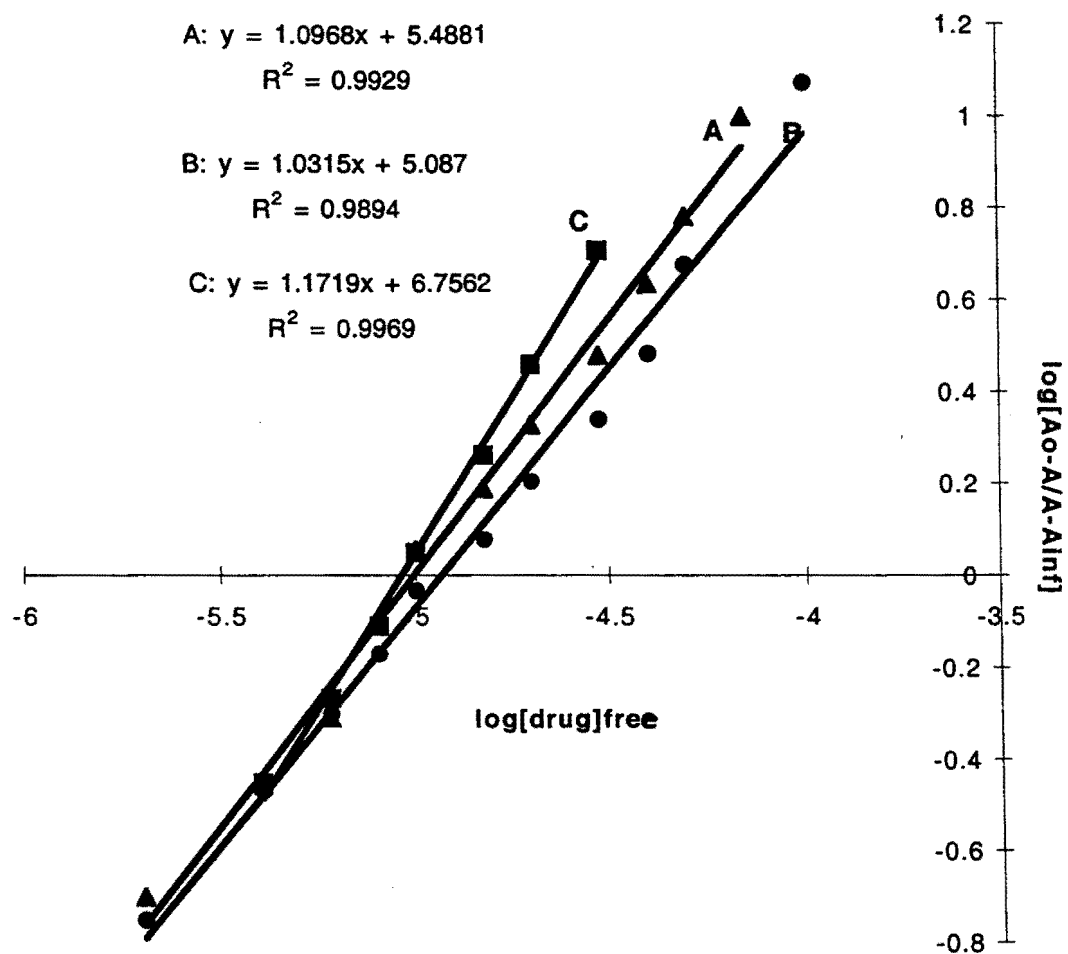
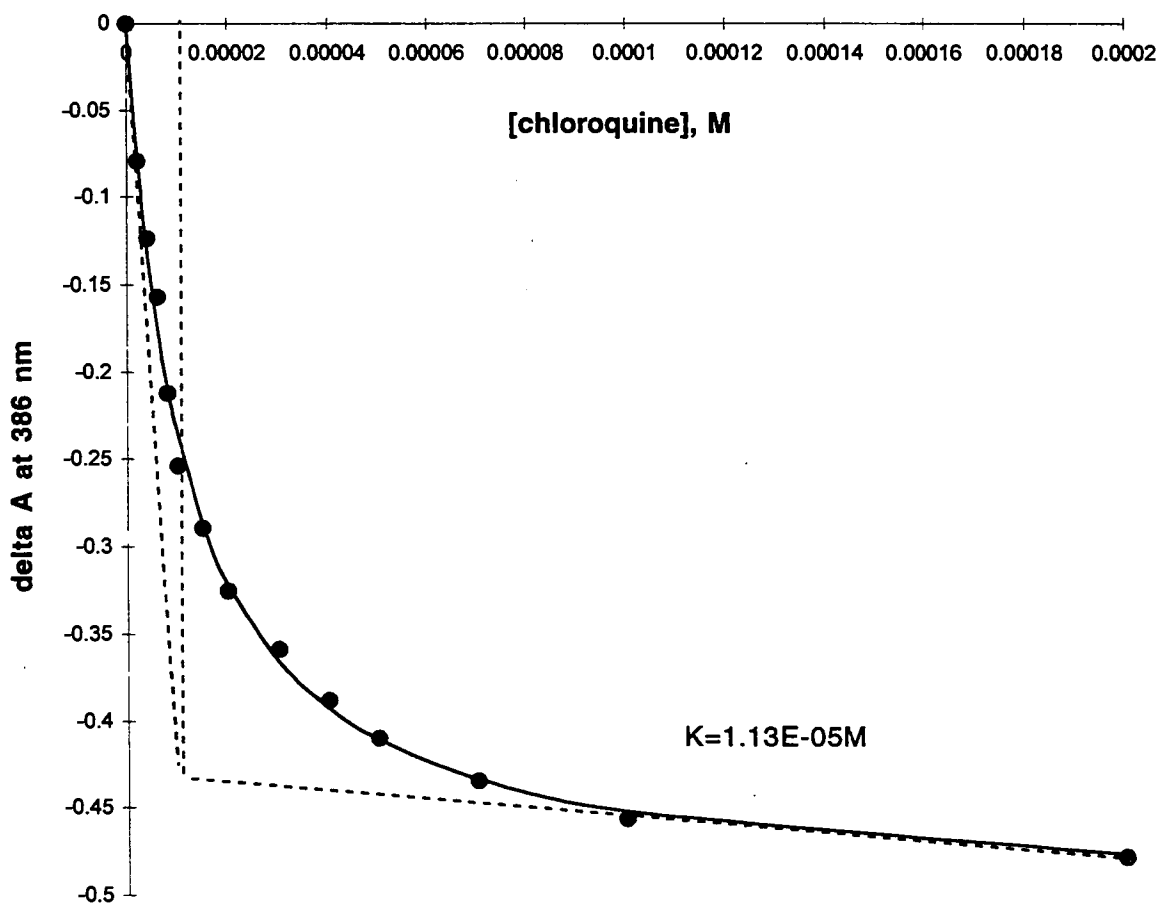


Figure 12. Hill plots of A: SnPP-chloroquine association, B: SnPP-quinine association, C: SnPP-X2 association at 386 nm, 10 μM SnPP concentration, pH 5.8, 25 $^{\circ}$



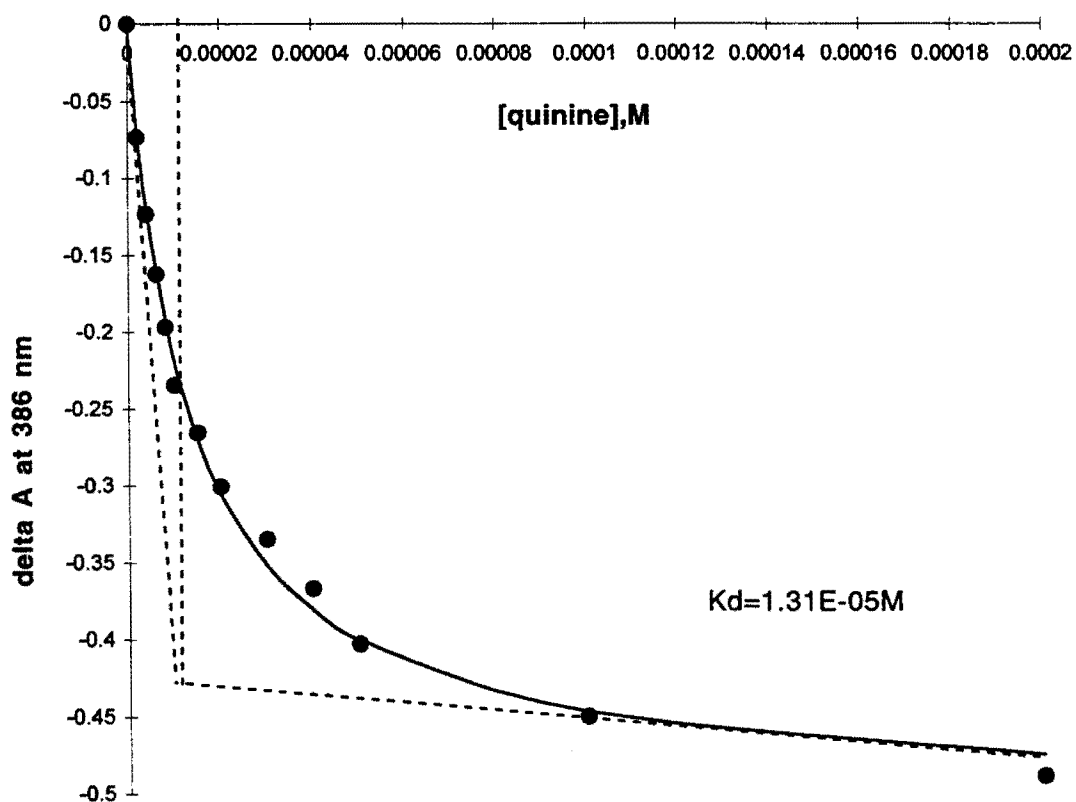


Figure 14. Variation in the absorbance at 386 nm of 10 μM SnPP with increasing concentration of quinine, pH 5.8, 25 $^{\circ}\text{C}$. The broken lines indicate the 'breaking point' of the plot, the solid lines is the least square fit to equation (21) of the text.

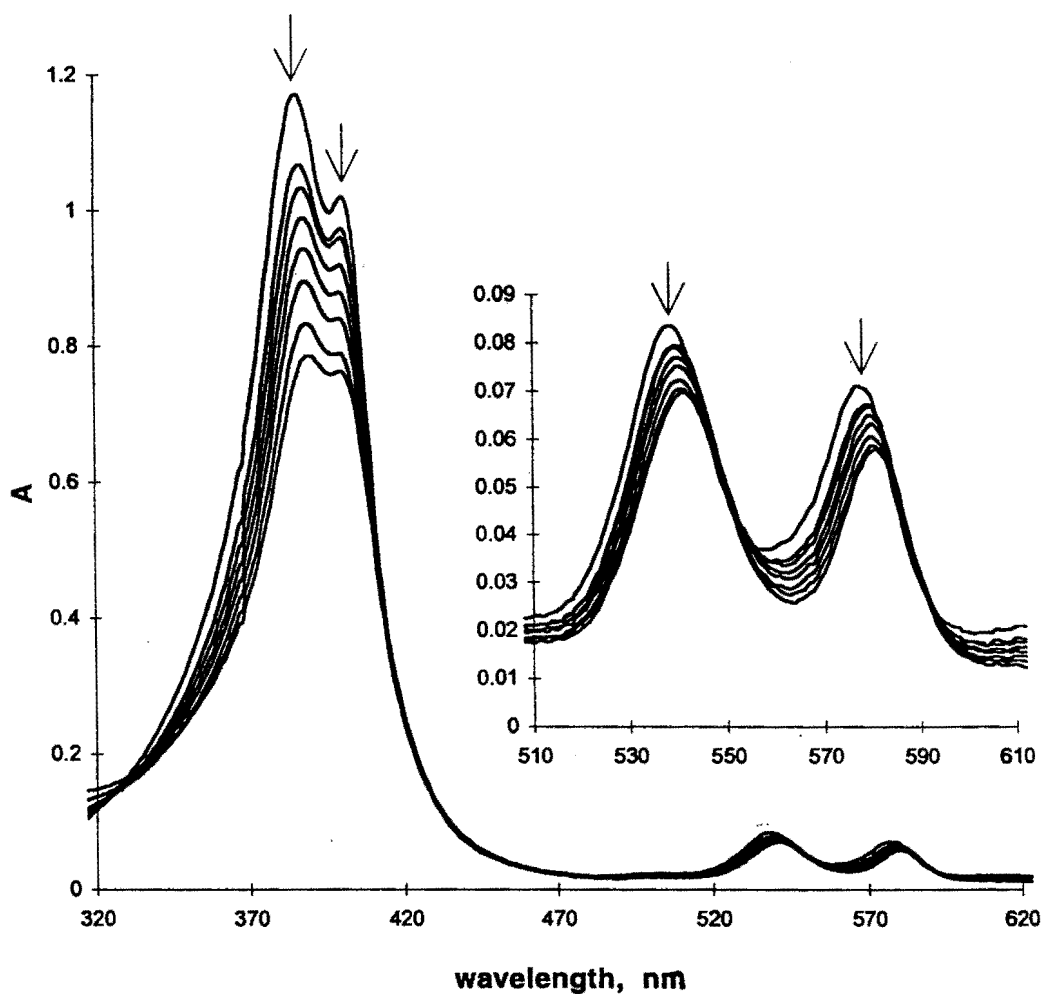


Figure 15. Optical titrations: SnPP-X2 spectroscopic changes, corrected for dilution, accompanying 2-300 μl additions of 1 mM X2 to 10.0 μM solution of SnPP. A: absolute spectra. B: difference spectra.

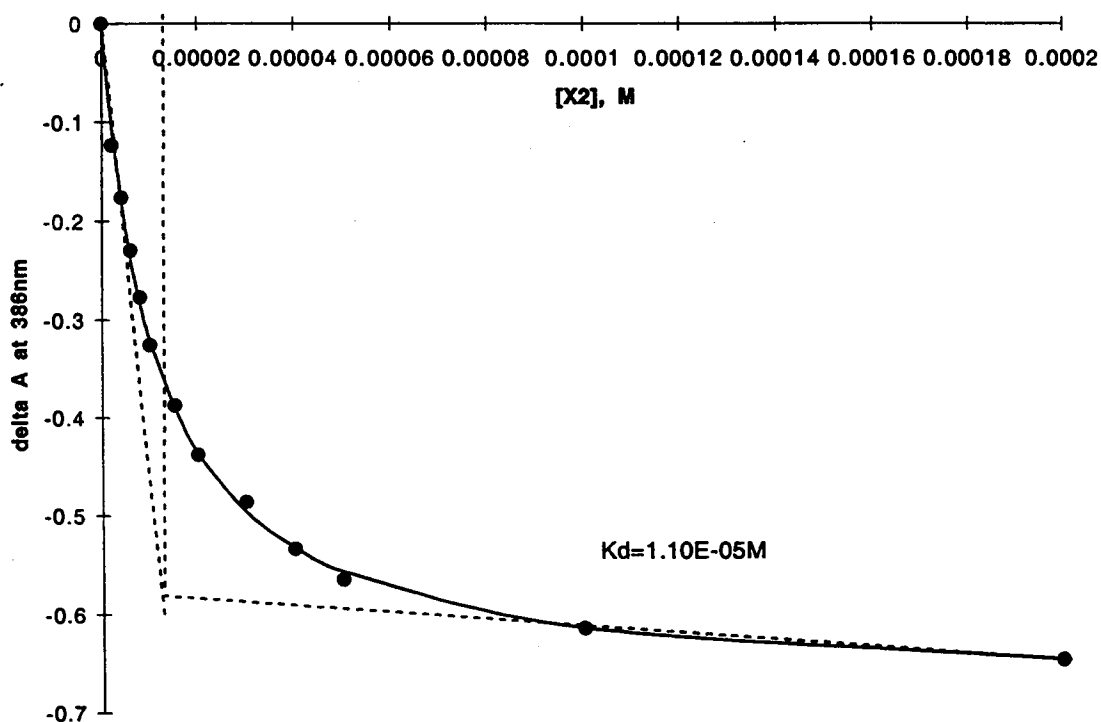


Figure 16. Variation in the absorbance at 386 nm of 10 μ M SnPP with increasing concentration of X2, pH 5.8, 25 $^{\circ}$ C. The broken lines indicate the 'breaking point' of the plot, the solid lines is the least square fit to equation (21) of the text.

CHAPTER 5

KINETIC STUDIES OF THE INTERACTIONS BETWEEN SnPP AND ANTIMALARIAL AGENTS

The conclusions derived from previous chapters indicate that chloroquine, quinine, and X2 bind heme or SnPP in aqueous solution at pH 5.8, and that these binding processes may alter the kinetic behavior of the porphyrin self-association. The investigation of the effects of binding between these antimalarial agents and SnPP on the kinetic behavior of SnPP is discussed in this chapter. SnPP was chosen because it is a well-behaved porphyrin under varying conditions of pH.

MATERIALS AND METHODS

Kinetic studies were performed with a Beckman Du-60 scanning spectrophotometer. Stock solutions of SnPP (1 mM) were prepared by dissolving the compound in H₂O with a few drops of 5% NaOH. For dimer formation processes, small aliquots of the stock solution of SnPP were diluted to pH 5.8 in phosphate buffer to a final concentration of 10 μ M. Optical spectra was measured immediately afterward (or after mixing with drugs to a 1:1 mole ratio) with a 32 second time intervals for total of six minutes. For monomer formation processes, dimeric SnPP (or a SnPP drug complex) formed from the above process was allowed to sit for 1 hour in order to allow the attainment of the dimer formation. The solution was then diluted to 1 μ M SnPP in the same buffer solution. Optical spectra were measured immediately afterward with a 3 minute time intervals for a total of 33 minutes.

RESULTS AND DISCUSSION

Effect of Chloroquine and X2 to the Dimer Formation Process of SnPP

SnPP exhibits an absorption spectrum typical of metalloporphyrins, with the maximum of the Soret bands at 386 nm (dimer) and 406 nm (monomer), as well as two bands at around 540 and 580 nm. In aqueous solutions the shapes of the Soret bands and their maximum are largely influenced by the pH of the medium and the SnPP concentration. at low pH values and at high porphyrin concentrations the maximum absorption is localized at 386 nm and gradually shifts to 406 as the pH increased and/or the concentration is decreased.

The optical spectra in Figure 17 demonstrate the time course for the Soret region from monomeric SnPP to dimeric SnPP by diluting stock solution of (largely monomer) SnPP (pH=12) into pH 5.8 phosphate solution. This series of spectra shows a drop in intensity of the monomeric peak (406 nm), accompanied by a gain in intensity of the dimeric peak (386 nm). A well defined isosbestic point is observed, suggesting only two species (monomer and dimer) are involved.

No dramatic changes were observed in optical spectra of dimer formation process of SnPP upon addition of chloroquine or X2 to SnPP. However, optical changes of SnPP at 386 nm (dimeric peak) were plotted versus time in order to elucidate the kinetics of the process, in particular the first order rate constant (Figure 18A). The rate of dimer formation of SnPP was found to be $9.54 \times 10^{-2} \text{ min}^{-1}$. The initial rate of SnPP dimer formation process was slightly enhanced ($1.09 \times 10^{-1} \text{ min}^{-1}$) upon complexation with chloroquine (Figure 18B). The process also reached steady state in slightly shorter time. Binding with X2 not only increased the initial rate of SnPP dimer

formation ($1.66 \times 10^{-1} \text{ min}^{-1}$), but also helped the process reach steady state in a noticeably shorter time (Figure 18C).

Effect of Chloroquine and X2 to the Dimer Dissociation Process of SnPP

Upon dilution of dimeric SnPP, optical spectra (Figure 19) clearly showed a drop in intensity of the dimeric peak (386 nm) accompanied by a gain in intensity of the monomeric peak (406 nm). The well defined isosbestic point was observed, suggesting only two species (monomer and dimer) appear to be involved. Binding with chloroquine or X2 did not significantly change the SnPP dimer dissociation process.

In order to understand the inhibition of chloroquine or X2 of the SnPP dimer dissociation process, optical changes of SnPP at 386 nm (dimeric peak) were plotted versus time (Figure 20A). The rate of dimer dissociation of SnPP was found to be $1.30 \times 10^{-3} \text{ min}^{-1}$. Initial rate of SnPP dimer dissociation process was slightly enhanced ($2.00 \times 10^{-3} \text{ min}^{-1}$) upon complexation with chloroquine (Figure 20B). The process reached steady state in slightly shorter time. Binding with X2 increased the initial rate of SnPP dimer dissociation ($2.80 \times 10^{-3} \text{ min}^{-1}$), and also helped the process reach to steady state in noticeably shorter time (Figure 20C).

CONCLUSION

At pH 5.8, 25°C, the rate of SnPP dimer formation is about 100 times faster than SnPP dimer dissociation. The effect of chloroquine or X2 on SnPP dimer formation is similar to the effect on SnPP dimer dissociation, SnPP binding with either chloroquine or X2 slightly increases the initial rate of the dimerization or

monomerization process, help to stabilize the final product. The initial rate constants for SnPP dimer formation and dissociation with and without drug are listed in Table 7.

Table 7. Apparent first order rate constant for SnPP dimer formation and dissociation at pH 5.8.

Species	Dimer Formation Rate	Dimer Dissociation Rate
SnPP	$9.54 \times 10^{-2} \text{ min}^{-1}$	$1.30 \times 10^{-3} \text{ min}^{-1}$
SnPP with chloroquine	$1.09 \times 10^{-1} \text{ min}^{-1}$	$2.00 \times 10^{-3} \text{ min}^{-1}$
SnPP with X2	$1.66 \times 10^{-1} \text{ min}^{-1}$	$2.80 \times 10^{-3} \text{ min}^{-1}$

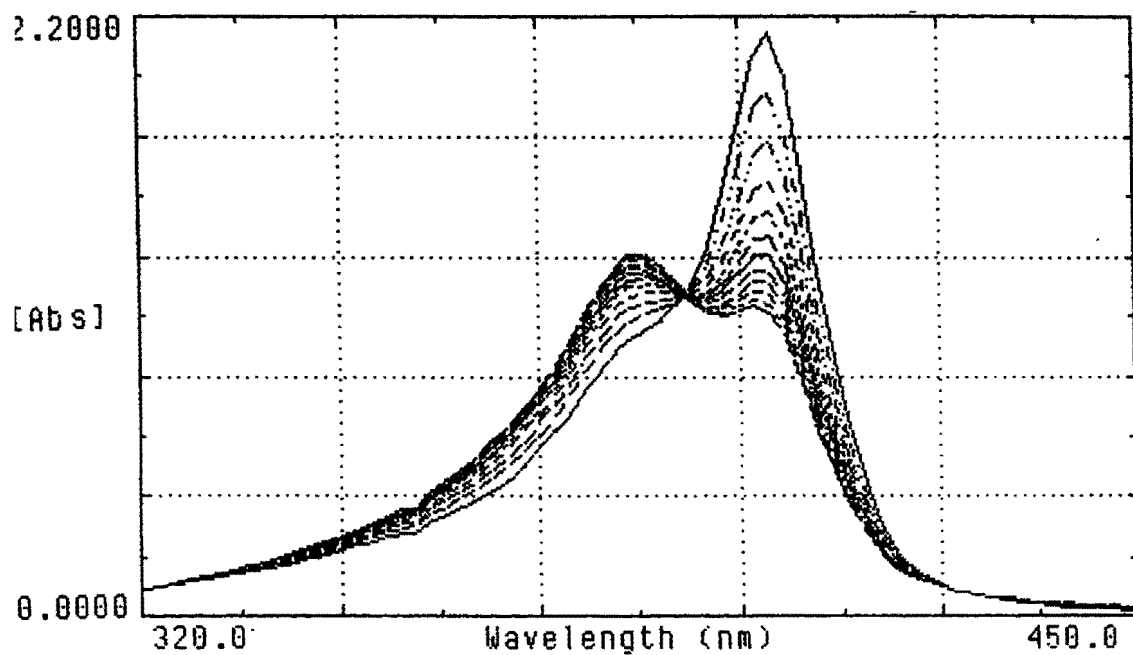


Figure 17. Optical spectra of the Soret region which reflect the conversion of SnPP monomer to SnPP dimer at pH 5.8.

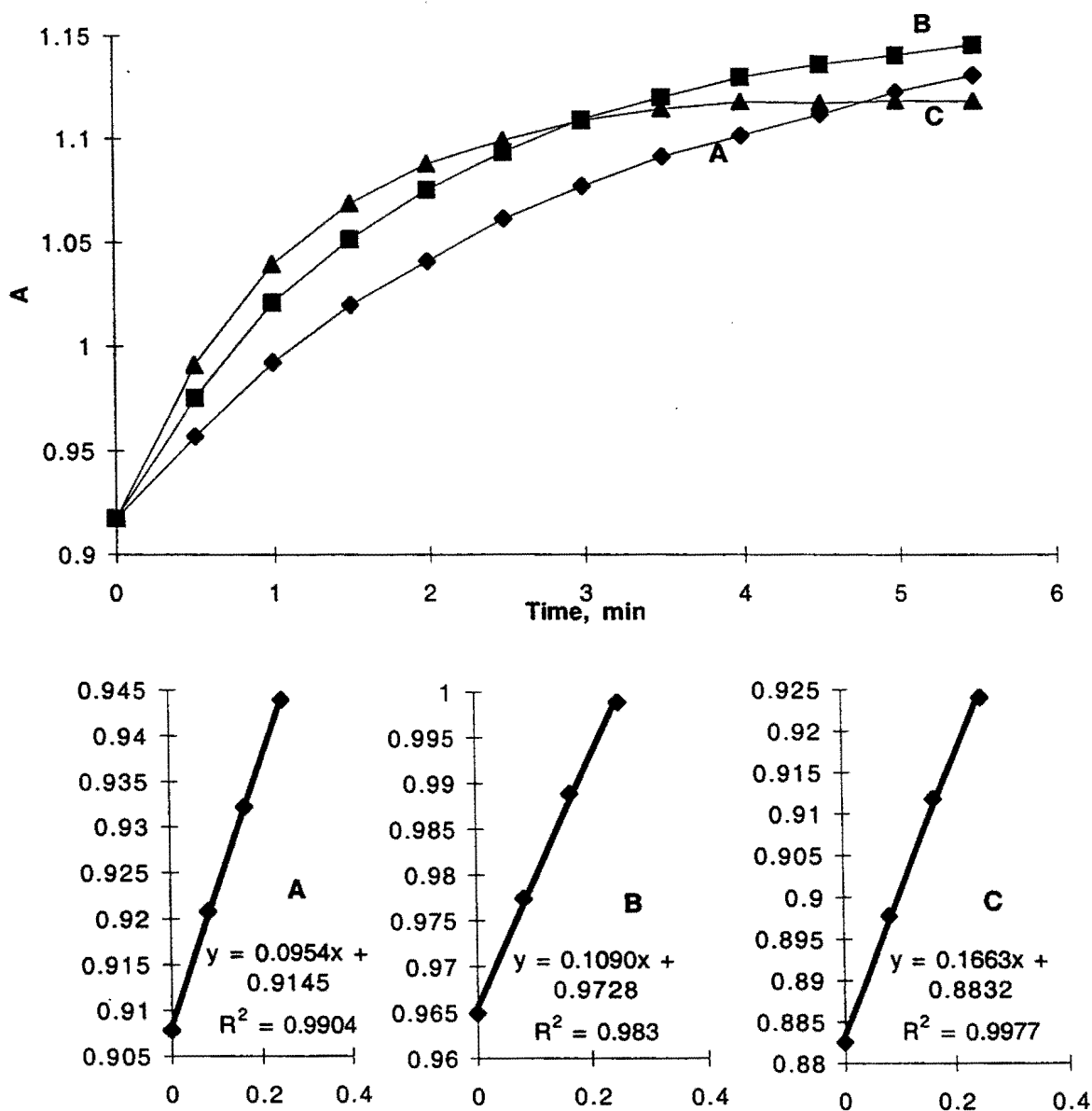


Figure 18. A plot of absorbance at 386 nm versus time at pH 5.8 for A: SnPP, B: SnPP with chloroquine, C: SnPP with X2 dimer formation process.

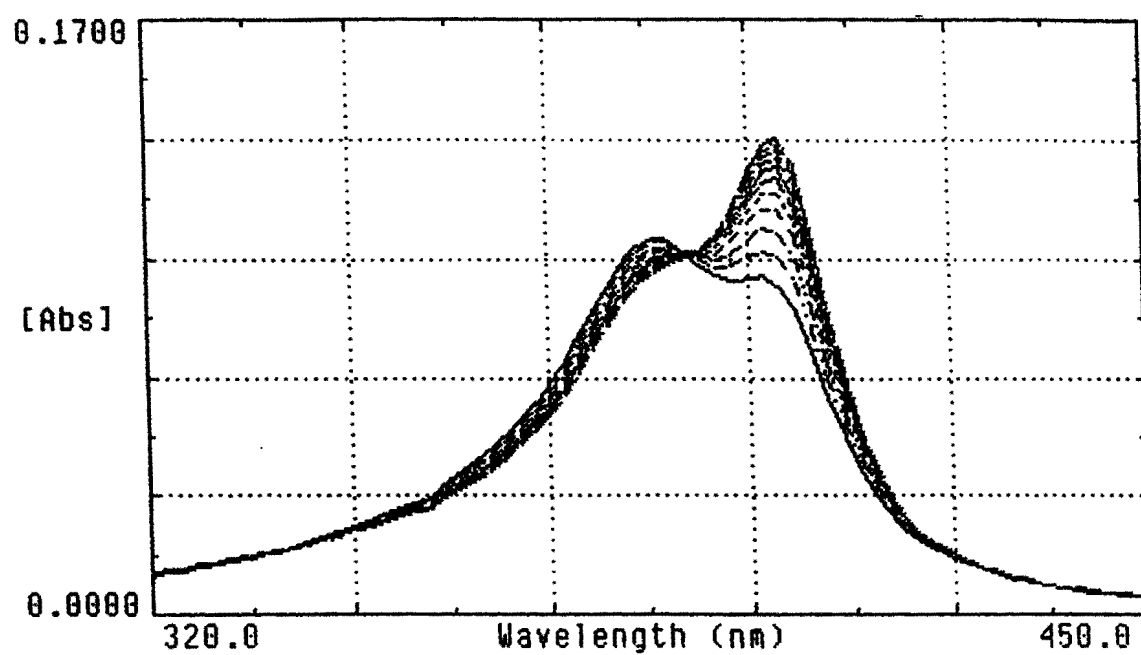


Figure 19. Optical spectra of the Soret region which reflect the conversion of SnPP dimer to SnPP monomer at pH 5.8.

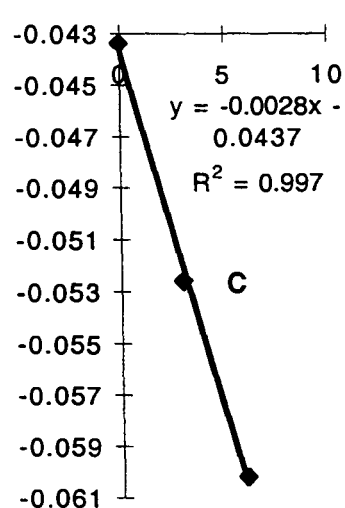
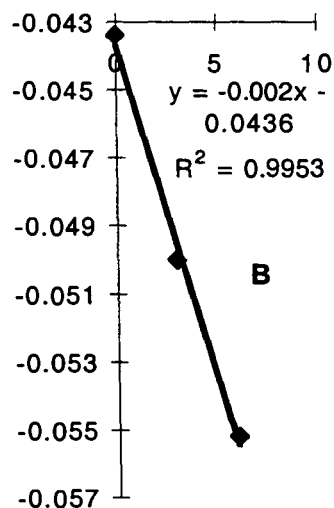
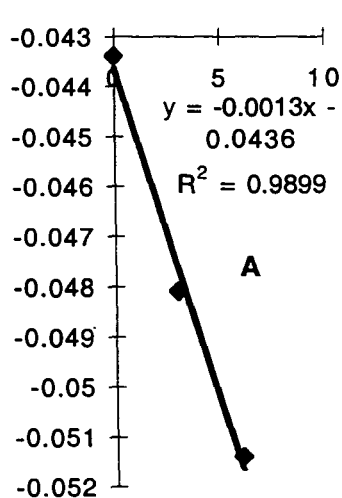
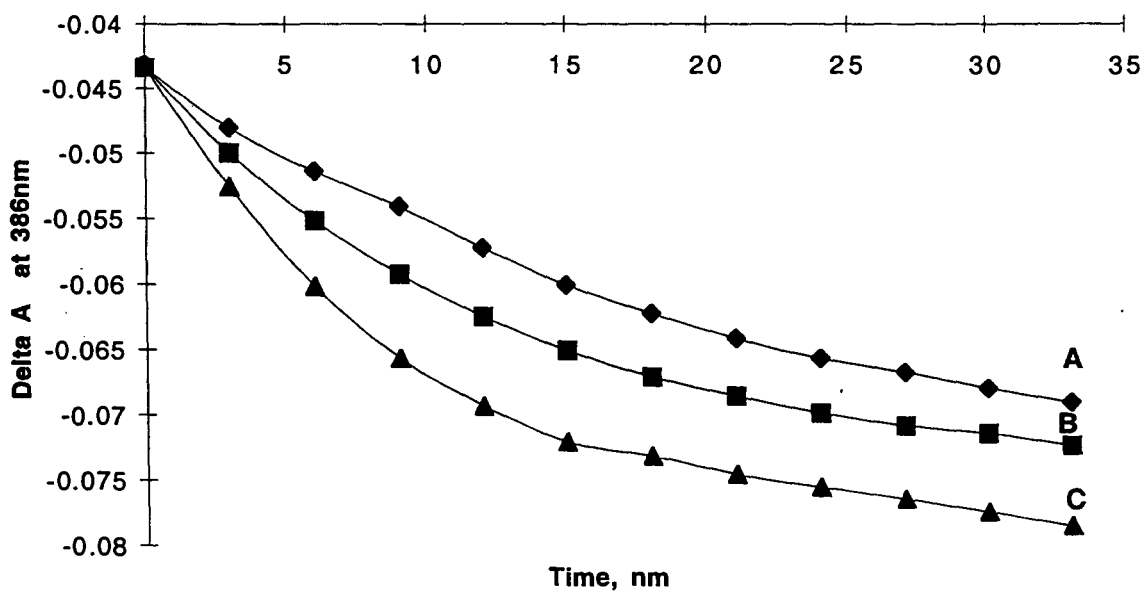
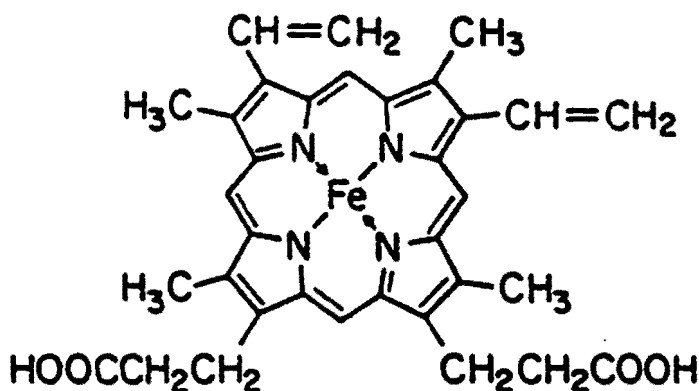


Figure 20. A plot of absorbance at 386 nm versus time at pH 5.8 for A: SnPP, B: SnPP with chloroquine, C: SnPP with X2 dimer dissociation process.

CHAPTER 6

NMR STUDY OF THE INTERACTION BETWEEN HEME AND X2

A study of the interactions between heme (the structure is shown below) and X2 using ^1H NMR to elucidate the nature and the geometry of the complex formed between them is presented in this chapter. The perturbations of the NMR spectra of X2 (1 mM) induced by addition of heme were measured. Two types of measurements were undertaken. The first study was carried out in aqueous medium (pH 9.5 and pH 11.5), and the second study was carried out in an organic solvent, DMSO.



The model of heme-X2 complex proposed by Ignatushchenko et al. is supported by the NMR analyses. In this model, the aromatic rings of X2 are stacked above the pyrrole rings of heme, in a π - π type interaction. The 1(8) protons of X2 face the center of the porphyrin, the iron ion coordinates with X2 via its carbonyl group, while the 4(5) position hydroxy groups of X2 participate in hydrogen bonding with the propionate side chain of heme.

MATERIALS AND METHODS

Heme was purchased from Sigma Chemical Company. D₂O was from Cambridge isotope Laboratories, and DMSO (Methyl sulfoxide-d₆) was from Aldrich. X2 was synthesized by Dr. Rolf Winter from the Portland VA Hospital.

Heme and X2 aqueous solutions were always prepared fresh for each experiment by adding minimum amount of NaOD to a D₂O suspension of the sample. The buffer system employed was 0.1 M phosphate at pH 9.5. Solutions of heme were adjusted to the correct pH for the studies with minimal amounts of DCl or NaOD. Repeated monitoring of the pH throughout all procedures was accomplished with a Radiometer Copenhagen pH meter 26 and an Ingold electrode.

All 1D ¹H NMR experiments were acquired on a Nicolet NT-500 MHz Spectrometer equipped with a 5 mm ¹H probe at 25°C, operating at 500 MHz. In aqueous solutions, NMR spectra were acquired with the zgpr pulse sequence as RD-90°_x-FID, in which the residual water resonance was suppressed with a long, low power pulse during the relaxation delay (RD). Chemical shifts are referenced to Me₄Si through the residual water signal at 4.76. In non-aqueous solutions, NMR spectra were acquired with the simple zgpr pulse sequence without solvent suppression, and spectra were referenced against internal Me₄Si (0.00 ppm). All ¹H NMR spectra were processed with MacNMR (Tecmag, Houston, TX, v.5.3).

RESULTS AND DISCUSSION

Interaction Between Heme and X2 in Aqueous Solution.

The resonance assignments for X2 have been previously discussed in Chapter 2 (Figure 1). There are slight chemical shift differences for the proton spectrum of X2 in water, compared with that in DMSO solutions. However, resonance assignments in D₂O were confirmed by comparison with the previous assignments.

Addition of small amounts of heme to a 1 mM aqueous solution of X2 at pH 9.5 resulted in a broadening of all the resonance lines and loss of intensity, as depicted in Figure 21. A second effect was a change in chemical shift of the various protons. A plot of induced shift versus the porphyrin/drug ratio is shown in Figure 22. All of the aromatic protons were shifted to high field; the aromatic 2(7) protons exhibited only a small change in chemical shifts, but the aromatic 1(8) and 3(6) protons showed large induced shifts, indicating strong interactions between the porphyrin ring and the aromatic nucleus of X2.

This pattern of induced shifts is interpretable in terms of a proposed geometry for the complex in solution. Previous calculations (Cross et al., 1985) of heme ring current induced shifts indicate that resonances of atoms in molecules that are located over the central part of the heme experience upfield shifts that are expected to vary with precise relative location (most easily rendered with cylindrical coordinates), the axial ligand occupies a region strongly shielded by the porphyrin ring current, and so the proton signals of the ligand upfield shifted the most are located closest to the metal. Resonances of atoms in molecules associated with a porphyrin, but which lie at the porphyrin periphery, may exhibit little induced shift or even downfield shifts. Ring current induced shifts for protons may be sizable. For example, these shifts can range between approximately +0.01 and -0.8 ppm for groups in well-characterized proximity to the heme in diamagnetic heme proteins (Cross et al., 1985).

The dramatic line broadening accompanying the titration with heme is a consequence of the pseudocontact dipolar interaction due to paramagnetic iron (III) atoms; yet some broadening also can be explained by the increased correlation time, thus indicating the formation of molecular complexes. Since heme (III) in aqueous solution has been identified as high-spin ferric species (Smith, 1975), a highly symmetric 6A orbital ground state is anticipated. The significant line broadening exhibited by X2 aromatic protons is understandable on this basis.

A slight upfield shift (of less than 0.01 ppm (0.008 ppm)) is experienced by the aromatic protons 2 and 7 in the presence of 75 mol % heme (heme to X2 is 3:1), suggesting that these protons are located on top of the pyrrole rings (near the heme periphery) of the porphyrin in a π - π type interaction. The largest induced shift (0.046 ppm) is observed at the 1(8) position protons, implying that these protons occupy a position at the heme plane where induced shifts as a result of combined effects of ring current and iron paramagnetism are large, and so are over or near the center of the porphyrin. This is the result that is consistent with the keto C=O moiety acting as an axially coordinating ligand to the heme iron. The upfield shift of protons 3(6) is almost as large (0.03 ppm) as those of protons 2(7), indicating a closer π - π interaction than those for protons 2(7), or closer proximity to the porphyrin core, the cause for this observation is unclear at this point, but with the investigation performed in the following chapters, an explanation of this mystery will be given in Chapter 9.

Figure 23 reveals the result of titrating heme into an aqueous solution of X2 at pH 11.5. It is important to notice that the aromatic X2 proton resonance changes are different than those for the same titration experiment performed in pH 9.5 in aqueous solution. In the presence of 23 mol % heme (heme to X2 = 0.3:1), a slight increase in linewidths are observed for the aromatic protons of X2, but no induced shift is

detectable. It thus appears that at this concentration of heme, no $\text{Fe}^{\text{III}}\text{O}=\text{C}<$ axial coordination, nor π - π interactions are detected. In the presence of 50 mol % heme (heme:X2 = 1:1) however, significant increase in linewidths and sizable downfield shifts of similar magnitudes for all aromatic X2 protons (about 0.082 ppm) are observed, no unusually large change in chemical shift for proton 1 and 8 is observed, indicating that the iron is not axially coordinated. In strongly basic solutions, the hydroxy groups of X2 tend to be deprotonated, precluding the possibility of hydrogen bonding with carboxylate side chain of heme. Meanwhile, strongly basic solvent, which is not only a Brønsted base, but also a Lewis base, can bind as a neutral donor ligand L to a metal ion behaving as Lewis acid, so it can compete with the X2 C=O group as the fifth (or sixth) axial ligand for the central iron. In this situation, xanthone complexed with heme is inferred as stacked over or near the porphyrin periphery (indicated by the downfield shift of X2 aromatic protons) with undefined geometry. At high concentration of heme, strong π - π interaction indicated by the significant line broadening occurs due to the close contact between heme and X2 and the high concentration of X2-heme complex. The close contact between heme and X2 can be explained by the lack of the steric hindrance caused by axial coordination and hydrogen bonding within the heme-X2 complex. Meanwhile, the equilibrium of X2 binding with heme shifted to the complexation side while the concentration of heme increases, leading to higher concentration of X2-heme complex. These observations in strongly basic solution preclude the possibility of mere π - π interaction between heme and X2, thus further supporting the idea of the iron and X2 keto coordination and hydrogen bonding between heme carboxylate/X2 hydroxy groups at lower pH, because π - π interactions rarely are solvent dependent (Smith, 1975). In fact, adding strong base to a

non-polar solution of metalloporphyrin is an established way to test for a metal atom axial coordination interaction (Smith, 1975).

Interaction Between Heme and X2 in Nonaqueous Solution (DMSO)

Effects on the proton NMR spectrum for X2 binding to heme in DMSO are shown by the titration in Figure 24. The most obvious effect is the strong line broadening for hydroxy protons compare to aromatic protons (even at the lowest mole percent of heme, 33 mol %). Typical concentration-dependent ring current induced upfield shifts of the order of 0.007 ppm at the presence of 83 mole % of heme (heme:X2 = 5:1) without dramatic line broadening for all aromatic protons of X2 were also observed.

The unusual line broadening for hydroxy protons of X2 strongly indicates the existence of hydrogen bonding for these protons. No unusually large upfield shift for protons 1(8) was observed here, suggesting no coordination between heme Fe and X2 C=O. The major reason for this may be that DMSO itself strongly coordinates with most of the transition metals (Meek et al., 1960), so that DMSO competes with the C=O group as the fifth (or sixth) axial ligand for the central iron of the porphyrin ring. Since hydrogen bonding between the 4 and 5 position hydroxy groups of X2 and carboxylate side chain of heme are likely formed in the aprotic solvent DMSO, X2 stacking over the heme porphyrin plane likely became orientated with 1 and 8 protons facing to the center of the heme core. Thus, X2 is stacked on top of the pyrrole rings of the heme instead of the porphyrin periphery. The concentration dependence of the shifts indicate that π - π interaction exists between heme and the X2 molecule in DMSO. Unlike in strongly basic aqueous solution, the hydrogen bonding between

these two molecules and the coordination between DMSO with central iron also causes the steric hindrance for X2 binding, as a result, the drug may be prevented from contacting heme, as well as from getting very close to the heme iron, so even at high concentration the complex still gives relatively sharp lines for X2. The geometry of X2 binding with heme in DMSO can be understood as X2 approaching to one side of heme with or without significant π - π interaction and hydrogen bonding to the carboxylates, while DMSO coordinates to the heme iron through the oxygen of DMSO on the other side of heme, assuming that this high-spin state iron is in five coordinated, allowing only single axial ligand (Smith, 1975).

Taken together, the observations in DMSO nonaqueous solution preclude the possibility of mere π - π interaction between heme and X2, thus further supporting the idea of the iron to X2 keto coordination and hydrogen bonding between heme carboxylate with X2 hydroxy groups in aqueous solution at pH 9.5.

CONCLUSION

All the above observations show that the interactions between the heme porphyrin plane and the aromatic nucleus of X2 can be considered as the sum of π - π interactions, axial coordination, and hydrogen bonding. These conclusions were inferred from the heme-induced broadening of aromatic lines and different degrees of upfield shifts for various protons in the NMR spectrum of X2. This view is strengthened by considering the effect upon the X2 spectrum caused by the presence of heme in strongly basic aqueous solution as well as DMSO solution. These observations support a model where the aromatic rings are stacked above the pyrrole rings of heme, in a π - π type interaction with the 1,8 protons facing the center of the

porphyrin, axial iron ion coordinating with X₂ via its carbonyl group, while the 4(5) position hydroxy groups of X₂ hydrogen bond with carboxylate side chain of heme. The 'true' geometry of X₂ binding with heme needs to be established with more information (a more fully described geometry is presented in more detail in Chapter 9). In Chapter 3, it was shown that X₂ binding to heme is noncooperative process, so it is suggested that π - π interactions, axial coordination, and hydrogen bonding between X₂ and heme are spontaneous.

The paramagnetism of the ferric ion in heme and the aggregation property of heme cause the difficulties in the investigation in detail of the structure of interactions between monomeric or dimeric metalloporphyrin and X₂. Hence, a NMR investigation with a well-studied diamagnetic metalloporphyrin, SnPP, is introduced in the next chapter.

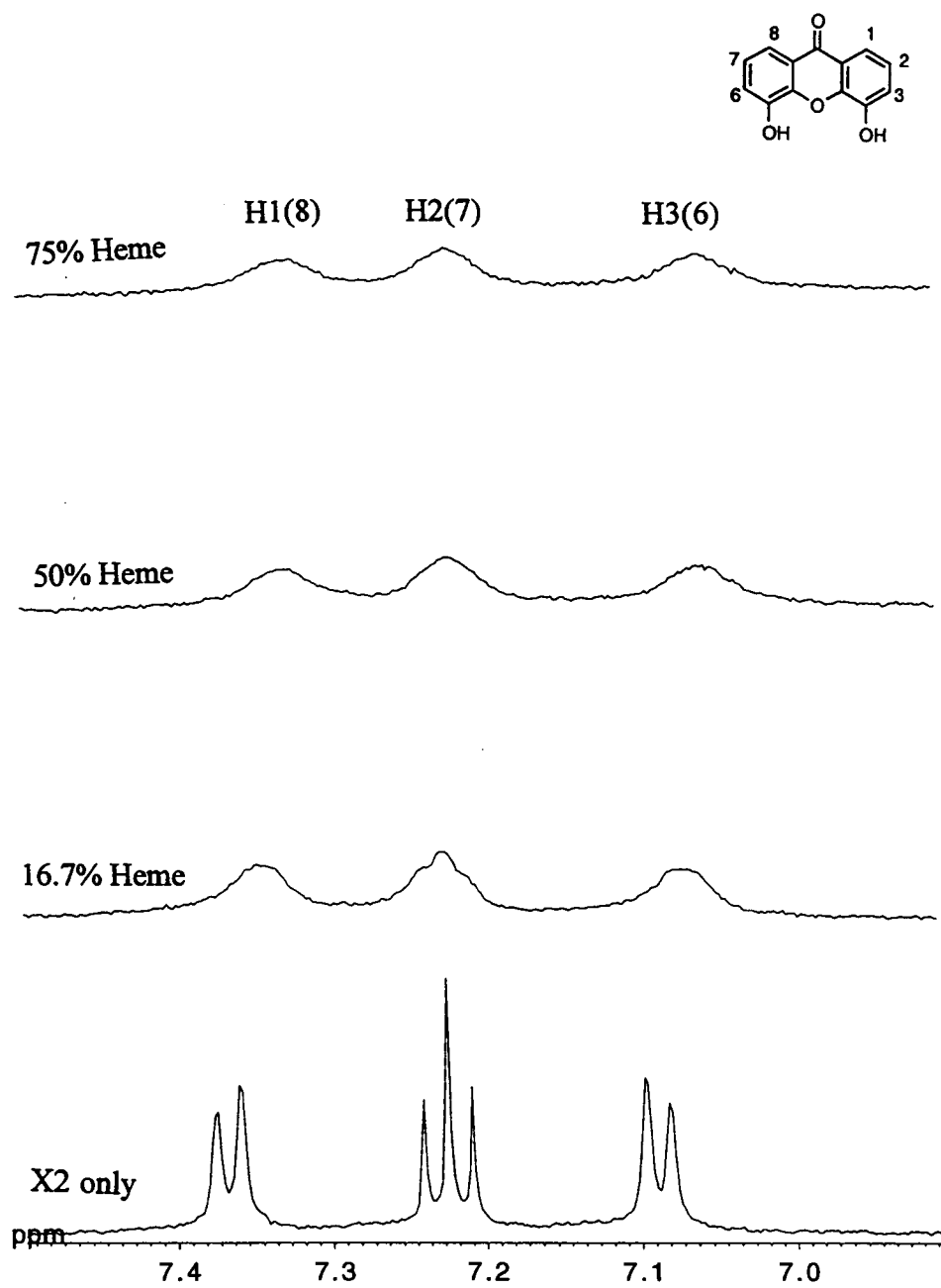


Figure 21. ^1H NMR spectra of X2 as a function of heme addition in mole percent at pH 9.5, 25 °C, 500 MHz.

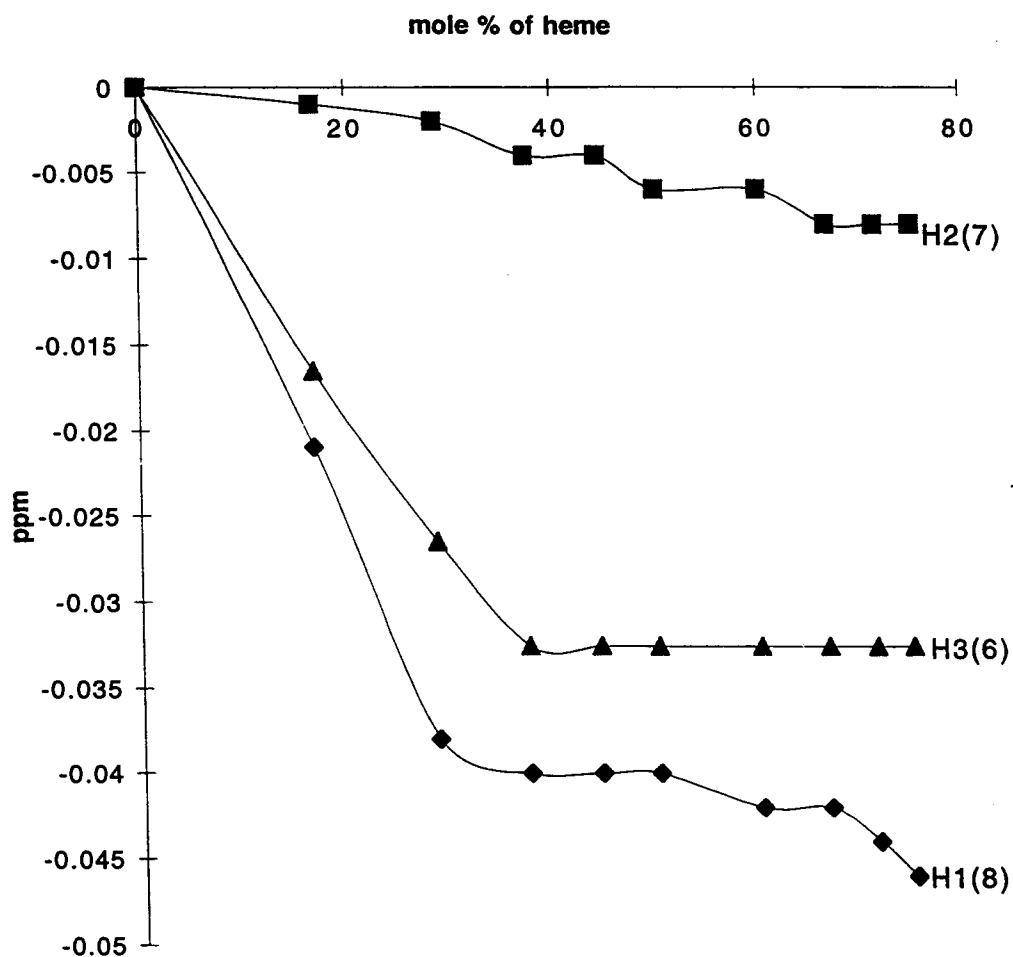


Figure 22. The high-field shifts ($\Delta\delta < 0$) of aromatic protons of X2 as a function of the molar fraction of heme, pH9.5, 25 °C

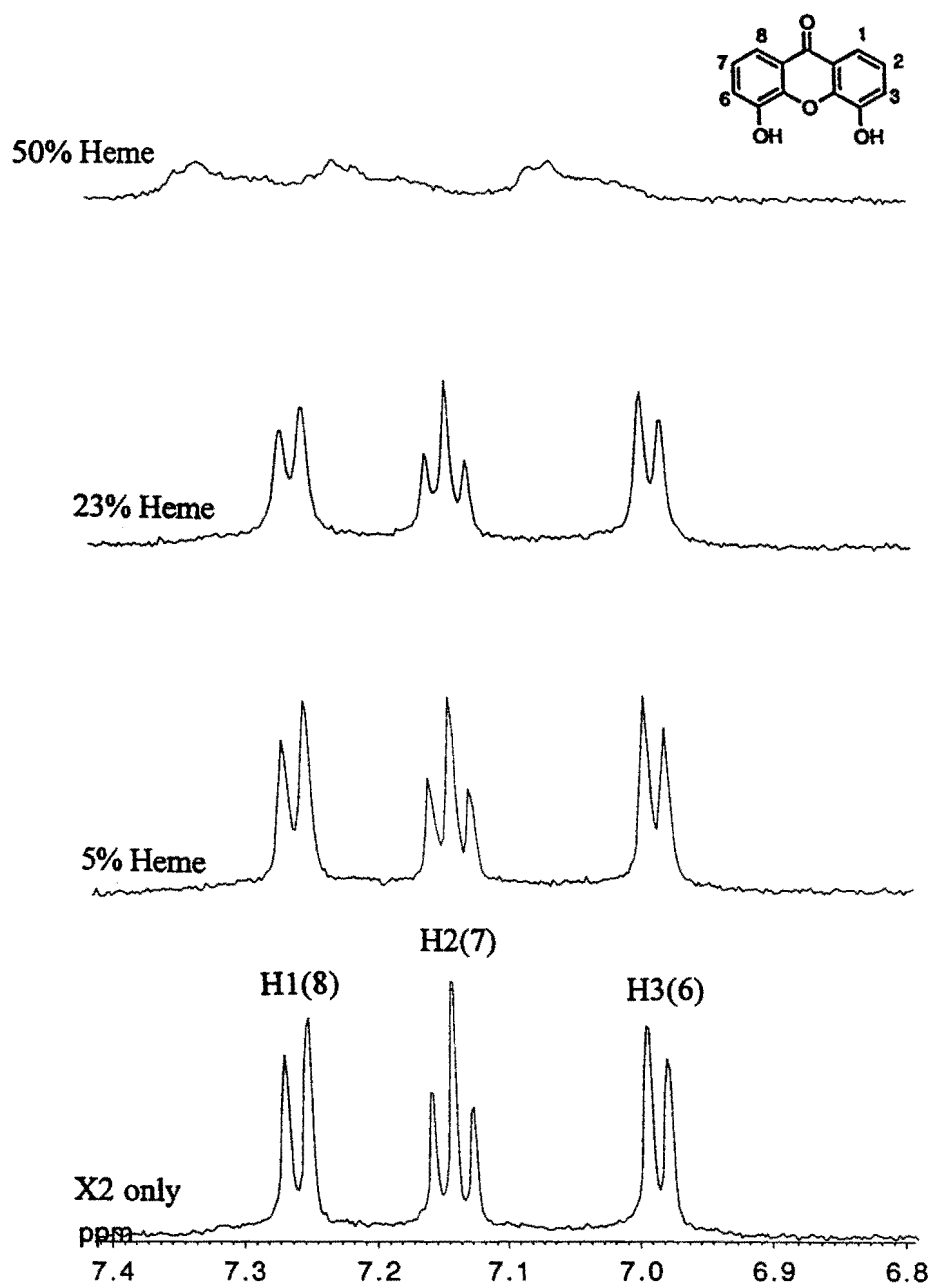


Figure 23. ^1H NMR of X2 as a function of heme addition in mole percent at pH 11.5, 25 °C, 500 MHz.

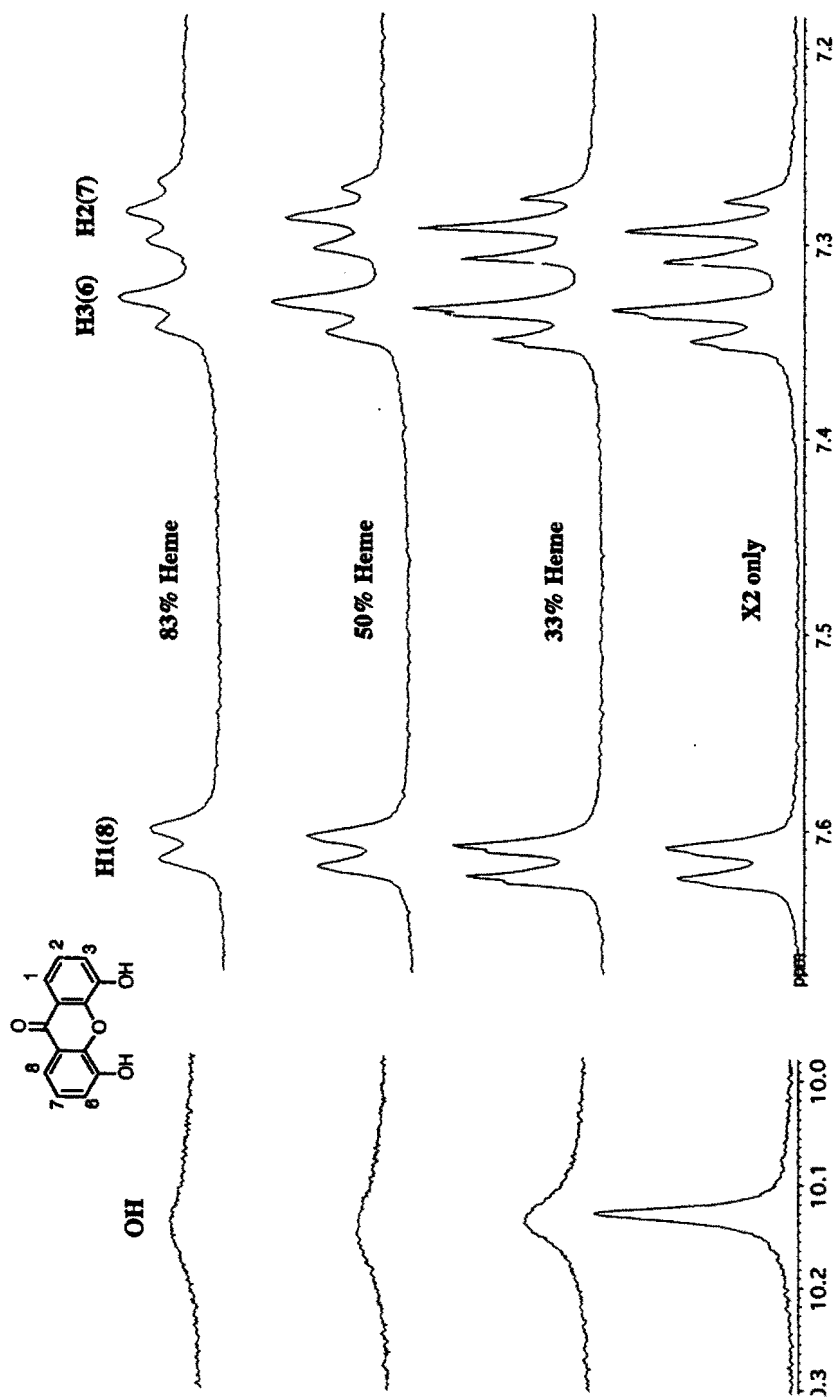


Figure 24. ^1H NMR spectra of X2 as a function of heme addition in mole percent in nonaqueous solution DMSO, 25 °C, 500 MHz.

titration of SnPP into X2 solution was performed, and the spectral changes upon addition of SnPP were analyzed afterward.

The complex formed between SnPP and X2 appears to be cofacial stacking, in which the aromatic rings of X2 are stacked above the pyrrole rings of SnPP in a π - π type interaction, with the 1(8) protons face the center of the porphyrin, the axial tin ion coordinates with X2 via its carbonyl group, and the 4(5) position hydroxy groups of X2 hydrogen bond with the carboxylate side chains of SnPP.

MATERIALS AND METHODS

SnPP was from Porphyrin Products. X2 was synthesized by Dr. Rolf Winter from Portland VAMC; DMSO (Methyl sulfoxide- d_6) was from Aldrich. SnPP solutions were always prepared fresh by dissolving the porphyrin in D_2O with a minimum amount of NaOD as required. All samples prepared were protected from light. 1H NMR spectra were recorded for SnPP and X2 in D_2O or DMSO at 25°C as described in Chapter 5. ^{119}Sn spectra were acquired on the AMX-400 NMR at 149.12 MHz using a 10 mm broadband probe at 25°C.

RESULTS AND DISCUSSION

1H NMR Study of Interaction Between SnPP and X2 in Aqueous Solution by Titrating X2 into SnPP.

Figure 25 shows that, at pH 7.2, SnPP primarily exists as a dimer (meso protons at 9.8 ppm). In the presence of 50 mole % of X2 (X2:SnPP = 1:1), virtually all of the SnPP proton resonances broaden and shift upfield. The line broadening

accompanying the titration with X2 is a consequence of the combination of increasing correlation time and the chemical exchange between free SnPP and bound SnPP with X2. The upfield shifts are an indication of the involvement of π - π interaction in the complexation between SnPP and X2. It is noticeable that the upfield shift and dipolar line broadening for $2H_{\beta c}$, $2H_{\beta t}$, $4H_{\beta c}$, $4H_{\beta t}$, and $6,7H_{\beta,\beta'}$ protons are smaller compared to other protons which are closer to the porphyrin pyrrole rings, and this can lead to the interpretation that these protons are located furthest from the range of X2's ring current effects. One significant observation is that when X2 was added to SnPP at pH 7.2, no precipitate was formed, while X2 alone precipitated out from the solution at this pH. This observation demonstrates that X2 binding to SnPP forms a soluble complex under neutral conditions.

At pH 9.5, SnPP and monomeric SnPP coexist in the solution, as shown by the NMR spectra in Figure 26. Upon titrating X2 into SnPP, line broadening and concentration-dependent upfield shifts throughout the whole spectra were observed, indicating a similar type of complexation between SnPP and X2 as at pH 7.2, but with both SnPP monomer and dimer complexing with X2 in a similar way. The interaction between SnPP with X2 shows no significant difference at pH 9.5 than at pH 7.0 (which is closer to the physiological condition). Thus pH 9.5 was often taken as an acceptable condition under which to run experiments of titrating SnPP into X2. At least 1 mM X2 concentration was required for some of these NMR studies, but at pH 7.0, X2 alone precipitates out of the solution if this concentration is attempted.

Effects on the SnPP proton NMR spectrum upon addition of X2 in strongly basic solution (pH 11.5) are shown in Figure 27. Up to the presence of 33 mol % of X2 (X2:SnPP = 0.5:1), there is no detectable change for the SnPP resonances; some slight line broadening and upfield shifting of the SnPP resonances are observed when

X2 concentration is raised to 50% (X2:SnPP = 1:1). As discussed in Chapter 5, in strongly basic solution, without axial coordination of metal (because the hydroxide Lewis base competes with X2 C=O for coordination with metal Sn) and hydrogen bonding, only weak and concentration dependent π - π interaction occurs between SnPP and X2. The evidence for this is that only at high concentration of X2 a significant fraction of SnPP interacts with the X2 aromatic ring. Dramatic line broadening was not observed in this case because the absence of paramagnetism.

In conclusion, these observations in strongly basic solution preclude the possibility of mere π - π interaction between heme and X2, thus further supporting the idea of the Sn (IV) and X2 keto coordination at lower pH.

¹H NMR Study of Interaction Between SnPP and X2 in Aqueous Solution by Titrating SnPP into X2.

Addition of small amounts of SnPP to a 1 mM aqueous solution of X2 at pH 9.5 resulted in a slight broadening of all the resonance lines with a loss of peak height, as depicted in Figure 28. A second effect was a shifting of the various proton resonances. The plot of induced shift versus the SnPP/X2 ratio is shown in Figure 29; all the aromatic protons were shifted to higher field, and the aromatic protons 2(7) and 3(6) exhibited only small shifts compared to the aromatic protons 1(8).

The slight line broadening is expected because SnPP is diamagnetic; minor line broadening can be explained in terms of increasing correlation time and chemical exchange effects, thus indicating the formation of molecular complexes and the chemical exchange between free SnPP and bound SnPP with X2.

The largest induced shift is observed at the 1(8) position proton (0.057 ppm), implying that they occupy a position over the center of the porphyrin, possibly

indicating X2 keto C=O axially coordinated with the Sn (IV) ion, because the axial ligand occupies a region strongly shielded by the ring current. Comparable, small upfield shifts of 0.019 ppm are experienced by the aromatic protons 2(7) and 3(6) in the presence of 75 mol % SnPP (SnPP:X2 = 3:1), suggesting that these protons located on top of the pyrrole rings of the porphyrin.

¹H NMR Study of Interaction Between SnPP and X2 in DMSO

Effects on the proton NMR spectrum upon X2 binding to SnPP in DMSO are shown in Figure 30. Slight line broadening for all aromatic protons is observed, indicating the formation of molecular complexes. The strong line broadening for hydroxy protons indicates the hydrogen bonding between 4(5) position hydroxy groups of X2 and carboxylate side chain of heme. The typical concentration-dependent ring current induced upfield shifts of X2 were not detected up to the presence of 90 mol % of SnPP (SnPP:X2 = 8:1). This can be explained as follows: the Sn in SnPP is expected to be six-coordinate, which allows two axial ligands. The steric hindrance caused by the coordination between DMSO with the central metal Sn on both sides of SnPP plane cause the distance between SnPP plane and X2 aromatic ring to be larger than the π - π coupling range, causing the loss of π - π interaction.

Since π - π interactions rarely are solvent dependent (Smith, 1975), the above observations in DMSO nonaqueous solution preclude the possibility of mere π - π interaction between heme and X2, thus further supporting the idea of the Sn (IV) and X2 keto coordination in aqueous solution at lower pH.

Further investigation of the coordination between the Sn of SnPP and C=O of X2 can be engaged by performing a ¹¹⁹Sn NMR of titration of SnPP with X2.

¹¹⁹Sn NMR Study of the Interaction Between SnPP and X2 in Aqueous Solution

The ¹¹⁹Sn NMR spectrum of SnPP shows that the dimeric and monomeric forms SnPP co-exist at pH 9.5, the ¹¹⁹Sn chemical shift change on going from monomeric SnPP to dimeric SnPP is 13.02 ppm with monomer gives rise to its resonance at downfield, dimer at upfield (shown in Figure 31). Figure 31 demonstrates the ¹¹⁹Sn resonance of SnPP with addition of X2. Line broadening and an upfield shift were observed for both the dimeric and monomeric Sn resonances, indicating that the central metal of porphyrin is involved in the complexation between X2 and SnPP. The axial coordination between Sn of SnPP and X2 C=O was suggested by the previous sections (if only π - π interaction occurs in the complex, the spectral changes would not have been solvent dependent), so the upfield shifts of Sn resonances may be caused mainly by the increased electron density as σ donor C=O approach metal Sn of the porphyrin. The plot of induced shift versus the porphyrin/X2 ratio is shown in Figure 32. The upfield shift for SnPP monomer is 2-fold larger than for SnPP dimer in the presence of 50 mol % of X2. This is the evidence of X2 binding on one side of each SnPP dimer plane (since dimeric SnPP was claimed to be μ -oxo bridged (Deeb, 1993)) while binding on both sides for SnPP monomer, through coordination between keto group of X2 and metal tin of SnPP in both cases. The proposed model for X2-SnPP association is shown in Figure 33 (for X2 association with SnPP monomer) and Figure 34 (for X2 association with SnPP dimer).

CONCLUSION

All the above observations show that interaction occurs between the SnPP porphyrin plane and the aromatic nucleus of X2, which may be a result of π - π interactions, axial

coordination, and hydrogen bonding. These conclusions were inferred from the SnPP-induced broadening of aromatic lines and different upfield shifts for various protons in the NMR spectrum of X2. This view is strengthened by considering the effect upon the X2 spectrum caused by the presence of SnPP in strong basic aqueous solution, in nonaqueous DMSO solution, as well as in ^{119}Sn NMR spectra. It is suggested that X2 binds to both sides of monomeric SnPP, as well as to both sides of the μ -oxo bridged dimeric SnPP. This conclusion is supported by ^{119}Sn NMR resonance changes of SnPP upon addition of X2, in which ^{119}Sn NMR resonances shows twice the magnitude of upfield shifts for monomeric SnPP than dimeric SnPP. At least in aqueous solutions, the complex formed between SnPP and X2 appears to be cofacial stacking, where the aromatic rings are stacked above the pyrrole rings of SnPP, in a π - π type interaction with the 1(8) protons facing the center of the porphyrin, with axial iron ion coordinate with X2 via its carbonyl group, and 4(5) position hydroxy group of X2 hydrogen bonding with carboxylate side chains of SnPP. Proposed models for the association of X2 with SnPP monomer and SnPP dimer are shown in Figure 33 and Figure 34, respectively. In Chapter 4, it was asserted that X2 binding to SnPP is noncooperative process, so it is suggested that π - π interactions, axial coordination and hydrogen bonding between X2 and SnPP are independent on each side of the porphyrin.

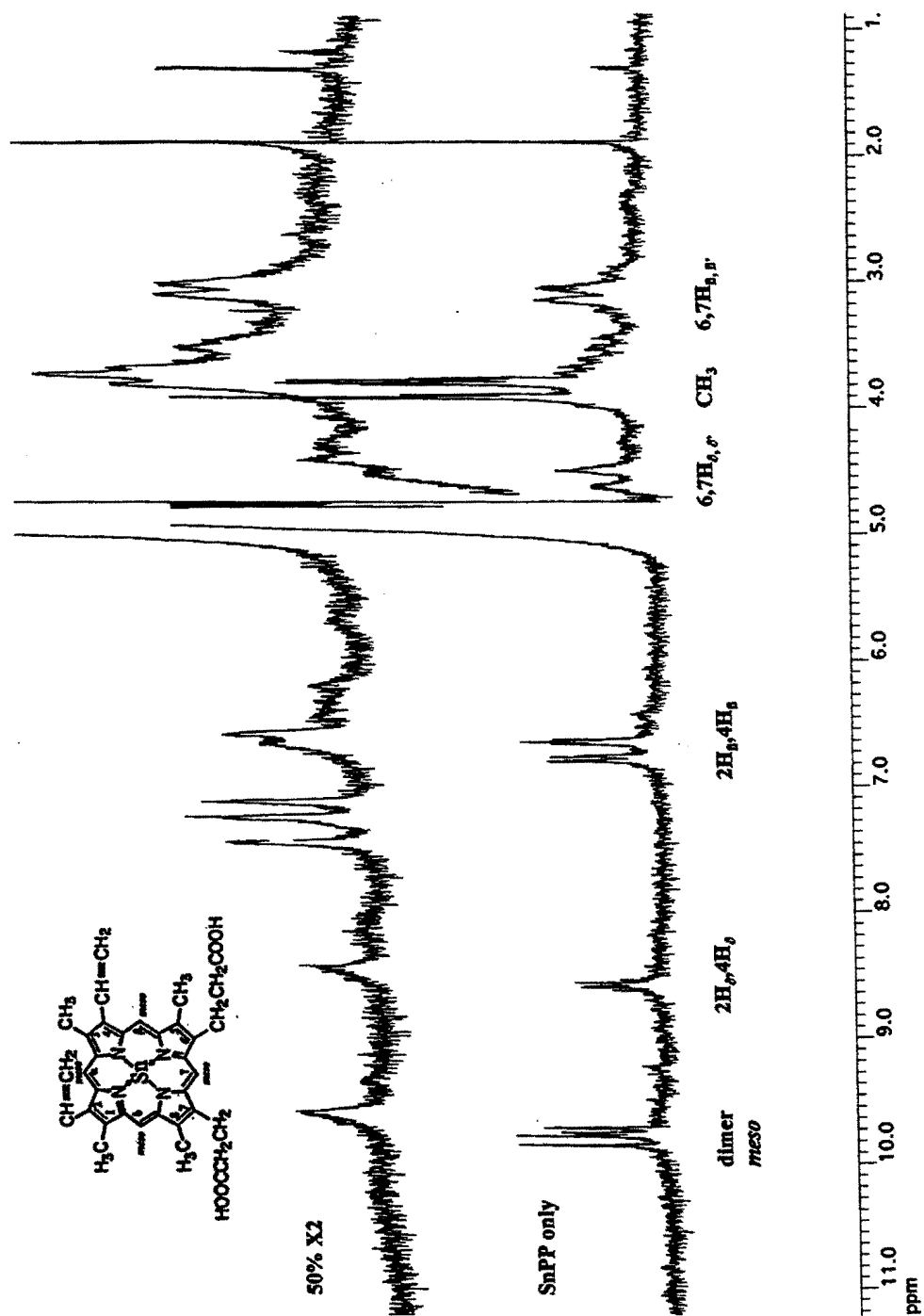


Figure 25. ^1H NMR spectra of SnPP as a function of X_2 addition in mole percent at pH 7.2, 25 °C, 500 MHz.

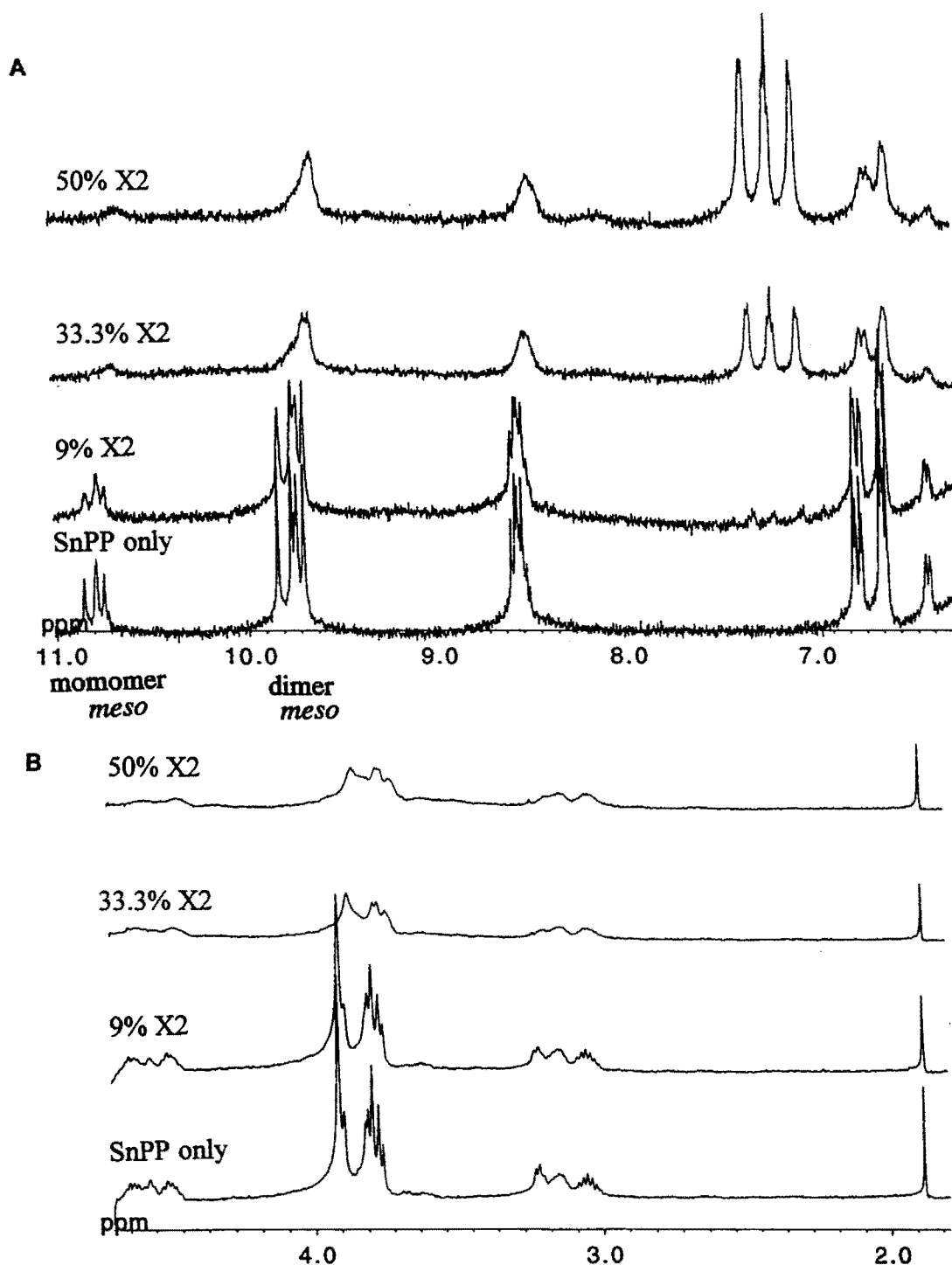


Figure 26. ^1H NMR spectra of SnPP as a function of X2 addition in mole percent at pH 9.5, 25 °C, 500 MHz. A: down field shifts from H_2O peak. B: upfield shifts from H_2O peak.

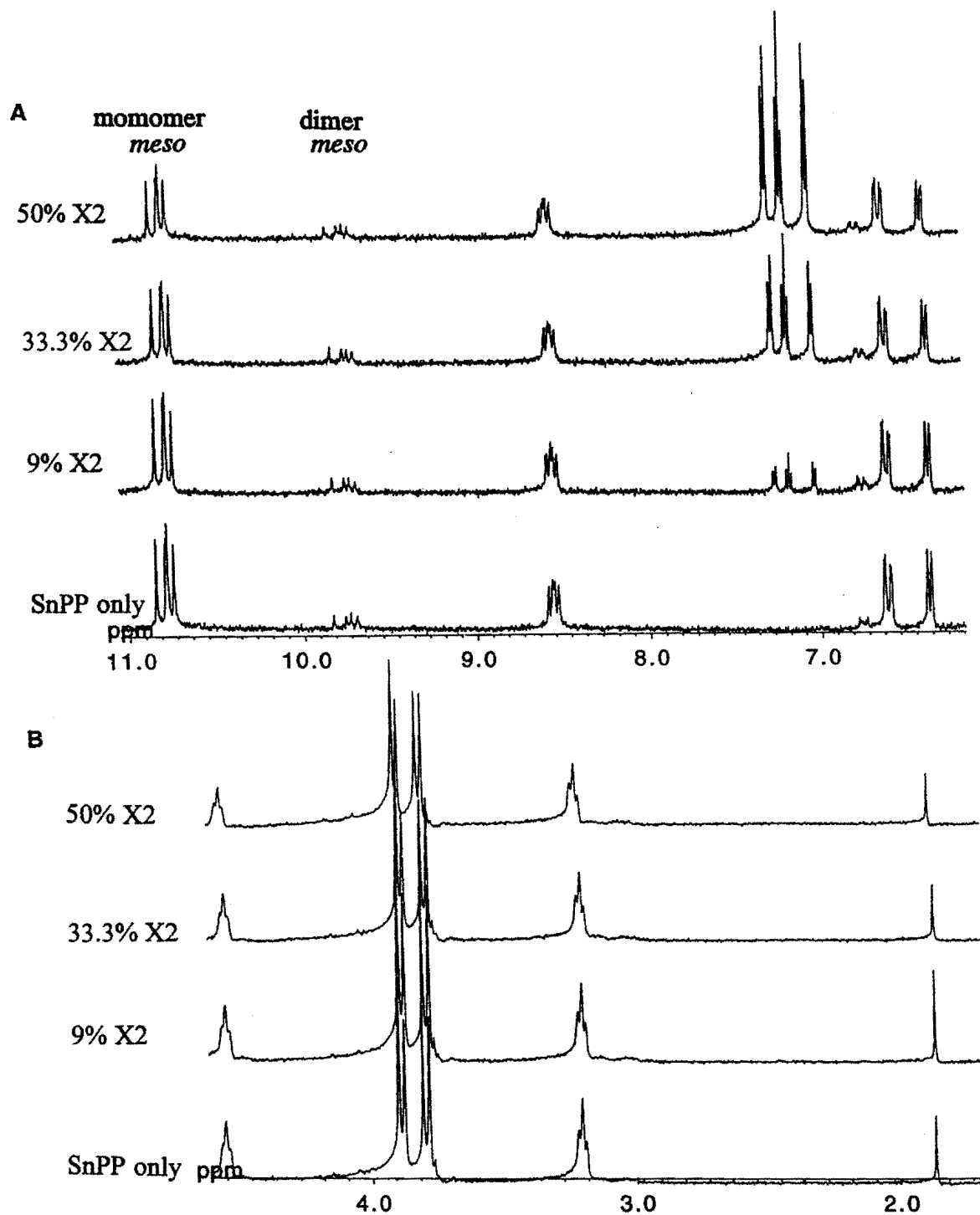


Figure 27. ^1H NMR spectra of SnPP as a function of X₂ addition in mole percent at pH 11.5, 25 °C, 500 MHz. A: down field shifts from H₂O peak. B: upfield shifts from H₂O peak.

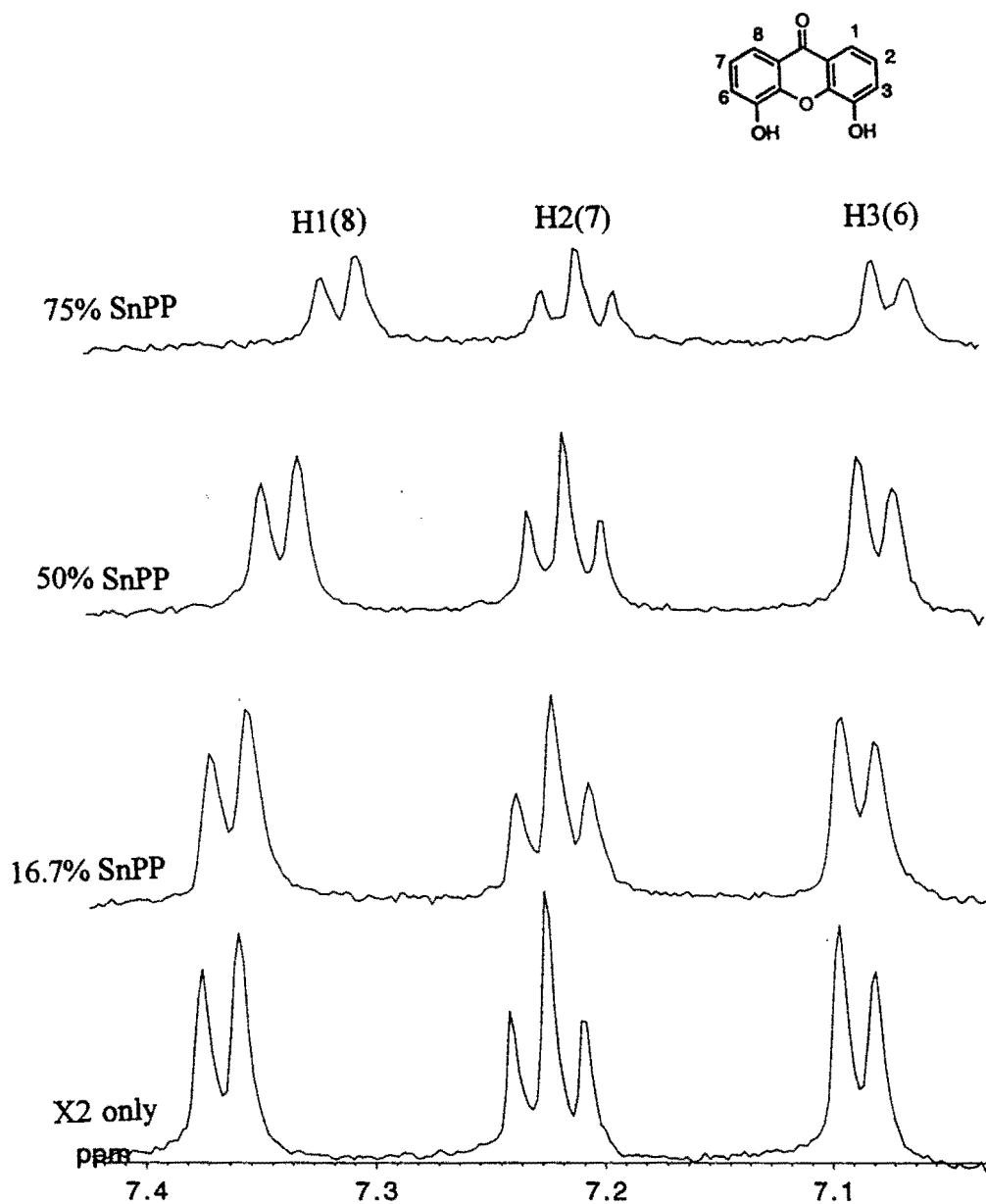


Figure 28. ^1H NMR spectra of X2 as a function of SnPP addition in mole percent at pH 9.5, 25 °C, 500 MHz.

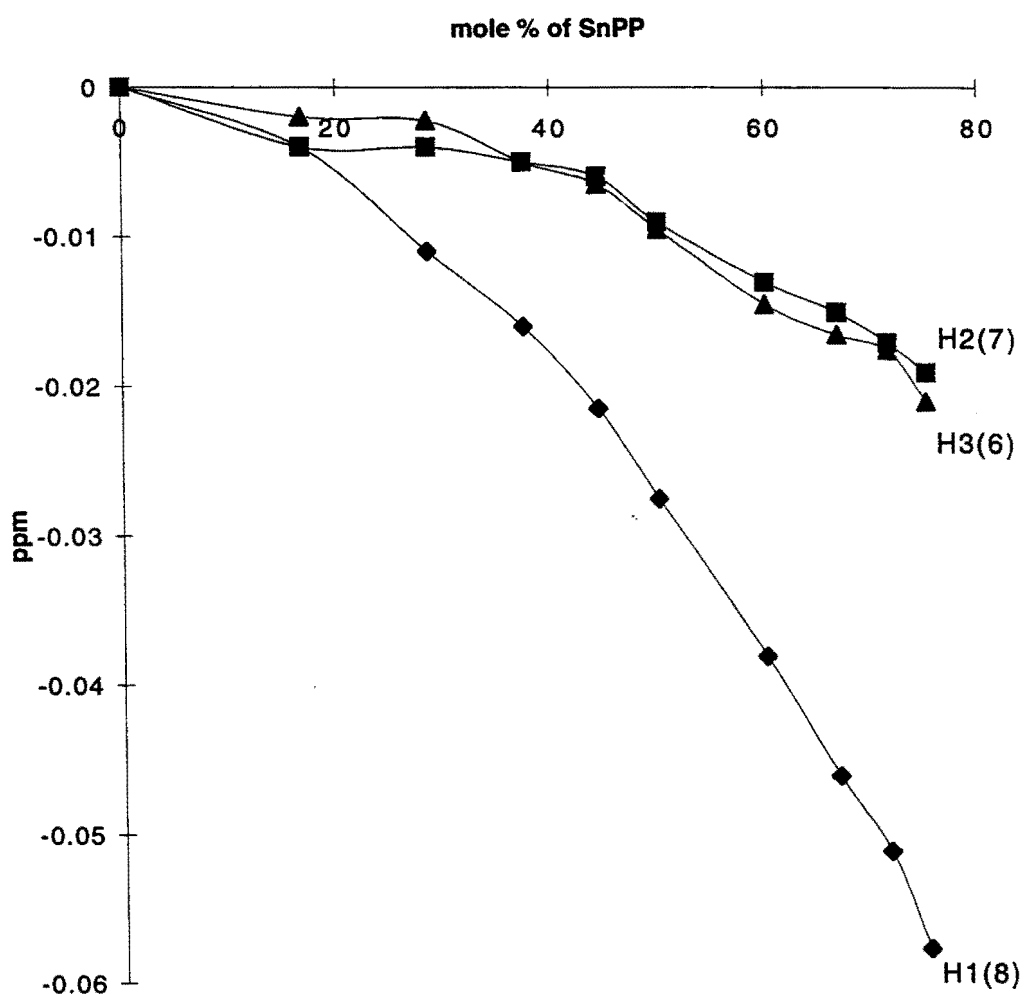


Figure 29. The high-field shifts ($\Delta\delta < 0$) of atomic protons of X2 as a function of the mole fraction of SnPP at pH 9.5.

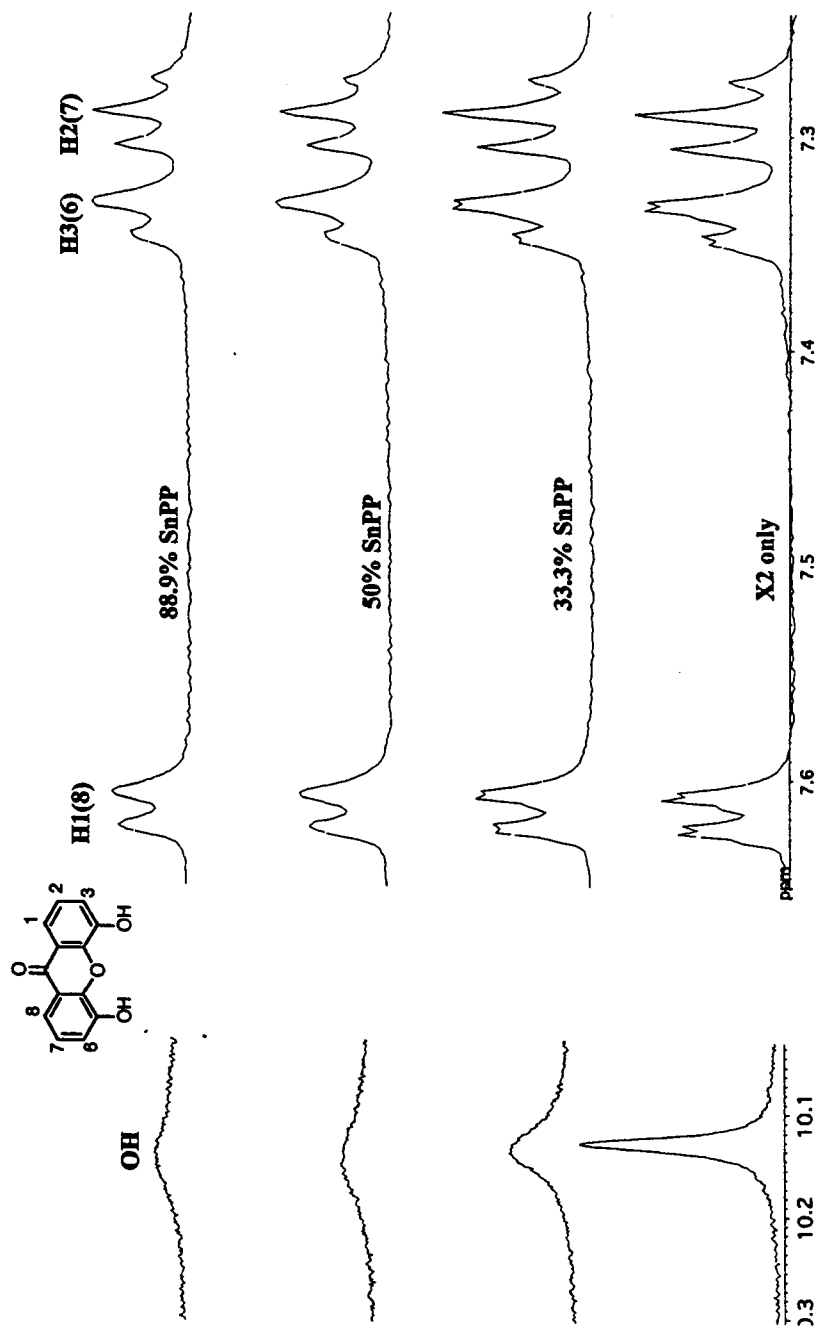


Figure 30. ^1H NMR spectra of X2 as a function of SnPP addition in mole percent in DMSO nonaqueous solution, 25 °C, 500 MHz.

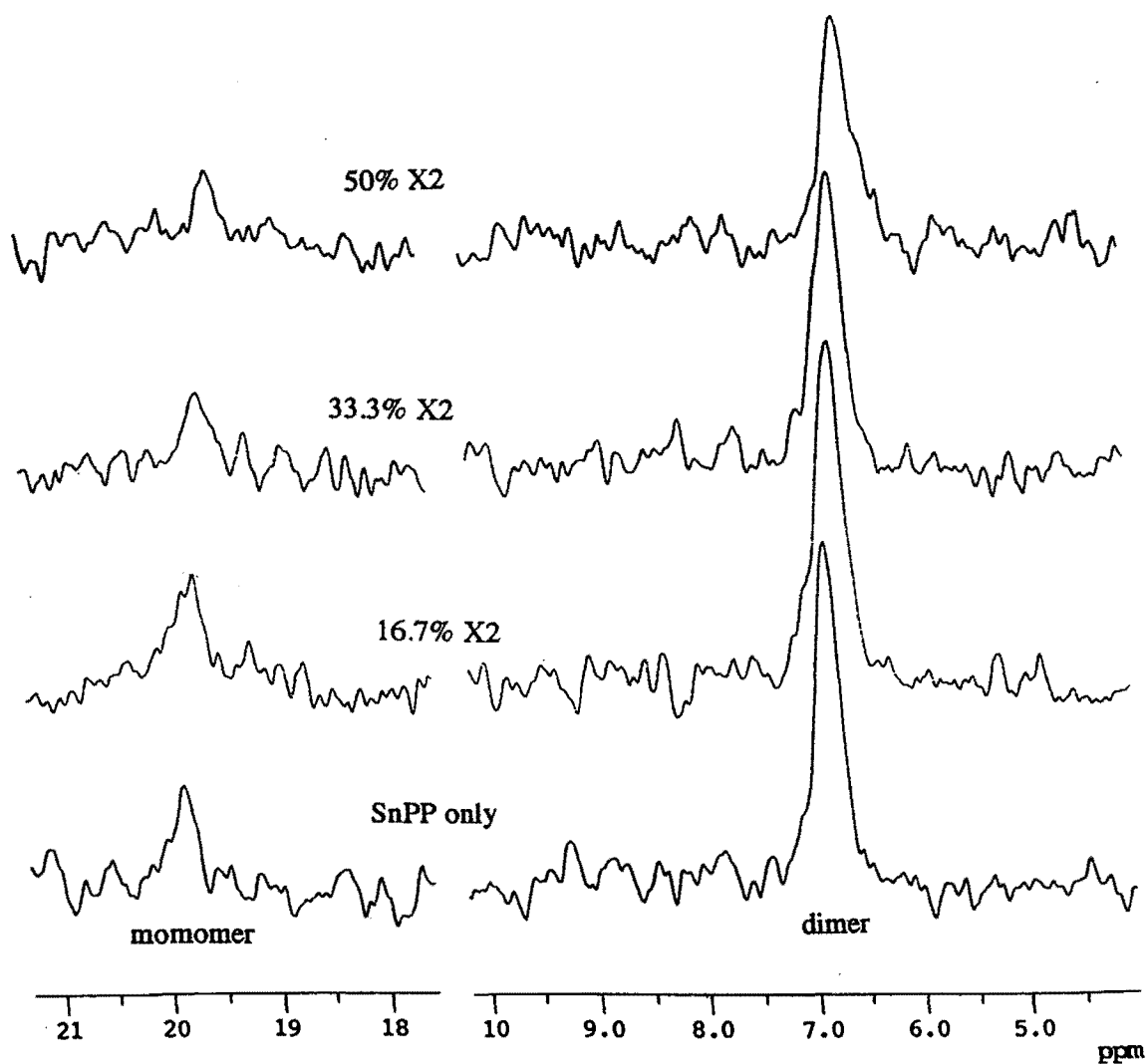


Figure 31. ^{119}Sn NMR spectra of SnPP as a function of X2 addition in mole percent at pH 9.5, 25 °C.

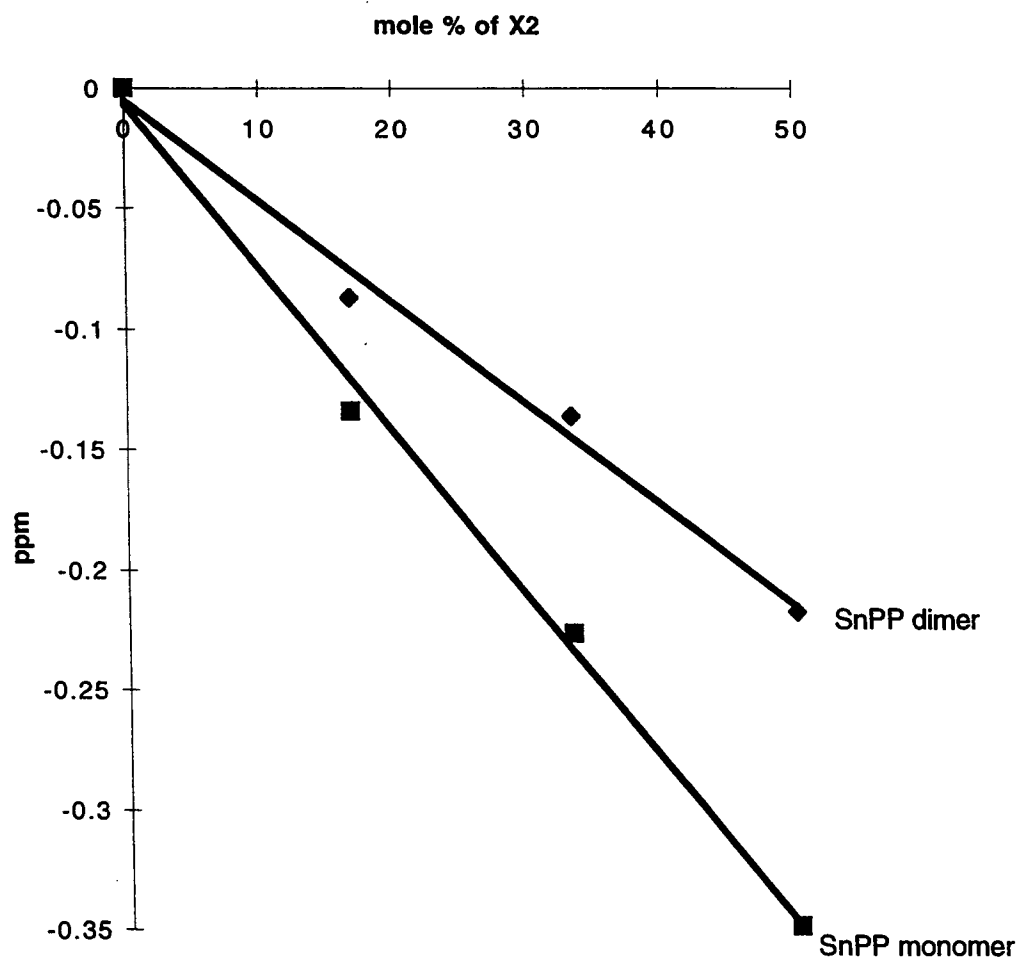


Figure 32. The dependence of induced shifts of the Sn resonance of SnPP on the concentration of X2, pH 9.5, 25 °C

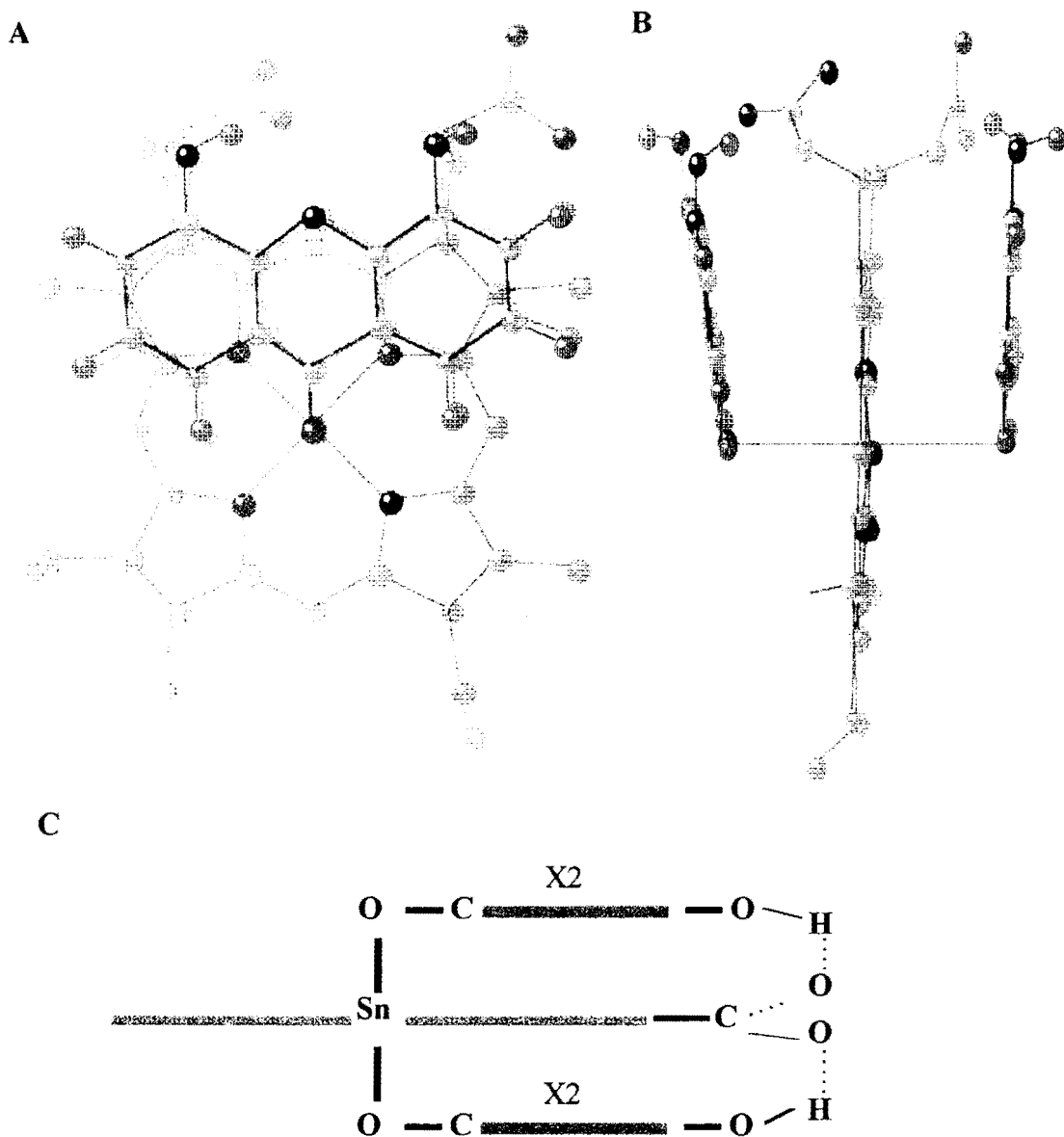


Figure 33. Proposed model for SnPP monomer-X2 complex in aqueous solution at pH 9.5. A: Top view. B: Side View C: Schematic structure

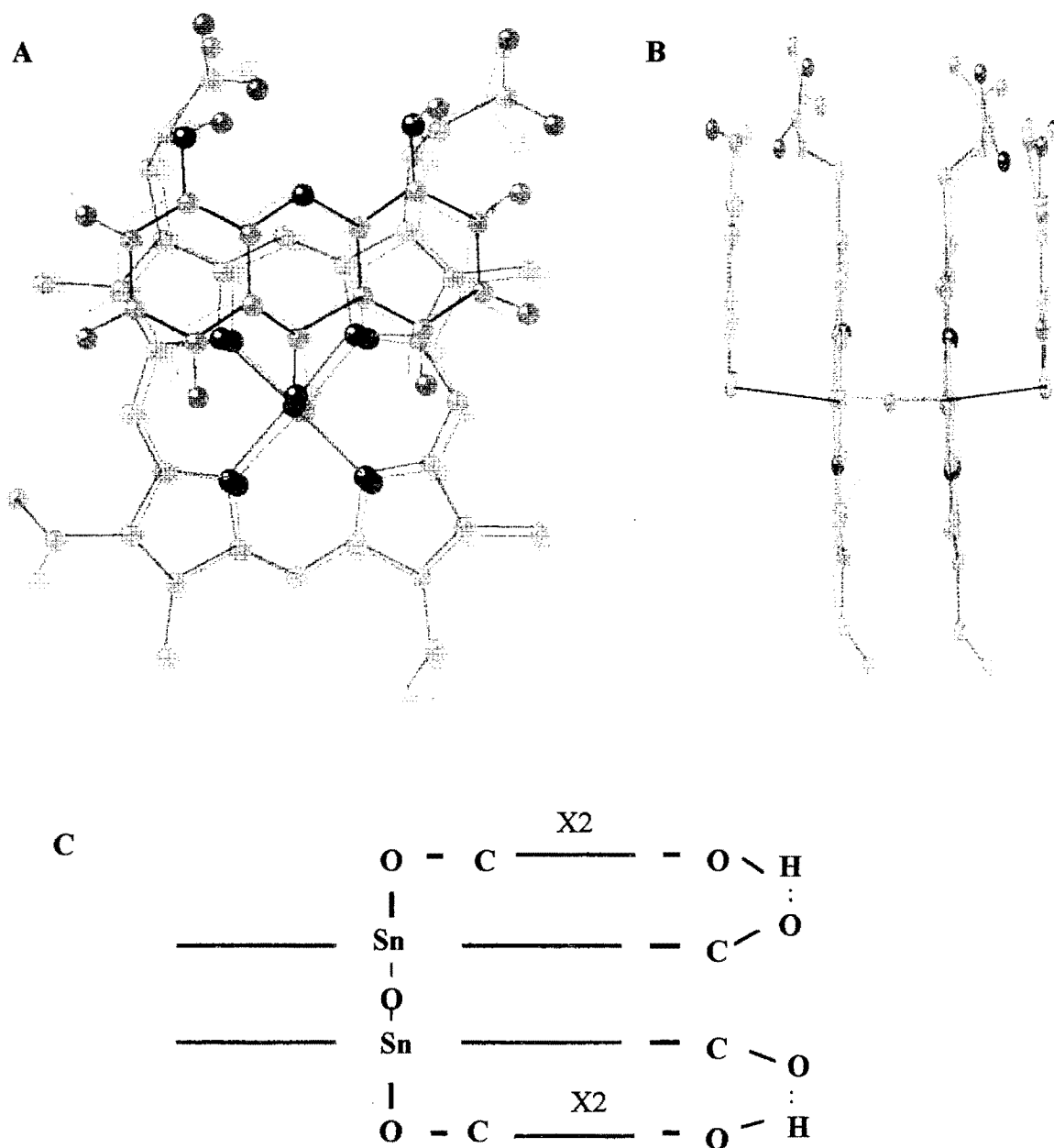
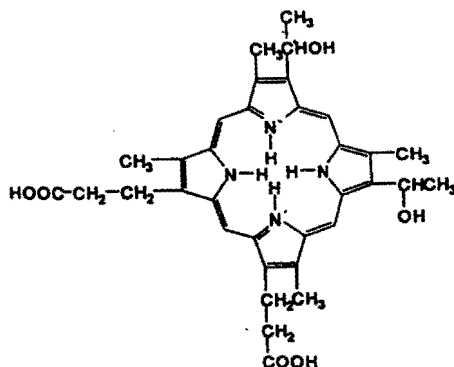


Figure 34. Proposed model for SnPP dimer-X2 complex in aqueous solution at pH 9.5. A: Top view B: Side view C: Schematic structure

CHAPTER 8

NMR STUDY OF THE INTERACTION BETWEEN HEMATOPORPHYRIN IX AND X2

The results derived from previous chapters together with the conclusion that the interaction of metalloporphyrin with X2 involves π - π interaction, led me to examine the interaction between X2 and non-metallated porphyrin. Hematoporphyrin IX (structure below) was chosen because of its high solubility in aqueous solution. The results from this chapter proves the existence of the π - π interaction in the complex formed between X2 and hematoporphyrin IX.



MATERIALS AND METHODS

Hematoporphyrin IX was supplied by Porphyrin Products. X2 was synthesized by Rolf Winter from Portland VA Hospital. Hematoporphyrin IX

solutions were always prepared fresh by dissolving the porphyrin in D₂O with a minimum amount of NaOD as required, and then adjusted to pH 9.5 in phosphate buffer. All samples prepared were protected from light. ¹H NMR spectra were recorded for hematoporphyrin IX and X2 in D₂O at 25°C as described in Chapter 5.

RESULTS AND DISCUSSION

In the case of X2 binding to hematoporphyrin IX, the absence of a porphyrin-coordinated central metal means unusually large upfield shifts may not be observed. Figure 35 shows the results of titrating hematoporphyrin IX into aqueous solution of X2 at pH 9.5. As expected, the main effect of addition of increasing concentration of hematoporphyrin IX is a high-field shift of the all aromatic protons of X2, with protons 1(8) slightly shifted more than the other protons, indicating the locations of these two protons are on top of the center of the porphyrin. A plot of induced shift versus the porphyrin/X2 ratio is shown in Figure 36. The overall upfield shifts for all aromatic protons are slightly larger than those shifts caused by π - π interactions for either heme-X2 association or SnPP-X2 association, suggesting X2 binding to hematoporphyrin IX on both sides of porphyrin. This view was supported by the stoichiometry of one porphyrin to two X2 derived from extrapolated intersection of the plot of induced shifts versus the mole fraction (shown in Figure 35, broken lines; 30% porphyrin means porphyrin:X2 = 0.5:1). The two X2 to one porphyrin stoichiometry can be explained by the structure of hematoporphyrin IX. Instead of two vinyl groups at positions 2 and 4 of the porphyrin like in heme and SnPP, there are two MeCHOH groups at positions 2 and 4 of the porphyrin, making it possible to form hydrogen bonding with 4(5) position hydroxy groups of the second X2 molecule.

A slight line broadening throughout the whole spectra was noted; this can be explained in terms of increasing rotational correlation time and the fast chemical exchange between free porphyrin and bound porphyrin with X2, thus reflecting the formation of molecular complexes.

CONCLUSION

The larger induced shift is observed at the 1(8) protons (0.037 ppm at presence of 50 mol % of porphyrin) compared to at 2(7) (0.023 ppm) and at 3(6) (0.012 ppm), implying that the 1(8) protons occupy a region more strongly shielded by the ring current, which is on the top of the center of the porphyrin (Cross et al., 1985). The overall upfield shifts are typical of a the π - π type of interaction (Cross et al., 1985) that occurs in the solution of X2 with hematoporphyrin. The 4(5) position of the X2 is located at the edge of the porphyrin (possibly with hydrogen bonding between 4(5) hydroxy group of X2 and carboxylate side chain of porphyrin). The possible stoichiometry for X2 binding to hematoporphyrin IX is that two X2 molecule binds to porphyrin with one X2 molecule on each side of the porphyrin. Such a complex formation supports the notion that π - π interaction is one of the binding forces involved between X2 and porphyrin ring, including heme and SnPP.

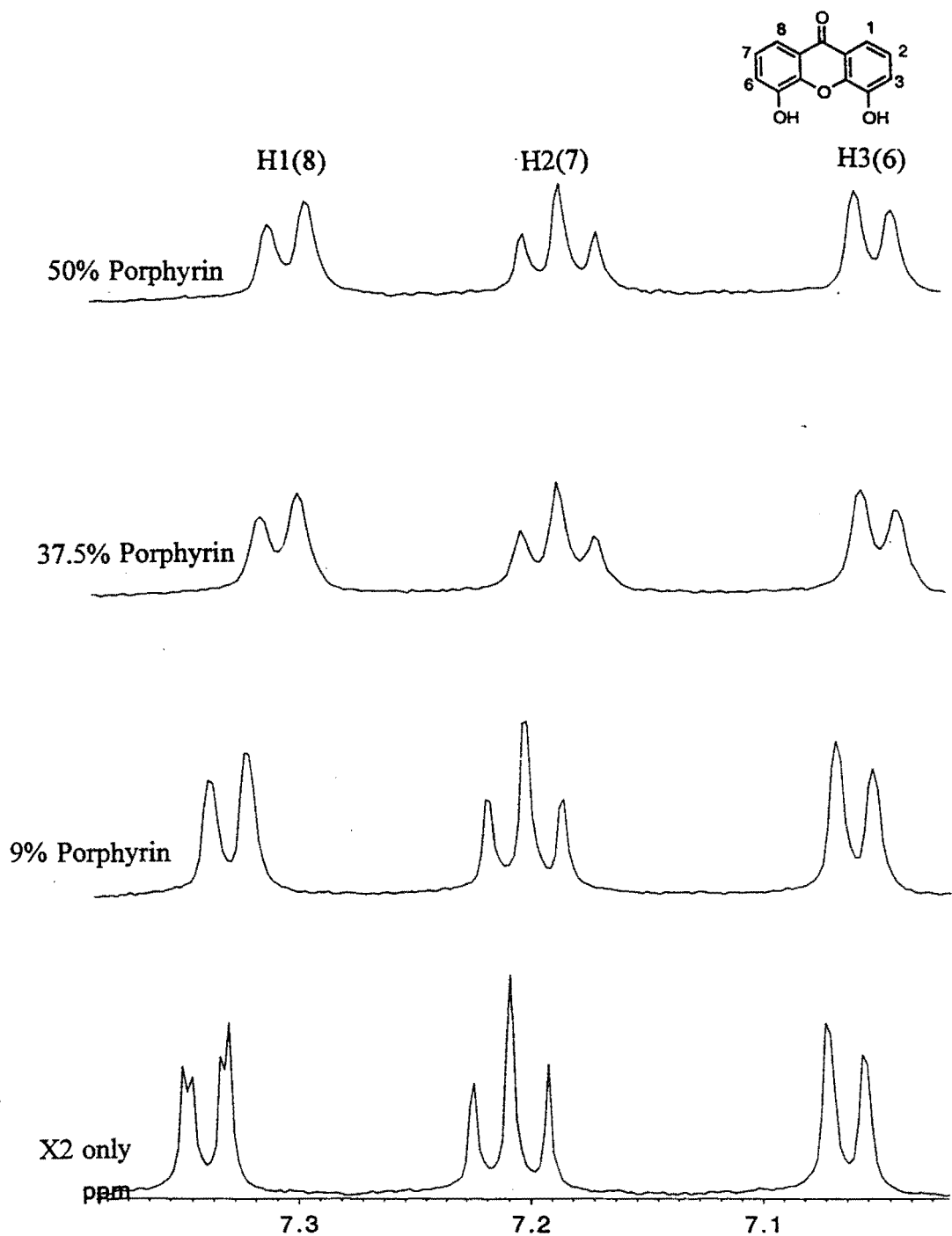


Figure 35. ^1H NMR spectra of X2 as a function of hematoporphyrin IX addition in mole percent at pH 9.5, 25 °C, 500 MHz.

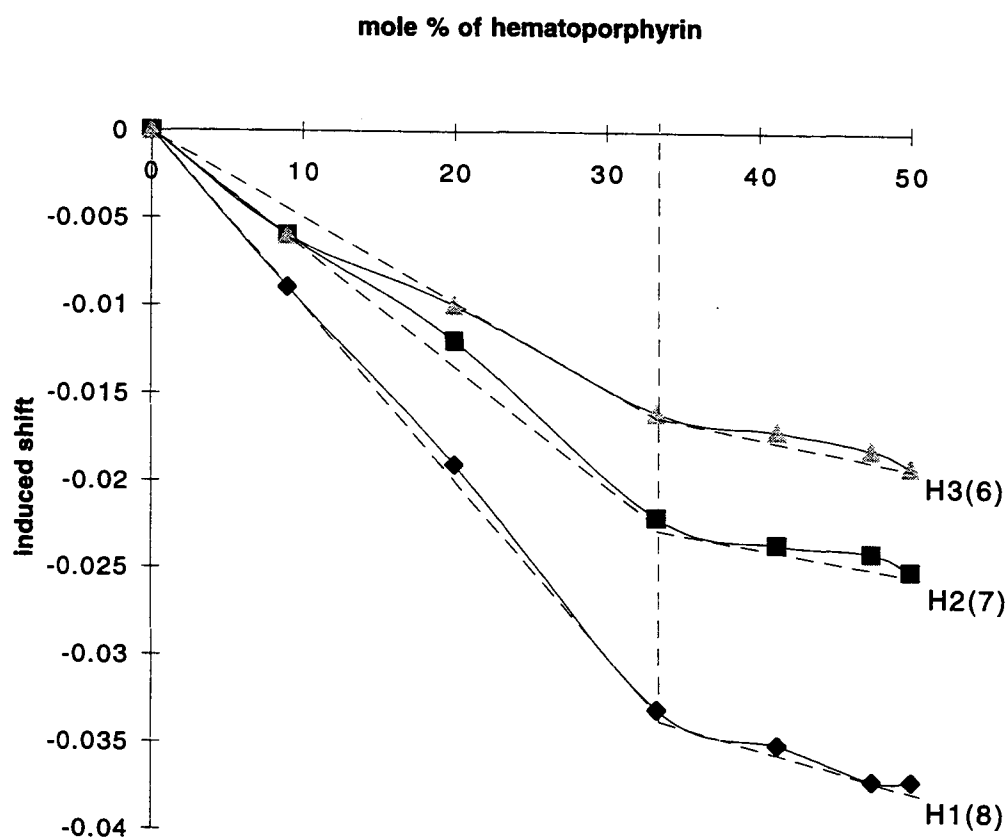
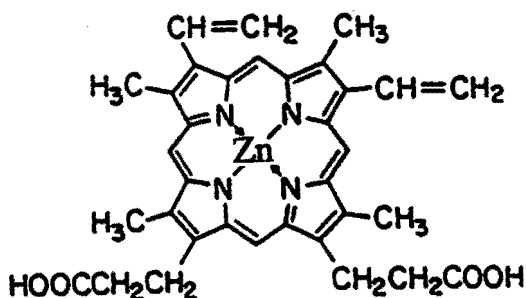


Figure 36. The upfield shifts of aromatic protons of X2 as a function of the molar fraction of hematoporphyrin IX.

CHAPTER 9

NMR STUDY OF THE INTERACTION BETWEEN ZINC PROTOPORPHYRIN AND X2

Interaction between zinc (II) protoporphyrin (ZnPP; the structure is shown below) and X2 was initially tested out of pure curiosity, but surprisingly, the result derived from NMR data is different than those derived from the interaction between X2 with heme or SnPP. A plausible explanation is also given in this chapter.



MATERIALS AND METHODS

ZnPP was from Porphyrin Products. X2 was synthesized by Dr. Rolf Winter from Portland VA Hospital. ZnPP solutions were always prepared fresh by dissolving the porphyrin in D₂O with a minimum amount of NaOD as required, and then adjusted to pH 9.5 in phosphate buffer. All samples prepared were protected from light. ¹H NMR spectra were recorded for SnPP and X2 in D₂O at 25°C as described in Chapter 5.

RESULTS AND DISCUSSION

Figure 37 shows the results from titrating ZnPP into X2 in aqueous solution at pH 9.5. Unlike the interaction between X2 with heme or SnPP where protons 1(8) of X2 experienced the largest upfield shift (compared to other aromatic protons), all of the aromatic protons of X2 show the upfield the same magnitude chemical shift change (about 0.023 ppm upfield shifted at presence of 80 mole % of ZnPP (ZnPP:X2 = 4:1)). This can be explained by the low charge of Zn (II) and the stereochemistry of ZnPP. The oxidation number of Zn in ZnPP is 2, which is smaller compared with Fe(III) in heme and Sn(IV) in SnPP. Consequencingly ZnPP has lower capability to accept a σ -donor ligands; meanwhile, a closed-shell d^{10} is formed after the formation of the equatorial ZnN_4 plane, and the complexing properties of the closed-shell d^{10} Zn(II) derives primarily from its unoccupied $4sp^3$ orbital, which would be weaker compared to inner shell complexing. Hence, all the above considerations may lead to a hindered the axial coordination between Zn metal of porphyrin and keto group from X2 molecule. The conclusion is that X2 binds to ZnPP primarily with π - π interaction, possibly accompanied by hydrogen bonding between the 4(5) hydroxy groups of X2 and carboxylate side chains of ZnPP.

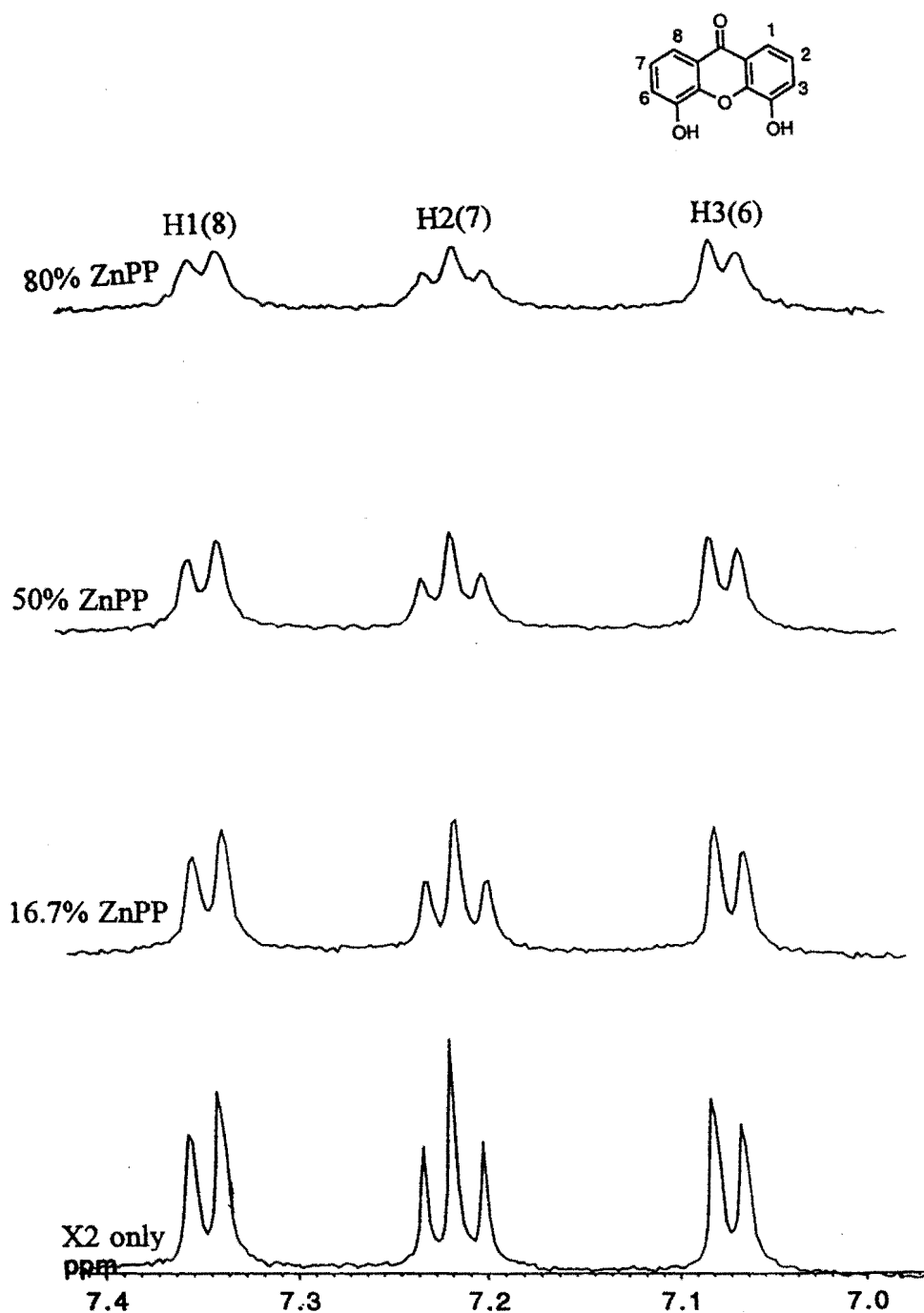


Figure 37. ^1H NMR spectra of X2 as a function of ZnPP addition in mole percent at pH 9.5, 25 °C, 500 MHz.

CHAPTER 10

MODE OF ACTION FOR X2 AS AN ANTIMALARIAL AGENTS

In this thesis I have presented evidences showing that X2 binds with both heme and SnPP in the following manner: axial coordination between C=O of X2 with Fe or Sn plays a key role in the complexation, accompanied by π - π interaction between aromatic ring of X2 and porphyrin plane, as well as with hydrogen bonding between 4(5) hydroxy groups of X2 with carboxylate side chains of the metalloporphyrin. The binding process is noncooperative (shown by Scatchard and Hill methods as described in Chapters 3 and 4) for both cases. It is suggested in Chapter 6 that X2 binds to both sides of the monomeric SnPP, as well as to both sides of the μ -oxo bridged dimeric SnPP. This conclusion is supported by ^{119}Sn NMR results.

The nature of heme in aqueous solution at low pH (pH 5.2-5.8, hemozoin range) is not clear. Slater et al. (1991) suggested that at this pH, heme exist as β -hematin, in which heme is linked between the central ferric ion of one heme and a carboxylate side-group oxygen of another, as shown in Figure 38. The bound iron in β -hematin is in a low-spin ferric state, while the unbound iron remain in a high-spin state. In any high-spin iron metalloporphyrin, the $3d_{x^2-y^2}$ and $3d_{z^2}$ orbitals in the metal atom retain each one unpaired electron. The presence of the electron in the $d_{x^2-y^2}$ orbital is responsible for the substantial displacement of the iron atom from the plane of the nitrogen atoms that is observed in every high-spin porphyrinato-iron species, and this large displacement is altogether favorable to the sterically unhindered complexing

of a single axial ligand. This makes the formation of stable high-spin six-coordinate species unusual (Smith, 1975).

Thus, X2 binding to a β -hematin dimer may be mainly through axial coordination between X2 C=O and unbound iron of the dimeric β -hematin as shown in Figure 38. This conclusion is strongly supported by the deference of binding stoichiometry between heme-X2 association and SnPP-X2 association, where one dimeric SnPP appears to bind with two X2 molecules, while one dimeric heme only binds with one X2 molecule. This theory is also supported by unusual large ^1H NMR upfield shift for the protons at the 3 and 6 position of X2, which was expected to experience the same magnitude shift with those for proton 2 and 7 if X2 is to bind with a μ -oxo dimeric heme. The large upfield shift for protons 3 and 6 may be the result of the ring current caused by the second heme plane which has its iron bond to the carboxylate oxygen of the first heme plane. Yet the above hypothesis does not preclude the possible effect of a significant contact shift caused by paramagnetic heme iron, because a spin transfer mechanism caused by the contact interaction through bound can lead to different (i.e., upfield and downfield) chemical shift changes for adjacent proton resonances.

This is then a happy ending with all puzzle pieces fitting into places, it may be that X2 acts in a unique fashion to bind with heme and 'put the cap' on the heme polymerization, hence killing plasmodium parasites. With little modification of the structure of X2, xanthone derivatives may make very potent antimalarial agents. This model should provide a good starting point for designing even better antimalarial drugs.

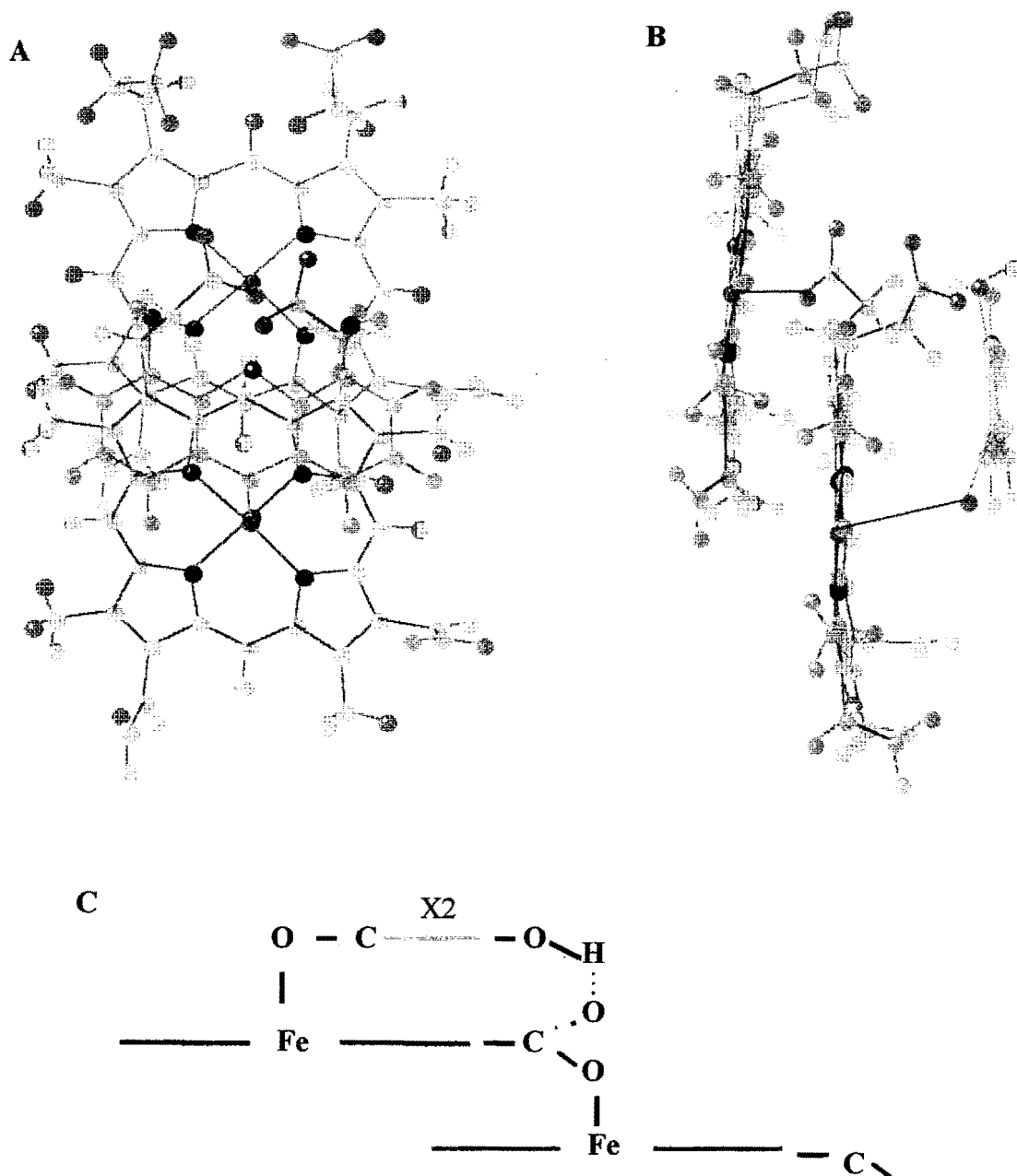


Figure 38. Proposed model for heme-X2 complex in aqueous solution at pH 9.5. A: Top view. B: Side view. C: Schematic structure

REFERENCES

- Ashong, J.O., Blench, I.P., Warhurst, D.C. (1989) *Trans. R. Soc. Trop. Med. Hyg.* 83, 167-172.
- Barracrough, D., Locksley, H.D., Scheinmann, F., and Taveira Magalhaes, (1970) *M. J Chem. Soc. (B)*, 603.
- Behere, D.V., Goff, H. M. (1984) *J. Am. Chem. Soc.* 106, 4945-4950.
- Blauer, G., and Ginsburg, H. (1982) *Biochem. Int.* 5, 519-523.
- Breslow, E., Cjamdra R., and Kappas, A. (1986) *J. Biol. Chem.*, 261 3135-3134.
- Cantor, C.R.; Schimmel, P.R. (1980) *Biophysical Chemistry, Part III*, W. H. Freeman: San Francisco, CA, pp1134-1138.
- Chou, A.C., Chevli, R., Fitch, C.D. (1980) *Biochemistry* 19, 1543-1549.
- Chou, A.C., Fitch, C.D. (1981) *J. Clin. Invest.* 68, 672-677.
- Connors, K.A (1980) *Binding Constant*, Wiley, NY pp241.
- Constantinidis I., and Satterlee, J. (1988) *J. Amer. Chem. Soc.* 110, 4391.
- Constantinidis, I., and Satterlee, J. (1988) *J. Amer. Chem. Soc.* 110, 927.
- Cross, K.J., Wright, P.E. (1985) *J. of Magn. Reson.* 64, 220-231.
- Deeb, R.S. (1993) *Nuclear Magnetic Resonance Investigation of the Interaction of Heme Binding Proteins with SnIV Protoporphyrin IX and Heme: Structure and Conformational Changes of Myoglobin and Hemopexin*, Ph. D Dissertation.
- Deeb, R.S., and Peyton, D.H. (1992) *Biochemistry* 31, 468-474
- Dorn, A., Stoffel, R., Matile, H., Bubendorf, A., Ridley, R.G. (1995) *Nature* 374, 269-271.
- Dorn, A., Vippagunta, S.R., Ridley, R.G. (1998) *Biochemucal Pharmacology* 55, 1-10.

- Fitch, C.D., Chevli, R., Banyal, H.S., Phillips, G., Pfaller, M.A., Krogstad, D.J. (1982) 21, 819-822.
- Fitch, C.D., Kanjanangkulpan, P. (1987) *J. Biol. Chem.* 262, 15552-15555
- Goldberg, D. E. and Slater, A.F.G.(1992) *Parasitol Today* 8, 280-283.
- Goldie, P., Roth, E.F.Jr, Oppenheim, J., Vanderberg, J.P. (1990) *Am. J. Trop. Med. Hyg.* 43, 584-596.
- Homewood, C.A., Warhurst, D.C., Peters, W., Baggaley, V.C. (1972) *Nature* 235, 50-52.
- Hostettmann, K., and Hostettmann, M. (1989) *Methods in Plant Biochemistry*, Academic Press Limited, 493.
- Ignatushchenko, M.V., Winter, R.W., Bachinger, H.P., Hinrichs, D.J., Riscoe, M.K., *FEBS Lett.* (1997) 409, 67-73.
- Martin, R.H., Defay, N., Greets-Evrard, F., Given, P.H., Jones, J.R., and Wedel, R.W. (1965) *Tetrahedron* 21, 1833.
- Meek, W., Straub, D., and Drago, R. (1960) *J. of Am. Chem. Soc.* 82, 6013
- Meshnick, S.R., Chang, K.P., (1977) *Cerami. A. Biochem. Pharmacol.* 26, 1923-1928.
- Moreau, S., Perly, B., and Biguet, J. (1982) *Biochemie* 64, 1015-1025.
- Moreau, S., Perly, B., Chachaty, C., and Deleuze, C. *Biochim. Biophys. Acta* 840, 107-116.
- Olliaro, P. and Goldberg, D.E. (1995) *Parasitol Today* 11, 294-297.
- Pople, J.A., Scheider, W.G., and Bernstein, J.H. (1959) *High resolution Nuclear Magnetic Resonance*, McGraw-Hill, New Yorkl, pp98.
- Prada, J., Malinowski, J., Muller, S., Bienzle, U., Kremsner, P.G. (1995) *Eur. Cytokine. Netw.* 6(2), 109-112.

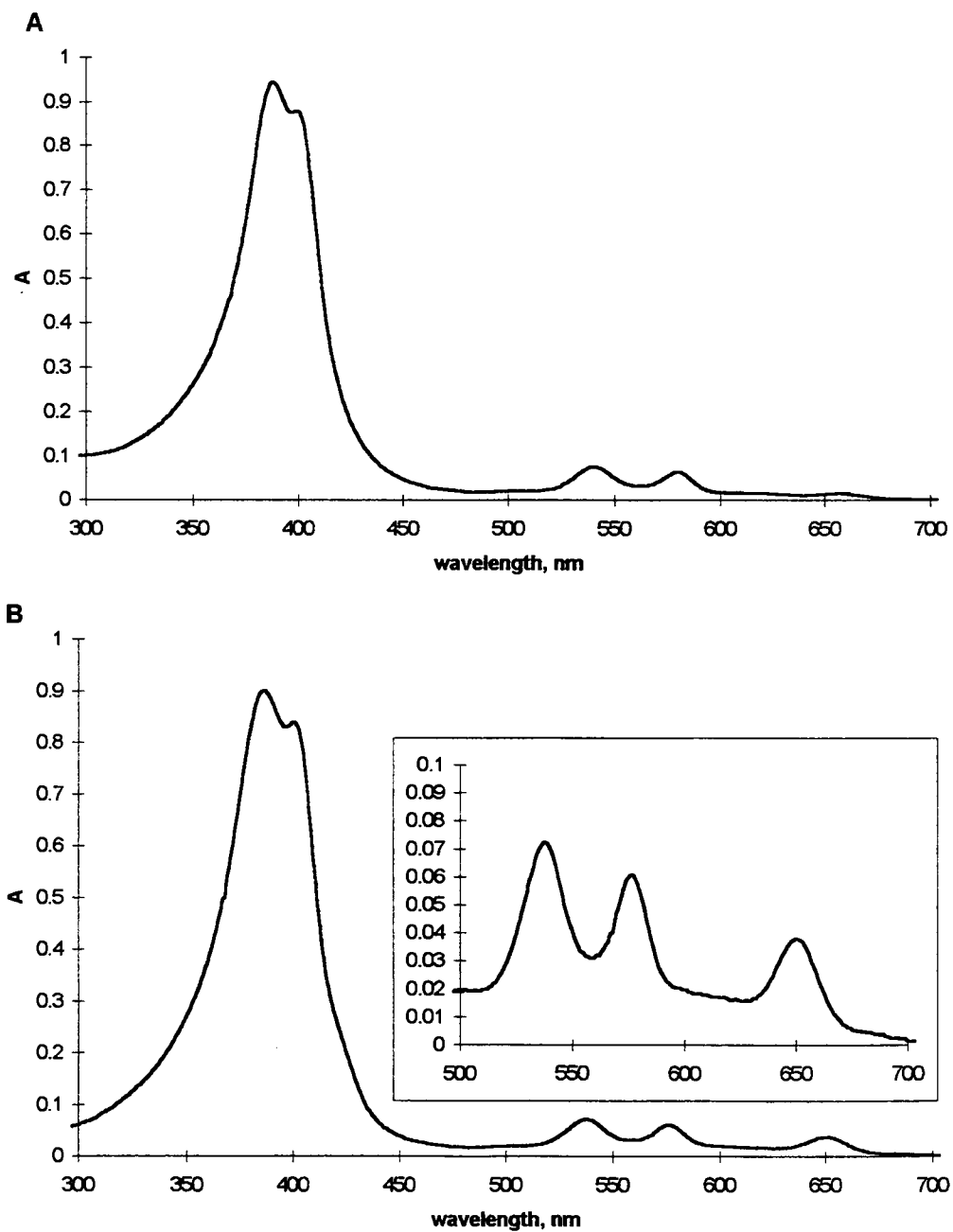
- Schwarzer, E., Turrini, F., Ulliers, D., Giribaldi, G., Ginsburg, H., Arese, P. (1992) *J. Exp. Med.* 176, 1033-1041.
- Sherman, I. W. (1979) *Microbiol. Rev.* 43, 453-495.
- Slater, A.F. (1992) *Experimental Parasitology* 74, 362-365.
- Slater, A.F. (1993) *Pharmacol. Ther.* 57, 203-235.
- Slater, A.F., Cerami, A. (1992) *Nature* 355, 167-169.
- Slater, A.F., Swiggard, W. J., Orton, B.R., Goldberg, D.E., Ceramin, A., and Henderson, G.B. (1991) *Biochemistry* 88, 325-329
- Slater, A.F., Swiggard, W.J., Orton, B.R., Flitter, W.D., Goldberg, D.E., Cerami, A., Henderson, G.B. (1991) *Proc. Natl. Acad. Sci. U. S. A.* 88, 325-329.
- Smith, K.M. (1975) *Porphyrins and Metalloporphyrins*, chapter 10, Elsevier Scientific, Amsterdam, The Netherlands.
- Van Hilde, K.E. (1971) *Physical Biochemistry*, Prentice Hall, Englewood Cliffs, NJ, pp62-64.
- Warhurst, D. C. (1987) *Ann. Trop. Med. Parasitol.* 81, 65-67.
- White, N. (1992). *J. Antimicrob. Chemo.* 30, 571-585.
- White, W.I. (1978) *The Porphyrins*, D. Dolphin, Ed., Academic Press, New York, Vol.V, pp7.

APPENDIX

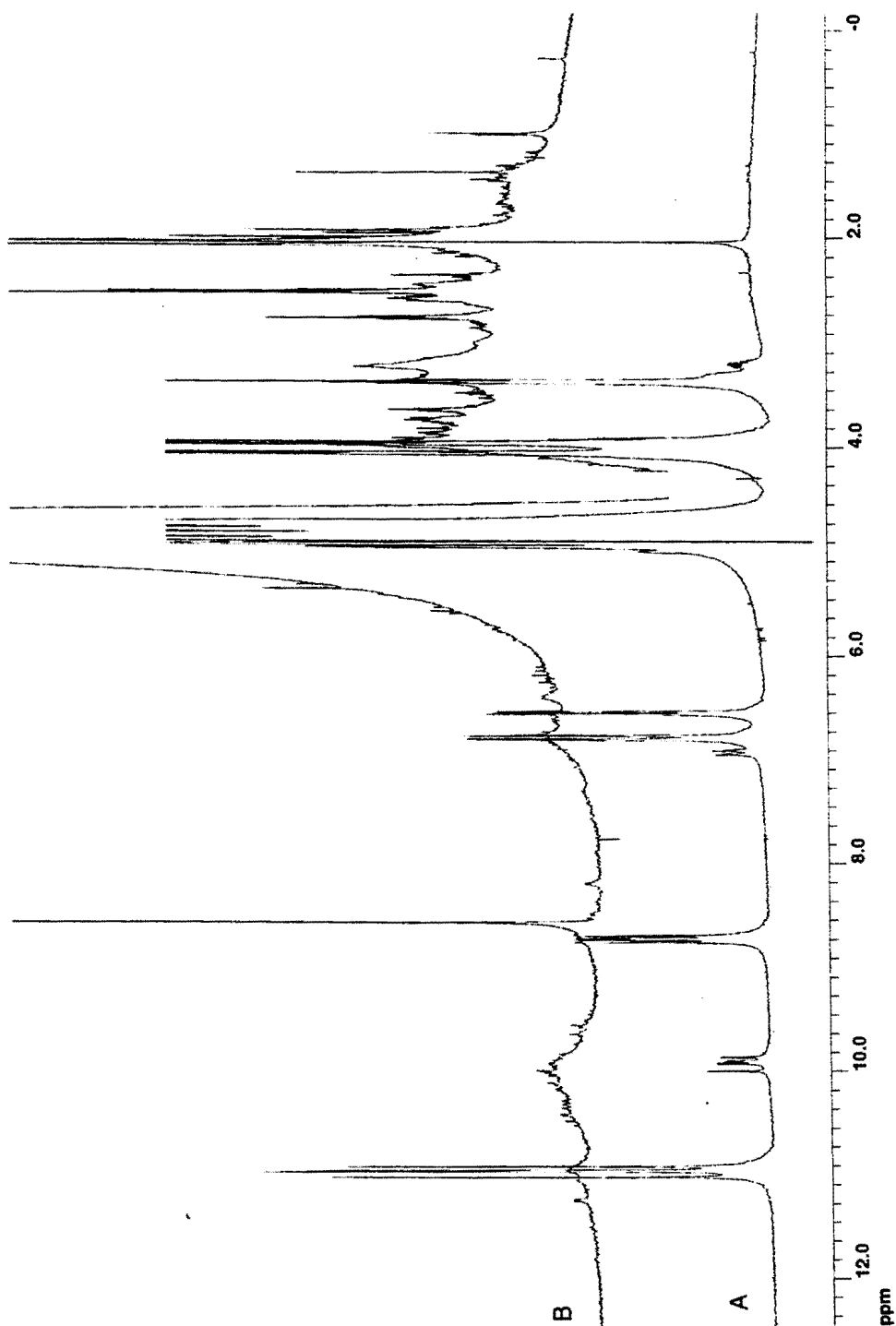
PHOTODEGRADATION OF SnPP

As discussed in Chapter 4, regular SnPP exhibits an absorption spectrum typical of metalloporphyrins with a maximum of the Soret band ranging between 386 and 406 nm as well as two bands peaking at around 540 and 580 nm (shown in Appendix Figure 1A). In aqueous solutions the shape of the Soret band and its maximum are largely influenced by the pH of the medium and the SnPP concentration. At low pH values and at high porphyrin concentrations the maximum absorption is localized at 386 nm (dimer) and gradually shifts to 406 nm (monomer) as the pH increases or the concentration decreased.

However, The absorption spectrum of SnPP undergoes significant modifications upon irradiation with light in the presence of oxygen. In particular, a new absorption band at 650 nm can be observed (shown in Appendix Figure 1B). This shows the NMR spectrum of the SnPP after photodegradation (Appendix Figure 2B) in comparison to regular SnPP (Appendix Figure 2A). The assignment of the NMR spectrum for photodegraded SnPP would need to be investigated in future studies in order to characterize the structure(s) of this resultant species.



Appendix Figure 1. UV-vis spectrum of A: regular SnPP, B: SnPP after photodegradation at pH 5.8, 25 °C.



Appendix Figure 2. ^1H NMR spectra of A: regular SnPP, B: SnPP after photodegradation at pH 10.5, 25 °C.